Doctoral Dissertation

Development of Carbon–Carbon Bond-Forming Reactions via the Cleavage of Carbon–Fluorine Bonds in Aryl Fluorides and Carbon–Silicon Bonds in Acylsilanes

Akihisa Matsuura

December 2024

Department of Applied Chemistry,
Graduate School of Engineering,
Osaka University

Preface and Acknowledgement

The research presented in this thesis was carried out under the direction of Professor Mamoru Tobisu of the Department of Applied Chemistry, Graduate School of Engineering, Osaka University. I was a student in Professor Shimada and Kamei's laboratory at The National Institute of Technology, Nara College from October 2016 to March 2018 and then moved to Osaka City University. I was a student in Professor Morimoto's laboratory from April 2019 to March 2020 and then moved to Professor Chatani's laboratory in Osaka University, where I was a student from April 2020 to March 2022. After Professor Chatani retired, I moved to Professor Tobisu's laboratory and have been a student there from April 2022 to March 2025. The thesis is concerned with development of carbon–carbon bond-forming reactions via the cleavage of carbon–fluorine bonds in aryl fluorides and carbon–silicon bonds in acylsilanes. This thesis could not have been completed without the support of numerous people. Here, I wish to express my sincerest appreciation to all of these people.

First, I would like to express my heartfelt gratitude to Professor Mamoru Tobisu for accepting me as a doctoral student and providing invaluable guidance throughout my three years of study. When I first joined the laboratory, I was an inexperienced researcher, but under his expert supervision, I was able to grow both academically and personally. His insightful advice and unwavering support were instrumental in enabling me to complete research papers that I am truly proud of. I am deeply thankful for the opportunity to learn and develop under his mentorship.

Second, I wish to express my sincere gratitude to Assistant Professor Takuya Kodama. His invaluable guidance on crystal structure analysis and his thoughtful advice during challenging times greatly supported me. I am also thankful for the enjoyable conversations beyond research, which made my time in the laboratory even more fulfilling.

Third, I would like to express my heartfelt gratitude to Assistant Professor Hayato Fujimoto. I am deeply grateful for his guidance and support, both in my research and personal life, and for the many valuable discussions we had.

I sincerely appreciate Professor Naoto Chatani, Associate Professor Yoshiya Fukumoto, Assistant Professor Yusuke Ano, Professor Yoshiki Morimoto, Lecturer Keisuke Nishikawa, Technical Staff Matsumi Doe, Professor Toyoshi Shimada, Associate Professor Toshiyuki Kamei for instructive advice based on their profound understanding of

chemistry. I also express my appreciation to the secretaries in our laboratory, including Ms. Kyoko Kawashima, and Ms. Junko Ohmagari for their generous assistance. I also wish to express my appreciation to the past and present laboratory members. The respectable and talented senior members: Dr. Tomoki Yoshida, Dr. Ryoma Shimazumi, Dr. Yasuaki Iyori, Dr. Qiyuan He, Dr. Hisayasu Ishibashi, Mr. Itsuki Nohira, Mr. Shizuki Monda, Mr. Natsuki Kawai, Ms. Nozomi Ohara, Dr. Kunihiro Matumura, Dr. Kento Nishikibe, Mr. Yuta Ogata, Mr. Takumi Ikeuchi, Mr. Takayuki Noguchi, Ms. Priscilla Yoong Mei Yen, Mr. Toshiki Niwa, Mr. Koki Kikuta, Mr. Tomoki Omoteno, Dr. Soushi Nishino, Dr. Hironobu Nakazawa. Thanks to them, my stay here was both fruitful and happy and it was able to advance my research through discussions with them. I also wish to express my thanks to my colleagues in laboratory: Mr. Hikaru Noguchi, Mr. Daichi Takahashi, Ms. Aoi Morishige, Ms. Haruka Kawakami, Mr. Tomoki Tsuruta, Mr. Yuichiro Fushii, Mr. Rikuto Yasuda, Mr. Kokoro Okumura. They were highly motivated, worked hard and were an inspiration to me. I also wish to express my appreciation to the younger members of laboratory: Mr. Tetsuya Inagaki, Mr. Kenta Uchida, Mr. Satoshi Ogawa, Mr. Riku Tanimoto, Mr. Bunta Nakayasu, Mr. Takahiro Ando, Mr. Ryota Shiraki, Mr.Nijito Mukai, Ms. Sakura Takahashi, Mr. Hiroki Morita, Mr. Shisato Yamamura, Mr. Yuki Akita, Mr. Taiki Arima, Mr. Kazuya Imachi, Mr. Tomoya Emmei, Ms. Namiki Takenaka, Mr. Tomoya Ueda, Mr. Takayuki Enomoto, Mr. Teruki Nishioka, Ms. Moe Morimoto, Ms. Yui Morimoto, Mr. Sota Iwasaki, Mr. Ryoichi Tabata. Mr. Sei Harada, Mr. Ibuki Hirai, Mr. Masayuki Mizutani, Mr. Haruki Hirosawa, Mr. Yuki Nakamoto, Mr. Kazumune Yo, Mr. Syun Watanabe, Ms. Nami Tanaka, Mr. Syoutaro Yano, Mr. Kippei Yamamura.

Furthermore, I wish to acknowledge the talented postdoc: Dr. Vishal Kumar Rawat, Dr. Supriya Rej, Dr. Shrikant Kahake Manmathappa, Dr. Sanjit Kumar Mahato, Dr, Amurita Das, Dr. Bernard Parker,

Lastly, I express my appreciation for my family; Mr. Mikiyoshi Matsuura, Ms. Masako Matsuura, younger brother Mr. Sosuke Matsuura, grandmather Mr. Ikuko Tanaka for their continuous and generous support.

Suita, Osaka

January 2024

Akihisa Matsuura

Contents

General Introduction

Chemical reactions are initiated by the bond cleavage of the starting molecules. As such, compounds with weaker bonds often serve as suitable substrates. For instance, in carbon–carbon bond formation reactions, a common strategy to make the reaction thermodynamically favorable is to employ substrates bearing π-bonds or carbon–halogen bonds, which have smaller bond energies than the carbon–carbon bonds (**Fig. 1a**). In recent years, significant progress has been made in the study of C–H activation, in which C–H bonds commonly found in organic compounds are utilized in organic synthesis.[1] There has also been growing interests in exploring the cleavage of unreactive bonds other than C–H bonds, which are generally less reactive, and utilizing them in organic synthesis. Notable examples include transformations involving the cleavage of C–O bonds in anisoles[2] and C–N bonds in anilines.[3] This study explores novel chemical reactions involving the cleavage of carbon–fluorine and carbon–silicon bonds, which are conventionally considered to be less reactive.

Direct transformation of unreactive bonds holds immense potential in organic synthesis, as it eliminates the need for pre-functionalized substrates and enables late-stage elaboration of complex molecules, bypassing tedious protection/deprotection steps (**Fig. 1b**).

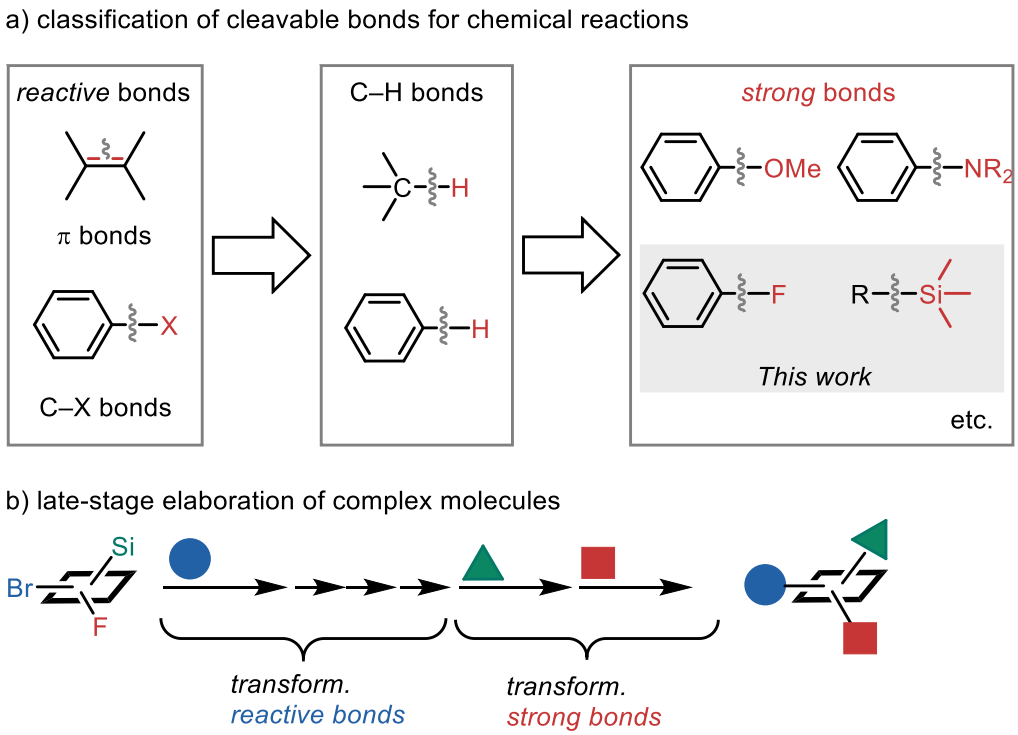

Fig. 1 Diversification of the Cleavable Bonds for Chemical Reactions.

Carbon-fluorine bonds are among the strongest covalent bonds involving carbon (e.g., BDE of Ph–F: 127 kJ/mol),[4] making its activation a significant challenge even in modern organic chemistry. Nucleophilic aromatic substitution (S_NAr) reactions are relatively well-studied transformations for carbon–fluorine bond cleavage (**Fig. 2a**).[5] The S_NAr reaction, which has been studied since the 1870s,[6] typically proceeds via a Meisenheimer intermediate. It generally which requires electron-withdrawing groups to stabilize the intermediate and promote reaction. Therefore, the aryl fluorides that efficiently react in conventional S_NAr reactions are limited to derivatives with strongly electron-withdrawing substituents such as a nitro group and reactivity is known to increase in order of Ar–F > Ar–Cl > Ar–Br > Ar–I. Recently, concerted nucleophilic aromatic substitution (cS_NAr) reactions have emerged, which proceed without intermediate formation and retain aromaticity in the transition state, thus enabling the use of simple aryl fluorides without electron-withdrawing groups (**Fig. 2b**).[7] The first example of the cS_NAr reaction were reported in 1980 by Pierre in the nucleophilic substitution of potassium hydride with aryl halides (**Fig. 2c**).[8] This pioneering study demonstrated an inverse reactivity trend of halides compared to classical S_NAr reactions (Ar–I > Ar–Br > Ar–Cl > Ar–F). Mechanistic insights into the cS_NAr reaction were provided by Fry and Pienta in 1985, who observed, through Hammett studies, a small influence of the electronic nature of the substrates.[9] Later, computational studies by Tuttele et al. in 2020 revealed that the effect of nucleophiles on adopting a concerted mechanism is minimal, while favorable electrostatic interactions between cations and fluorine atoms play a crucial role.[10] These findings suggest that designing nucleophiles capable of reacting with nonactivated aryl fluorides via the cS_NAr mechanism is challenging, emphasizing the importance of selecting a suitable combination of nucleophile and base. To date, nucleophilic aromatic substitution reactions of simple aryl fluorides predominantly involves heteroatom nucleophiles (e.g., alkoxides), with limited examples employing carbon nucleophiles (**Fig. 2d**). This study expands the scope of carbon nucleophiles applicable to nucleophilic aromatic substitution of simple aryl fluorides.

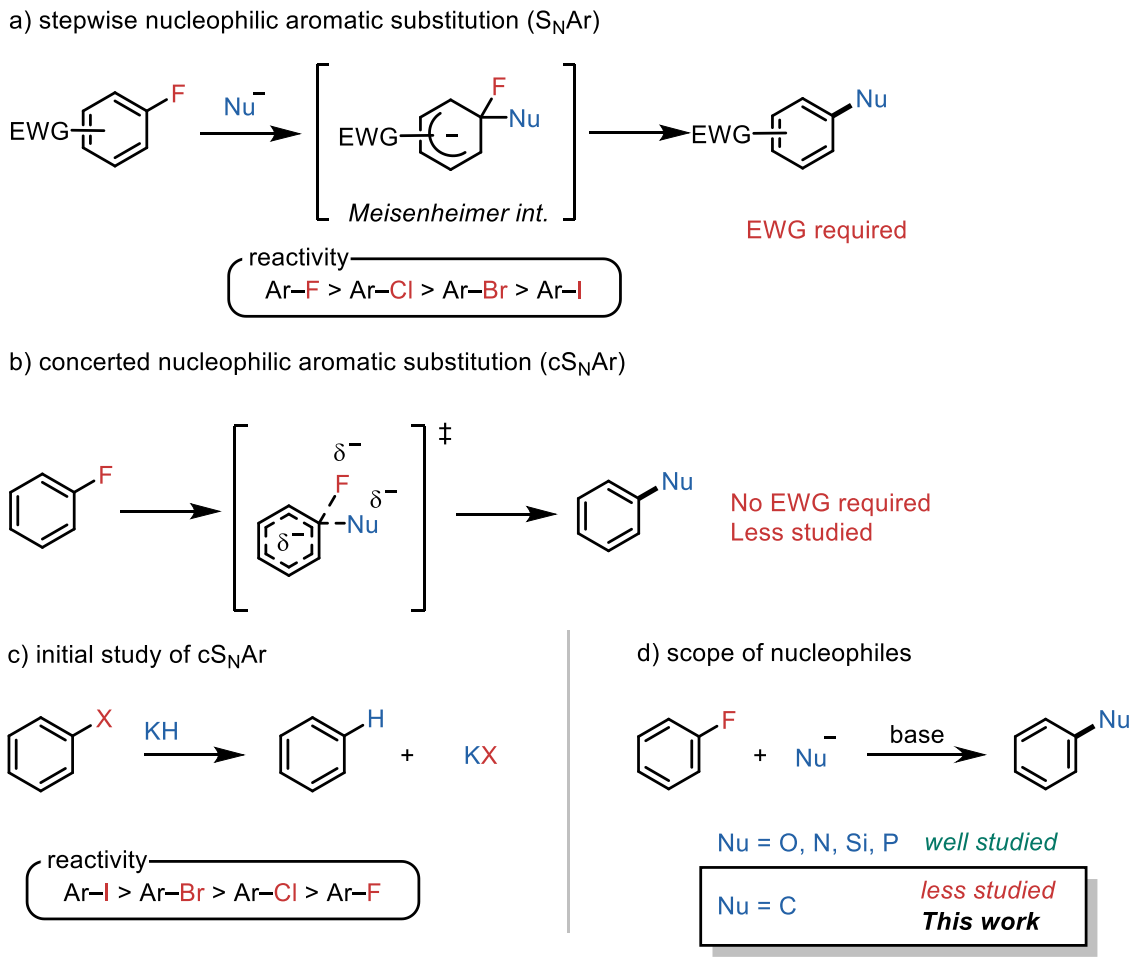

Fig. 2 Nucleophilic Aromatic Substitution: Reaction Mechanisms and Scope.

Another type of aromatic carbon–fluorine bond transformation involves transition metal catalysts. Transition-metal-catalyzed transformations of carbon–fluorine bonds often proceed via oxidative addition to a low-valent metal complex. Similar to S_NAr reactions, these transformations generally require substrates with electron-withdrawing groups, such as perfluorobenzene (**Fig. 3a**).[11] It should be noted that C–F bond dissociation energy of perfluorobenzene (114 kcal/mol) is significantly smaller compared to that of fluorobenzene (127 kcal/mol).[12] In contrast, there are few examples of catalytic carbon–carbon bond formation reactions using simple aryl fluorides without electron-withdrawing groups. While most reported reactions involve strong nucleophiles like Grignard reagents, few examples utilize other organometallic reagents or stabilized carbanions (**Fig. 3b**).[13] Herein, a novel annulation reaction of simple aryl fluorides with alkynes, which avoids the use of nucleophilic reagents, is presented (**Fig. 3c**).

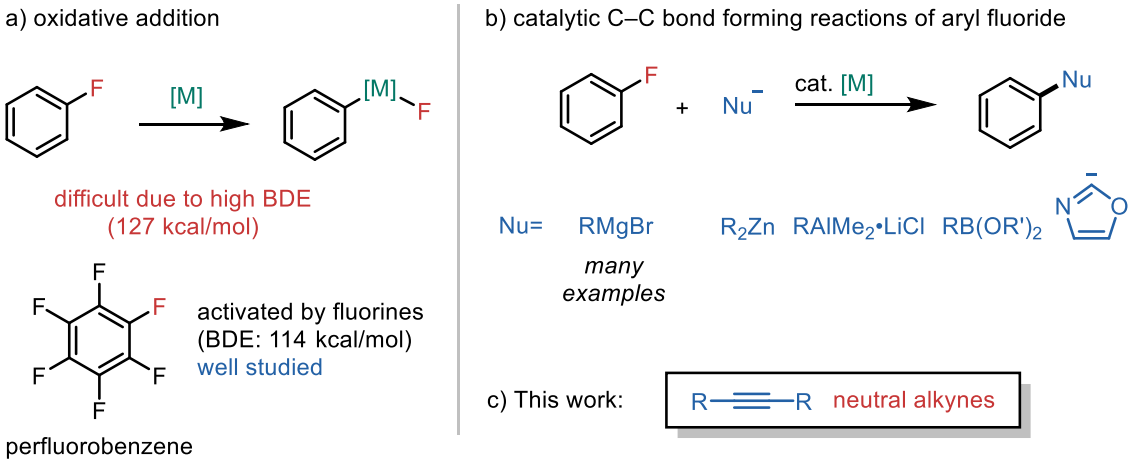

Fig. 3 Aryl C–F Bond Functionalization: Transition Metal Catalysis.

Regarding the cleavage of carbon–silicon bonds, this study focuses on the reaction of acylsilanes, a versatile class of compounds. Several methods for the conversion of carbon–silicon bonds in acylsilanes have already been reported. [14] In terms of transition metal catalysis, the most common mechanism involves transmetalation, where the silicon group acts as a leaving group and is lost during the reaction (**Fig. 4a**). The transmetalation process is well-utilized in several cross-coupling reactions using acylsilanes as the acyl source (**Fig. 4b**). [15]

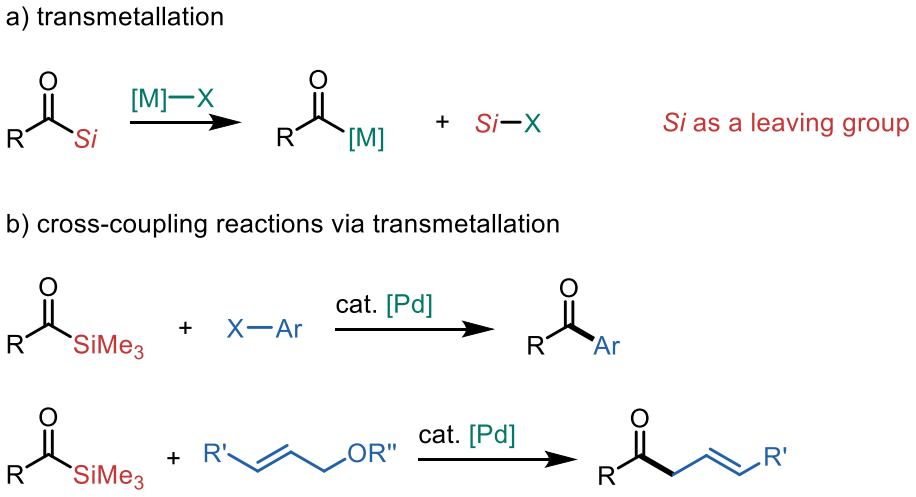

Fig. 4 C–Si Bond Cleavage of Acylsilanes via Transmetallation: Transition Metal Catalysis.

Another mechanism for cleavage of carbon–silicon bonds by transition metal complexes is oxidative addition (**Fig. 5a**). In contrast to transmetalation, the silicon group remains on the transition metal and is finally incorporated into the product. However, the reactions of acylsilanes via oxidative addition

have been limited to transformations involving decarbonylation (**Fig. 5b)**. [16] This work investigates novel siloxycarbene complex formation via oxidative addition of acylsilanes, followed by silicon rearrangement, unlocking new catalytic transformations that preserve the silicon moiety (**Fig. 5c**).

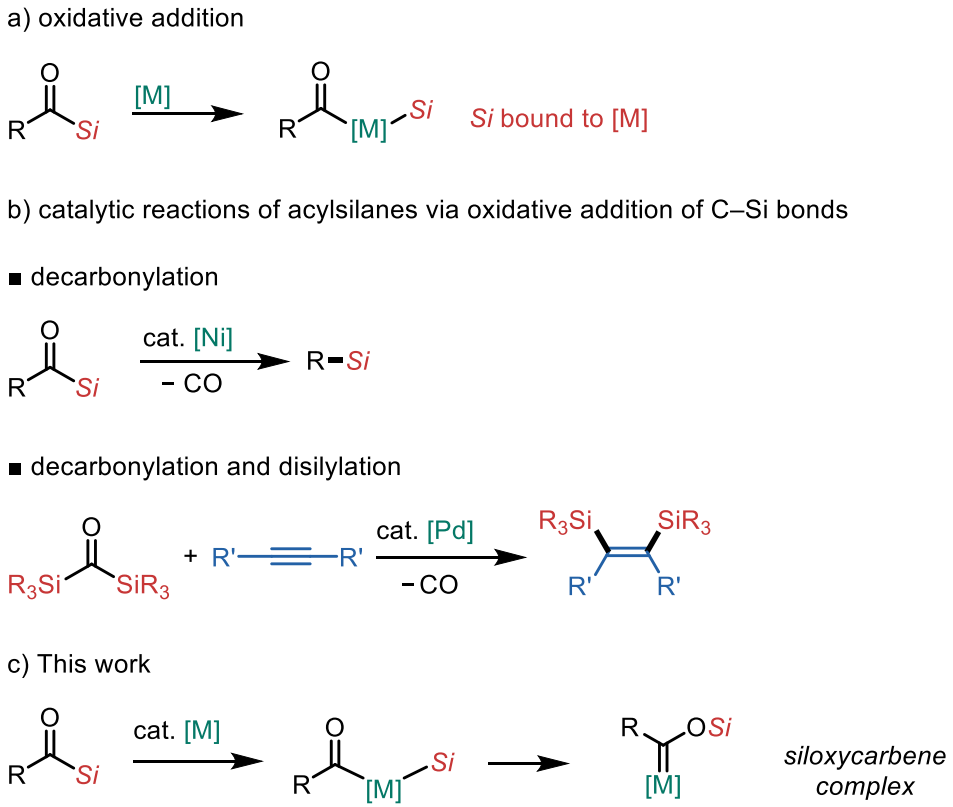

Fig. 5 C–Si Bond Cleavage of Acylsilanes via Oxidative Addition: Transition Metal Catalysis.

This study consists of the following three chapters (**Fig. 6**). In Chapter 1, the annulative coupling reaction of aryl fluorides with alkynes involving a directed carbon–fluorine bond clevage is described. This reaction represents the first example of carbon-fluorine bond activation using a carboxylic acid as a directing group. In Chapter 2, nucleophilic aromatic substitution reactions of non-activated aryl fluorides with amido enolates is described. In Chapter 3, the nickel-catalyzed reaction of acylsilanes with norbornenes is described. This is the first example of nickel-catalyzed formation of Fischer carbene complexes from acylsilanes.

This work advances understanding and application of carbon–fluorine and carbon–silicon bond transformations, providing innovative strategies in organic synthesis.

Chapter 1. Nickel-Catalyzed C–F/O–H Annulation with Alkynes

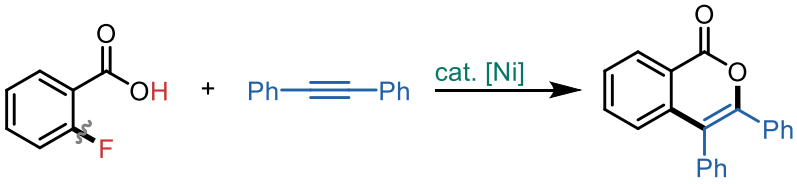

Chapter 2. cS_NAr Reaction of Non-Activated Aryl Fluorides with Aliphatic Amides

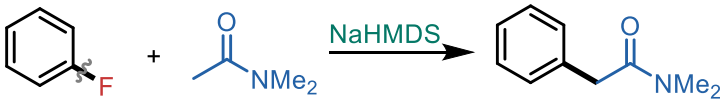

Chapter 3. Nickel-Catalyzed Synthesis of Silyl Enol Ethers Using Acylsilanes and Norbornene

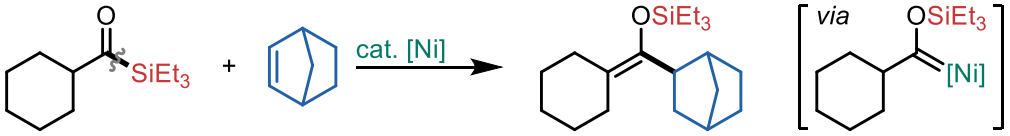

Fig. 6 Carbon–Carbon Bond-Forming Reactions via the Cleavage of Carbon–Fluorine and Carbon–Silicon Bonds.

References

(1) (a) Yang, L.; Huang, H. *Chem. Rev.* **2015**, *115*, 3468–3517. (b) Ali, W.; Prakash, G.; Maiti, D. *Chem. Sci.* **2021**, *12*, 2735–2759.

(2) (a) Tobisu, M.; Chatani, N. *Springer International Publishing: Cham*, **2019**; pp 103–140. (b) Li, P.; Zhang, M.; Zhang, L. *Top Curr Chem* **2024**, *382*, 38.

(3) García-Cárceles, J.; Bahou, K. A.; Bower, J. F. *ACS Catal.* **2020**, *10*, 12738–12759.

(4) Wang, Z.; Sun, Y.; Shen, L.-Y.; Yang, W.-C.; Meng, F.; Li, P. *Org. Chem. Front.* **2022**, *9*, 853–873.

(5) Bunnett, J. F.; Zahler, R. E. *Chem. Rev.* **1951**, *49*, 273–412.

(6) Faust, Aug. *Chem. Ber.* **1873**, *6*, 1022–1023.

(7) (a) Rohrbach, S.; Smith, A. J.; Pang, J. H.; Poole, D. L.; Tuttle, T.; Chiba, S.; Murphy, J. A. *Angew. Chem., Int. Ed.* **2019**, *58*, 16368–16388. (b) Rohrbach, S.; Murphy, J. A.; Tuttle, T. *J. Am. Chem. Soc.* **2020**, *142*, 14871–14876.

(8) Handel, H.; Pasquini, M. A.; Pierre, J. L. *Tetrahedron* **1980**, *36*, 3205–3208.

(9) Fry, S. E.; Pienta, N. J. *J. Am. Chem. Soc.* **1985**, *107*, 6399–6400.

(10) Rohrbach, S.; Murphy, J. A.; Tuttle, T. *J. Am. Chem. Soc.* **2020**, *142*, 14871–14876.

(11) Ahrens, T.; Kohlmann, J.; Ahrens, M.; Braun, T. *Chem. Rev.* **2015**, *115*, 931–972.

(12) Liu, X.; Dong, S.; Zhu, J.; Inoue, S. *J. Am. Chem. Soc.* **2024**, *146*, 23591–23597.

(13) (a) Amii, H.; Uneyama, K. *Chem. Rev.* **2009**, *109*, 2119–2183. (b) Fu, L.; Chen, Q.; Nishihara, Y.

Chem. Rec. **2021**, *21*, 3394–3410. (c) Das, A.; Chatani, N. *ACS Catal.* **2021**, *11*, 12915–12930. (d) Hooker, L. V.; Bandar, J. S. *Angew. Chem., Int. Ed.* **2023**, *62*, e202308880.

(14) Zhang, H.-J.; Priebbenow, D. L.; Bolm, C. Acylsilanes: *Chem. Soc. Rev.* **2013**, *42*, 8540–8571.

(15) (a) Schmink, J. R.; Krska, S. W. *J. Am. Chem. Soc.* **2011**, *133*, 19574–19577. (b) Ramgren, S. D.; Garg, N. K. *Org. Lett.* **2014**, *16*, 824–827. (c) allylic ester: Obora, Y.; Ogawa, Y.; Imai, Y.; Kawamura, T.; Tsuji, Y. *J. Am. Chem. Soc.* **2001**, *123*, 10489–10493.

(16) (a) Nakatani, S.; Ito, Y.; Sakurai, S.; Kodama, T.; Tobisu, M. *J. Org. Chem.* **2020**, *85*, 7588–7594. (b) Srimontree, W.; Lakornwong, W.; Rueping, M. *Org. Lett.* **2019**, *21*, 9330–9333. c) Sakurai, H.; Yamane, M.; Iwata, M.; Saito, N.; Narasaka, K. *Chem. Lett.* **1996**, *25*, 841–842.

Chapter 1
Nickel-Catalyzed C–F/O-H [4+2] Annulation of *ortho*-Fluoro Aromatic Carboxylic Acids with Alkynes

1.1. Introduction

The use of chelation-assistance is one of the more reliable strategies for activating, not only C–H bonds,[1] but other unreactive bonds, such as C–O,[2] C–N,[3] and C–F bonds[4,5] to achieve site-selective activation at specific positions. The reaction represents a topic of great interest in the field of organic chemistry. A wide variety of directing groups has been designed and used for developing new transformations that involve the activation of such strong and unreactive bonds. Among them, carboxylate directing groups are particularly advantageous, since they are widely available in great structural diversity and at low cost. In fact, carboxylic acids have been extensively used as a weakly coordinating or traceless directing group in C–H functionalization reactions.[6] To the best of our knowledge, a carboxylate directing group has not yet been used for activating unreactive bonds other than C–H bonds. Although carboxylate moieties readily bind to high oxidation state metal complexes through an anion exchange process, such as Ru(II), Rh(II) and Pd(II). The resulting complexes then activate C–H bonds through S_EAr or CMDS but a carboxylate anion typically does not readily interact with electron-rich low oxidation state complexes. If this were to occur, the complexes that are generated would be expected to participate in the oxidative addition of unreactive bonds, such as C–O and C–F bonds. We wish to report herein on the Ni-catalyzed [4+2] annulation of *ortho*-fluoro aromatic carboxylic acids with alkynes, leading to the production of 1*H*-isochromen-1-one derivatives, in which a carboxylate moiety functions as a directing group for the activation of C–F bonds and is then incorporated into the final product (Scheme 1).

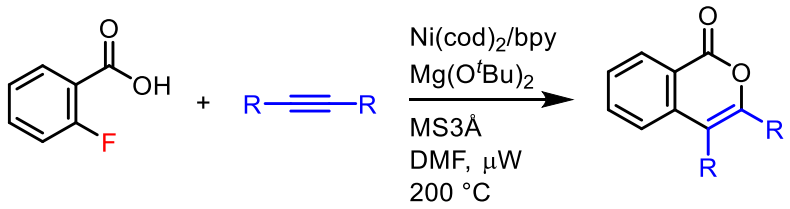

Scheme 1. Ni-catalyzed C-F/O-H annulation of 2-fluorobenzoic acids with internal alkynes.

1.2. Results and Discussion

The reaction of *ortho*-iodo aromatic acids with terminal alkynes leading to the production of 1*H*-isochromen-1-one derivatives was previously reported.[7] These reactions appear to proceed through Sonogashira-type coupling followed by the intramolecular cyclization of the resulting *ortho*-alkynylated products. Guo reported the $CuCl_2$-catalyzed reaction of *ortho*-halo aromatic acids with

acetylenedicarboxylate esters.[8] To the best of our knowledge, this is the only example of the production of 1*H*-isochromen-1-one derivatives by reactions of *ortho*-halo aromatic acids with internal alkynes. However, 4-octyne and diphenylacetylene were not applicable for the reaction. In addition, the reactivity of carboxylic acids decreased as follows I > Br > Cl and *ortho*-fluoro substrates were not examined.

Table 1. Optimization of reaction conditions.

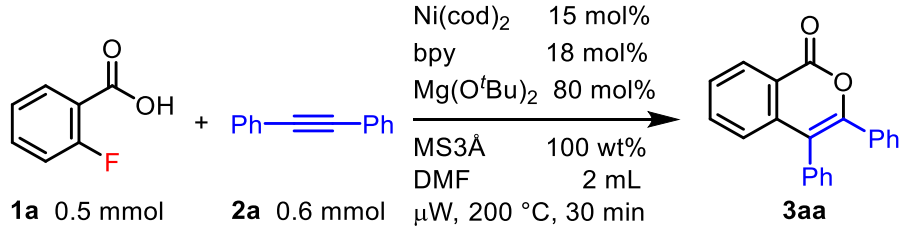

1a 0.5 mmol **2a** 0.6 mmol **3aa**

Entry	Deviations from the standard reaction conditions	NMR yields **3aa**/**1a** (%)
1	-	80 (77)/0
2	dtbpy in place of bpy	79/0
3	btfbpy in place of bpy	7/82
4	Me_4Phen in place of bpy	74/4
5	dmbpy in place of bpy	77/5
6	MS4Å in place of MS3Å	66/0
7	$Ni(cod)_2$ 0.05 mmol, Ligand 0.06 mmol	72/13
8	$Mg(O^tBu)_2$ 0.35 mmol	67/16
9	$Mg(O^tBu)_2$ 0.5 mmol	76/5
10	KO^tBu 0.5 mmol in place of $Mg(O^tBu)_2$	21/62
11	NaO^tBu 0.5 mmol in place of $Mg(O^tBu)_2$	27/61
12	1,4-dioxane in place of DMF	7/78
13	toluene in place of DMF	3/94
14	no catalyst	0/85
15	no ligand	1/84
16	no base	0/98
17	no MS3Å	70/5
18	No microwave irradiation, 160 °C, 24 h	70/18

A number in parentheses refers to isolated yield.

We recently reported the Ni-catalyzed reaction of 2-fluorobenzamides with alkynes using a base-promoted strategy, in which a C–F bond at the *ortho*-position is selectively activated under both mild

reaction and ligand-free conditions.[5d] We hypothesized that this strategy could also be used in reactions involving 2-fluorobenzoic acids. However, this was not that simple, probably because of the low coordination ability of the carboxylate anion to Ni(0), as we anticipated. No reaction occurred when the reaction of 2-fluorobenzoic acid (**1a**) was performed under the standard reaction conditions used in the previous report.[5d] After extensive experiments directed toward optimizing the reaction conditions using **1a** as the substrate, we determined the following conditions as standard reaction conditions (Table 1). The reaction of **1a** (0.5 mmol), diphenylacetylene (**2a**) (0.6 mmol), $Ni(cod)_2$ (15 mol%), bpy (2,2'-bipyridine, 18 mol%), $Mg(O^tBu)_2$ (0.4 mmol), MS3Å (100 wt%), in DMF (2 mL) under microwave irradiation (200 °C) for 30 min gave 3,4-diphenyl-1*H*-isochromen-1-one (**3aa**) in 80% NMR yield (entry 1). While the use of dtbpy (4,4'-di-tert-butyl-2,2'-dipyridyl), Me_4Phen (3,4,7,8-tetramethyl-1,10-phenanthroline), and dmbpy (4-4'-dimethoxy-2-2'-bipyridine) gave **3aa** in good yields (entries 2, 4, and 5), btfbpy (4,4'-bis(trifluoromethyl)-2,2'-bipyridine) was not effective as a ligand (entry 3). Decreasing the catalyst loading (10 mol%) resulted in a slight decrease in the product yield (entry 7). It was found that $Mg(O^tBu)_2$ was superior to KO^tBu or NaO^tBu as a base (entry 10 and 11), although the exact role of the Mg cation is not clear."

The use of a polar solvent was crucial for the reaction to proceed (entry 1 vs 12 and 13). When the reaction was carried out under no microwave irradiation conditions, the product yield was decreased (entry 18).

The scope of the reaction for *ortho*-fluorobenzoic acid derivatives bearing various substituents is shown in Scheme 2. The presence of an electron-donating group on the aromatic ring gave the corresponding products in good yields, as exemplified by **3ba**, **3ca**, and **3fa**. On the other hand, an electron-withdrawing group on the aromatic ring retarded the reaction. Even a sterically congested C–F bond was activated to give the **3ha** as the product. The reaction of 4-fluoronicotinic acid gave 3,4-diphenyl-1H-pyrano[3,4-c]pyridin-1-one **3ia**. The scope of alkynes was also investigated (Scheme 2). An alkyl-substituted alkyne, such as 6-dodecyne, also gave the corresponding 1*H*-isochromen-1-one **3ad** in 52% yield. The reaction with an unsymmetrical alkyne, such as 1-phenylpentyne gave the corresponding product **3ae** in a regioselective manner.

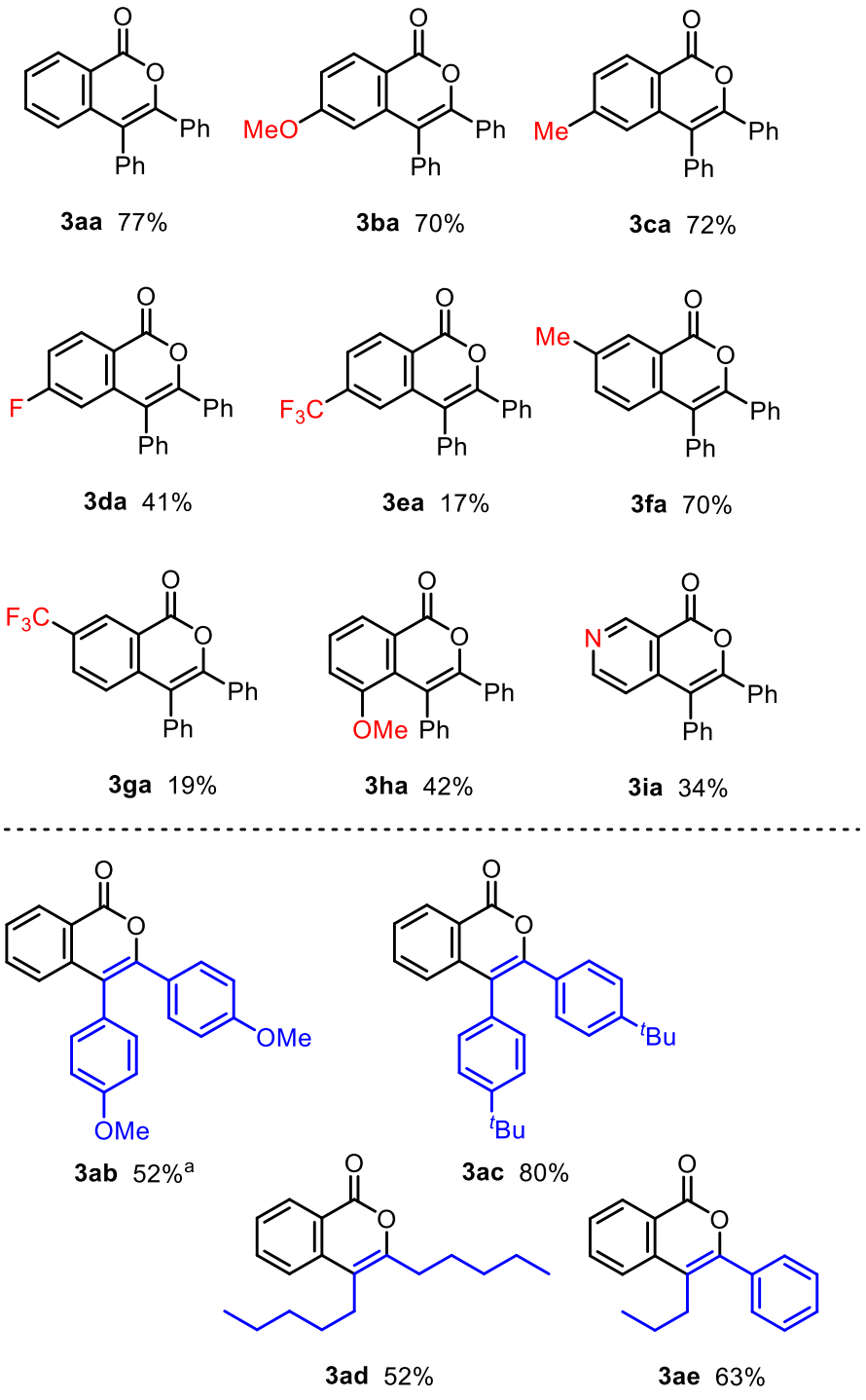

Scheme 2. Scope of the reaction. Reaction conditions: aromatic carboxylic acid 1 (0.5 mmol), alkyne 2 (0.6 mmol), Ni(cod)2 (0.075 mmol), bpy (0.09 mmol), MgOtBu2 (0.4 mmol), MS3Å (100 wt%), DMF (2 mL) under microwave irradiation (200 °C) for 30 min. [a] This compound was isolated by MPLC (Medium Pressure Liquid Chromatography) and then recrystallization.

We attempted to isolate the key oxanickelacycle intermediate from **1**, but all of these attempts to isolate an oxanickelacycle species failed. However, we were able to isolate a sample of the oxanickelacycle **4** by the reaction of phthalic anhydride with equimolar amounts of $Ni(cod)_2$ and dbbpy in THF at rt for 3 days and the structure of **4** was confirmed by an X-ray crystallographic analysis (Scheme 3a).[9] We used the complex **4** in further mechanistic studies. The reaction of the complex **4** with diphenylacetylene under the standard conditions in the absence of $Ni(cod)_2$ gave **3aa** in 67% yield (Scheme 3b). It was found that this reaction proceeded even in the absence of the base. In addition, the complex **4** showed catalytic activity. The use of **4** as a catalyst in place of $Ni(cod)_2$ gave **3aa** in 81% yield (Scheme 3c).

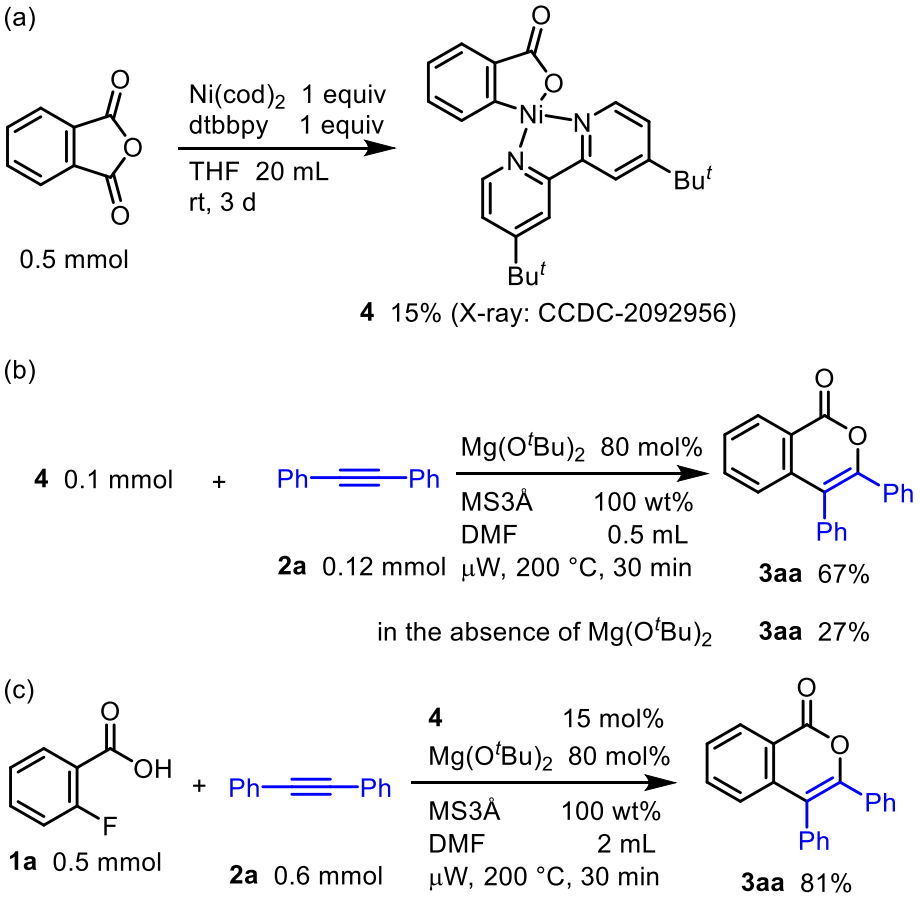

Scheme 3. Mechanistic studies.

A proposed mechanism for the above reaction is shown in Scheme 4. Deprotonation of the O-H proton in **1a** by $Mg(O^tBu)_2$ generates the carboxylate anion **A**. The reaction of **A** with Ni(0) gives the nickel ate complex **B**, in which a nickel center is sufficiently close to the ortho C–F bond to allow it to be activated. The cleavage of the ortho C–F bond gives the five-membered nickelacycle **C**. The

insertion of an alkyne into the C–Ni bond in **C** gives the seven-membered nickalacycle **D**. Reductive elimination gives the isochromen-1-one **3** with the regeneration of Ni(0). The presence of a base is essential for the reaction, indicating that the generation of **A** is key for the success of the reaction.

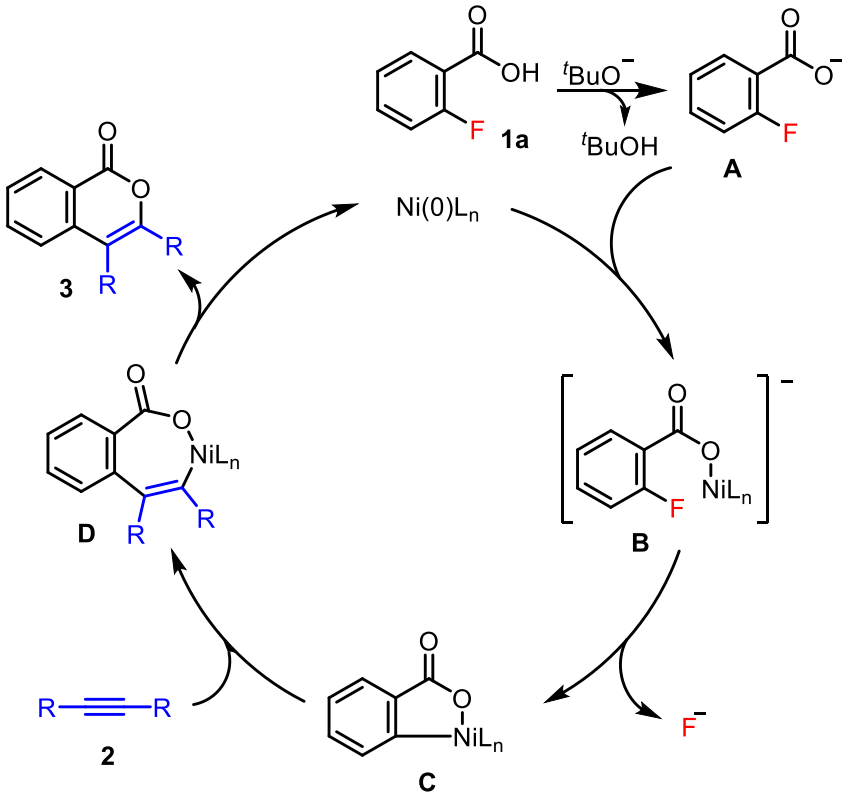

Scheme 4. Proposed mechanism.

1.3. Conclusion

In summary, we report herein the Ni-catalyzed C–F/O-H [4+2] annulation of *ortho*-fluoro-substituted aromatic acids with internal alkynes, leading to the production of isochromen-1-one derivatives, in which activation of C–F bond is a key step. To the best of our knowledge, this is the first example that a carboxylate directing group is used for activating unreactive bonds other than C–H bonds.[10] Studies of the use of this methodology are currently underway and will be reported in due course.[11]

1.4. Experimental Section

I. General Information

^{1}H, ^{13}C and ^{19}F NMR spectra were recorded on a JEOL ECZ-400S spectrometer in $CDCl_3$ with tetramethylsilane as an internal reference standard. The chemical shifts in ^{1}H NMR spectra were recorded relative to tetramethylsilane (δ: 0.0). The chemical shifts in ^{13}C NMR spectra were recorded relative to $CDCl_3$ (δ: 77.0). Data are given as follows: chemical shifts in ppm (δ), multiplicity (s =

singlet, d = doublet, t = triplet, q = quartet, brs = broad singlet, brd = broad doublet, m = multiplet, c = complex), coupling constant (Hz), and integration. Infrared spectra (IR) were recorded on a JASCO FT/IR-4000 spectrometer using the ATR method. Absorption data are reported in reciprocal centimeters from 800 to 3500 cm-1 with the following relative intensities: s (strong), m (medium), or w (weak). Mass spectra were obtained using a SHIMADZU QP-2010 spectrometer with a quadrupole mass analyzer at 70 eV. Data were recorded as follows: mass/charge ratio and relative intensity to base peak at 100%. High-resolution mass spectra (HRMS) were obtained using a JEOL JMS-T100LP spectrometer with a time-of-flight mass analyzer. Melting points were determined on a Stanford Research Systems MPA100 apparatus equipped with a digital thermometer and are uncorrected. Medium-pressure liquid chromatography (MPLC) was performed with Biotage Isolera®.

II. Materials

Toluene (super dehydrated), 1,4-dioxane (super dehydrated), DMF (super dehydrated), $Ni(cod)_2$, dtbpy, dtfbpy, Me_4Phen, dmbpy, $Mg(O^tBu)_2$, and KO^tBu were purchased and used as received. Bpy, benzoic acid (**1**), diphenylacetylene (**2a**) and phthalic anhydride were purchased and recrystallized from hexane and EtOAc before use. 6-Dodecyne (**2d**) and 1-phenyl-1-butyne (**2e**) were purchased and distilled over CaH_2 before use.

1,2-Bis (4-methoxyphenyl)ethyne (**2b**), 1,2-bis(4-tert-butyl)ethyne (**2c**), were prepared according to the reported procedure. [12]

III. General Procedure for the Ni-Catalyzed C–F/O-H Annulation with Alkynes

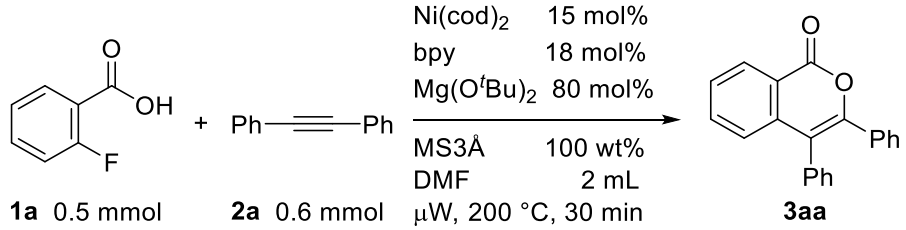

1a 0.5 mmol **2a** 0.6 mmol **3aa**

To an oven-dried 5 mL special microwave tube in a glove box, $Ni(cod)_2$ (21.7 mg, 0.075 mmol), bpy (14.1 mg, 0.09 mmol), $Mg(O^tBu)_2$ (68.2 mg, 0.4 mmol), 2-fluorobenzoic acid (**1a**, 104.1 mg, 0.5 mmol), diphenylacetylene (**2a**, 106.9 mg, 0.6 mmol), MS3Å (68.2 mg, 100 wt%), and DMF (2 mL) were added in sequential order. The mixture was stirred under microwave irradiation at 200 °C for 30 min and then allowed to cool to rt. The resulting mixture was washed with 1 M HCl aq. (5 mL) and extracted with EtOAc (30 mL). The organic layer was washed with water and filtered through a silica pad. The filtrate was concentrated to dryness in vacuo and the residue was purified by MPLC

(hexane/EtOAc = 8/1) to afford the desired product **3aa** (115.1 mg, 77%) as a white solid.

3,4-Diphenylisocoumarin (3aa) [CAS No. 1684-07-7]

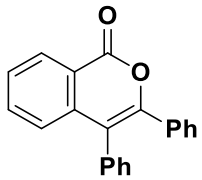

Yellow solid. Mp = 171.6-172.4 °C. R_f = 0.26 (hexane/EtOAc = 8/1). Yield = 77%, m = 115.1 mg.

^{1}H NMR (399.78 MHz, CDCl3) δ 7.15-7.27 (m, 6H), 7.33 (, 1.8Hz, 2H), 7.38-7.44 (m, 3H), 7.49-7.53 (c, 1H), 7.61-7.65 (c, 1H), 8.4 (dd, *J* = 7.8, 0.9 Hz, 1H).

^{13}C NMR (100.53 MHz, CDCl3) δ,116.8, 120.3, 125.3, 127.8, 128.0, 128.1, 128.9, 129.0, 129.1, 129.5, 131.1, 132.8, 134.2, 134.6, 138.8, 150.8, 162.2.

IR (ATR) 3059 w, 3025 w, 1734 s, 1723 s, 1077 m.

MS: *m/z* (EI, relative intensity, %) 299 (23), 298 (100, M^+), 270 (26), 221 (32), 165 (11), 105 (56), 77 (30).

HRMS ($[M+H]^+$) Calcd for $C_{21}H_{15}O_2$: 299.10666; Found: 299.10614.

6-Methoxy-3,4-diphenylisocoumarin (3ba) [CAS No. 56412-81-8]

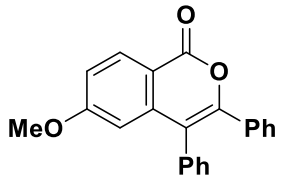

Yellow solid. Mp = 176.9-177.6 °C. R_f = 0.25 (hexane/EtOAc = 8/1). Yield = 70%, m = 121.8 mg.

^{1}H NMR (399.78 MHz, CDCl3) δ 3.73 (s, 3H), 6.57 (d, *J* = 2.3 Hz, 1H), 7.04 (dd, *J* = 8.9, 2.5 Hz, 1H), 7.15-7.22 (m, 3H), 7.23-7.26 (m, 2H), 7.30-7.33 (m, 2H), 7.37-7.43 (m, 3H), 8.32 (d, *J* = 8.7 Hz, 1H).

^{13}C NMR (100.53 MHz, CDCl3) δ 55.4, 108.3, 113.5, 115.5, 116.7, 127.7, 128.0, 128.8, 129.0, 129.1, 131.1, 131.8, 132.9, 134.2, 141.1, 151.4, 161.9, 164.5.

IR (ATR) 3057 w, 3026 w, 2965 w, 2934 w, 2842 w, 1725 s, 1604 s, 1262 s, 1074 m.

MS: *m/z* (EI, relative intensity, %) 329 (24), 328 (100, M^+), 300 (20), 251 (34), 105 (54), 78 (24.

HRMS ($[M+H]^+$) Calcd for $C_{22}H_{17}O_3$: 329.11722; Found: 329.11717.

6-Methyl-3,4-diphenyl-1*H*-2-benzopyran-1-one (3ca) [CAS No. 935762-75-7]

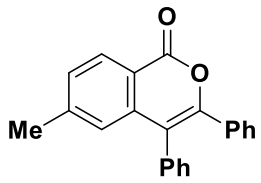

Yellow solid. Mp = 185.5-186.1 °C. R_f = 0.26 (hexane/EtOAc = 10/1). Yield = 72%, m = 114.6 mg.

^{1}H NMR (399.78 MHz, CDCl3) δ 2.37 (s, 3 H), 6.97 (br, 1H), 7.16-7.27(m, 6H), 7.30-7.35(m, 3H), 7.40-7.44(m, 3H), 8.30 (d, *J* = 8.0 Hz, 1H).

^{13}C NMR (100.53 MHz, CDCl3) δ 22.2, 116.8, 118.0, 125.2, 127.8, 128.0, 128.8, 129.0, 129.2, 129.5, 129.6, 131.2, 133.0, 134.4, 138.8, 145.7, 151.0, 162.3.

IR (ATR) 3057 w, 2914 w, 2850 w, 1726 s, 1073 m.

MS: *m/z* (EI, relative intensity, %) 313 (23), 312 (100, M^+), 284 (21), 235 (31), 105 (50), 77 (21), 69 (16).

HRMS ($[M+H]^+$) Calcd for $C_{22}H_{17}O_2$: 313.12231; Found: 313.12163.

6-Fluoro-3,4-diphenylisocoumarin (3da) [CAS No. 1493899-37-8]

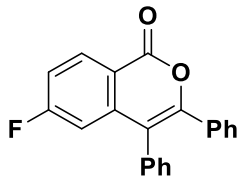

Yellow solid. Mp = 154.8-155.5 °C. R_f = 0.5 (hexane/EtOAc = 8/1). Yield = 41%, m = 65.5 mg.

^{1}H NMR (399.78 MHz, $CDCl_3$) δ 6.84 (dd, J = 10.2, 2.4 Hz, 1H), 7.17-7.28 (m, 6H), 7.32-7.35 (m, 2H), 7.41-7.46 (m, 3H), 8.42 (dd, J = 8.9, 5.7 Hz, 1H).

^{13}C NMR (100.53 MHz, $CDCl_3$) δ 111.3(d, *J* = 24.0 Hz), 116.3 (d, *J* = 23.0 Hz), 116.3(d, *J* = 2.9 Hz), 116.8(d, *J* = 1.9 Hz), 116.8, 116.8, 127.9, 128.4, 129.2, 129.2, 131.0, 132.5, 132.8(d, *J* = 9.6 Hz), 133.7, 141.8(d, *J* = 9.9 Hz), 152.1, 161.3, 166.7(d, *J* = 253.9 Hz).

^{19}F NMR (376.17 MHz, $CDCl_3$) δ -101.6.

IR (ATR) 3060 w, 3020 w, 1735 s, 1610 m, 1253 m, 1073 m.

MS: *m/z* (EI, relative intensity, %) 317 (12), 316 (100, M^+), 288 (10), 241 (28), 239 (29), 167 (23), 105 (54), 77 (32).

HRMS ($[M+H]^+$) Calcd for $C_{21}H_{14}O_2F$: 317.09723; Found: 317.09720.

6-Trifluoromethyl-3,4-diphenylisocoumarin (3ea) [CAS No. 944938-36-7]

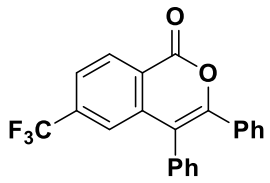

Yellow solid. Mp = 191.5-191.9 °C. R_f = 0.50 (hexane/EtOAc = 8/1). Yield = 17%, m = 37.1 mg.

^{1}H NMR (399.78 MHz, $CDCl_3$) δ 7.19-7.29 (m, 5H), 7.32-7.35 (m, 2H), 7.42-7.48 (m, 4H), 7.74 (dd, *J* = 8.2, 1.1 Hz, 1H), 8.53 (d, *J* = 8.2 Hz, 1H).

^{13}C NMR (100.53 MHz, $CDCl_3$) δ 116.3, 122.4 (q, *J* = 3.8 Hz), 122.7, 123.2 (q, *J* = 272 Hz), 124.3 (q, *J* = 3.8 Hz), 128.0, 128.6, 129.2, 129.4, 130.6, 131.0, 132.3, 133.2, 136.1 (q, *J* = 32.6 Hz), 139.3, 152.3, 161.1, one signal is obscured by overlap with other signals.

^{19}F NMR (376.17 MHz, $CDCl_3$) δ -63.2.

IR (ATR) 3062 w, 2923 w, 2853 w, 1736 s, 1610 m, 1316 m, 1125 s.

MS: *m/z* (EI, relative intensity, %) 367 (15), 366 (100, M^+), 338 (17), 289 (23), 105 (55), 77 (27).

HRMS ($[M+H]^+$) Calcd for $C_{22}H_{14}O_2F_3$: 367.09404; Found: 367.09339.

7-Methyl-3,4-diphenyl-1*H*-2-benzopyran-1-one (3fa) [CAS No. 93743-65-8]

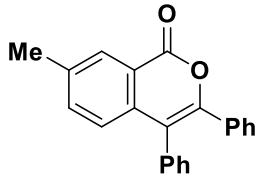

Yellow solid. Mp = 174.9-175.8 °C. R_f = 0.48 (hexane/EtOAc = 8/1). Yield = 70%, m = 109.6 mg.

^{1}H NMR (399.78 MHz, $CDCl_3$) δ 2.46 (s, 3H), 7.09 (d, *J* = 8.2 Hz, 1H), 7.15-7.21 (m, 3H), 7.22-7.26 (m, 2H), 7.31-7.34 (m, 2H), 7.38-7.45 (m, 4H), 8.21 (c, 1H).

^{13}C NMR (100.53 MHz, $CDCl_3$) δ 21.2, 116.8, 120.2, 125.3, 127.7, 128.0, 128.7, 128.9, 129.1, 129.2, 131.1, 132.9, 134.4, 135.8, 136.3, 138.4, 150.0, 162.4.

IR (ATR) 3058 w, 3023 w, 1725 s, 1495 m, 694 m.

MS: *m/z* (EI, relative intensity, %) 313 (24), 312 (100, M^+), 284 (18), 235 (34), 105 (50), 77 (19).

HRMS ($[M+H]^+$) Calcd for $C_{22}H_{17}O_2$: 313.12231; Found: 313.12193.

7- Trifluoromethyl-3,4-diphenyl-1*H*-2-benzopyran-1-one (3ga) [CAS No. 2095700-24-4]

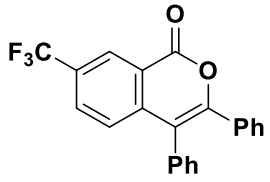

Yellow solid. Mp = 126.1-127.2 °C. R_f = 0.58 (hexane/EtOAc = 8/1). Yield = 19%, m = 36.4 mg.

^{1}H NMR (399.78 MHz, $CDCl_3$) δ 7.19-7.30 (m, 5H), 7.32-7.36 (m, 3H), 7.43-7.46 (m, 3H), 7.83 (ddd, *J* = 8.5, 2.1, 0.5 Hz, 1H), 8.68 (q, *J* = 0.7 Hz, 1H).

^{13}C NMR (100.53 MHz, $CDCl_3$) δ 116.2, 120.4, 123.4 (q, *J* = 271 Hz), 126.2, 127.0 (q, *J* = 3.8 Hz), 128.0, 128.5, 129.2, 129.3, 129.5, 130.0 (q, *J* = 33.5 Hz), 130.8 (q, *J* = 2.8 Hz), 131.0, 132.2, 133.5, 141.6, 152.9, 161.2.

^{19}F NMR (376.17 MHz, $CDCl_3$) δ -62.6.

IR (ATR) 3059 w, 3023 w, 1744 s, 1317 s, 1132 s, 697 m.

MS: *m/z* (EI, relative intensity, %) 367 (21), 366 (100, M^+), 338 (26), 289 (30), 105 (58), 177 (37).

HRMS ($[M+H]^+$) Calcd for $C_{22}H_{14}O_2F_3$: 367.09404; Found: 367.09372.

5-Methoxy-3,4-diphenyl-1*H*-2-benzopyran-1-one (3ha) [CAS No. 1975152-79-4]

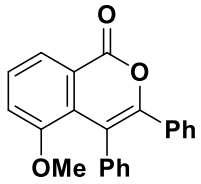

3ha

White solid. Mp = 174.3-174.9 °C. R_f = 0.25 (hexane/EtOAc = 10/1). Yield = 42%, m = 68.2 mg.

^{1}H NMR (399.78 MHz, $CDCl_3$) δ 3.34 (s, 3H), 7.11-7.25 (m, 12H), 7.47 (t, *J* = 8.0 Hz, 1H), 8.05 (dd, *J* = 7.8, 1.1 Hz, 1H).

^{13}C NMR (100.53 MHz, $CDCl_3$) δ 56.0, 115.6, 117.6, 122.0, 122.2, 126.8, 127.4, 127.7, 127.8, 128.6, 129.2, 129.7, 130.7, 132.5, 133.6, 137.8, 151.0, 156.2, 162.4.

IR (ATR): 3056 w, 3023 w, 2929 w, 2836 w, 1726 s, 1271 m.

MS: *m/z* (EI, relative intensity, %): 329 (23), 328 (100, M^+), 297 (15), 251 (21), 250 (15), 105 (65), 77 (22).

HRMS ($[M+H]^+$) Calcd for $C_{22}H_{17}O_2$: 329.11722; Found: 329.11677.

3,4-Diphenyl-1*H*-Pyrano[3,4-*c*]pyridin-1-one (3ia)

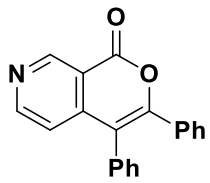

Brown solid. Mp = 143.1-143.7 °C. R_f = 0.20 (hexane/EtOAc = 8/1). Yield = 34%, m = 50.1 mg.

^{1}H NMR (399.78 MHz, $CDCl_3$) δ 7.20-7.31 (m, 5H), 7.32-7.36 (m, 2H), 7.43-7.49 (m, 3H), 8.15 (dd, *J* = 5.3, 0.9 Hz, 1H), 8.65 (d, *J* = 0.7 Hz, 1H), 8.79 (d, *J* = 5.0 Hz, 1H).

^{13}C NMR (100.53 MHz, $CDCl_3$) δ 114.7, 120.9, 125.7, 128.0, 128.6, 129.2, 129.4, 129.5, 131.0, 132.1,

132.5, 148.4, 148.6, 152.5, 160.8.

IR (ATR) 3055 w, 3029 w, 1744 s, 1079 m, 764 m, 693 m.

MS: *m/z* (EI, relative intensity, %) 300 (15), 299 (100, M^+), 298 (25), 271 (10), 105 (31), 77 (18), 69 (20).

HRMS ($[M+H]^+$) Calcd for $C_{20}H_{14}NO_2$: 300.10191; Found: 300.10171.

3,4-Bis(4-methoxyphenyl)-1*H*-2-benzopyran-1-one (3ab) [CAS No. 123290-68-6]

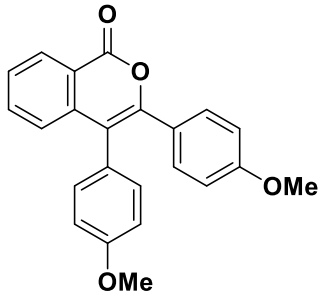

This compound was isolated by MPLC and then recrystallization from EtOAc/hexane. White solid. Mp = 162.3-162.7 °C. R_f = 0.28 (hexane/EtOAc = 10/1). Yield = 52%, m = 93.2 mg.

^{1}H NMR (399.78 MHz, $CDCl_3$) δ 3.78 (s, 3H), 3.87 (s, 3H), 6.71-6.75 (m, 2H), 6.95-6.99 (m, 2H), 7.16-7.22 (m, 3H), 7.28-7.32 (m, 2H), 7.47-7.51 (m, 1H), 7.60-7.64 (m, 1H), 8.38 (dd, J = 7.8, 1.1 Hz, 1H).

^{13}C NMR (100.53 MHz, $CDCl_3$) δ 55.2, 55.3, 113.3, 114.6, 115.3, 120.2, 125.1, 125.4, 126.6, 127.6, 129.4, 130.6, 132.3, 134.5, 139.4, 150.8, 159.2, 159.8, 162.4.

IR (ATR): 3072 w, 3006 w, 2957 w, 2909 w, 2837 w, 1724 s, 1602 m, 1249 s.

MS: *m/z* (EI, relative intensity, %): 359 (23), 358 (100, M^+), 331 (16), 330 (86), 315 (49), 135 (27), 69 (12).

HRMS ($[M+H]^+$) Calcd for $C_{22}H_{17}O_2$: 359.12779; Found: 359.12845.

3,4-Bis[4-(1,1-dimethylethyl)phenyl]-1*H*-2-benzopyran-1-one (3ac) [CAS No. 2267265-57-4]

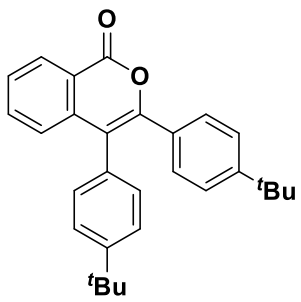

Brown solid. Mp = 179.5-181.0 °C. R_f = 0.50 (hexane/EtOAc = 8/1). Yield = 80%, m = 164.9 mg.

^{1}H NMR (399.78 MHz, $CDCl_3$) δ 1.26 (s, 9H), 1.38 (s, 9H), 7.18-7.20 (m, 5H), 7.27 (m, 2H), 7.43-

7.50 (m, 3H), 7.59-7.63 (c, 1H), 8.38 (dd, *J* = 8.0, 1.1 Hz, 1H).

^{13}C NMR (100.53 MHz, $CDCl_3$) δ 31.1, 31.3, 34.6, 34.6, 116.3, 120.2, 124.7, 125.4, 125.9, 127.7, 128.7, 129.3, 130.0, 130.7, 131.3, 134.4, 139.3, 150.7, 151.1, 151.9, 162.3

IR (ATR) 3072 w, 3026 w,2962 m, 2904 w, 2868 w, 1739 s, 1721 s, 1480 m, 773 m, 754 m.

MS: *m/z* (EI, relative intensity, %) 411 (17), 410 (76, M^+), 395 (10), 355 (20), 354 (100).

HRMS ($[M+H]^+$) Calcd for $C_{29}H_{31}O_2$: 411.23186; Found: 411.23143.

3,4-Dipentyl-1*H*-2-benzopyran-1-one (3ad) [CAS No. 1975152-85-2]

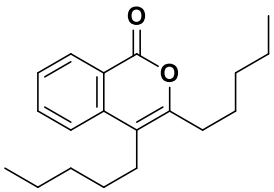

Yellow oil. R_f = 0.14 (hexane/EtOAc = 8/1). Yield = 52%, m = 73.4 mg.

^{1}H NMR (399.78 MHz, $CDCl_3$) δ 0.89-0.95 (m, 6H), 1.34-1.42 (m, 8H), 1.52-1.59 (m, 2H), 1.68-1.75 (m, 2H), 2.56-2.62 (m, 4H), 7.43-7.47 (c, 1H), 7.52 (d, *J* = 8.0 Hz, 1H), 7.71-7.75 (c, 1H), 8.31 (dt, *J* = 8.6, 0.7 Hz, 1H).

^{13}C NMR (100.53 MHz, $CDCl_3$) δ 13.9, 14.0, 22.4, 22.5, 26.2, 27.6, 29.4, 30.8, 31.5, 31.9, 112.2, 120.8, 122.6, 127.0, 129.8, 134.5, 138.0, 154.2, 162.9

IR (ATR) 2955 w, 2928 m, 2859 w, 1725 s, 1083 m, 769 m.

MS: *m/z* (EI, relative intensity, %) 287 (23), 286 (100, M^+), 230 (13), 229 (76), 211 (14), 173 (93), 147 (33), 145 (24), 131 (38), 117 (13), 115 (13).

HRMS ($[M+H]^+$) Calcd for $C_{19}H_{27}O_2$: 287.20056; Found: 287.20083.

3-Phenyl-4-propyl-1*H*-2-benzopyran-1-one (3ae) [CAS No. 1458720-54-1]

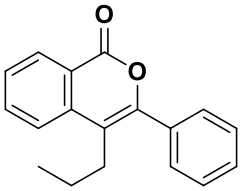

Yellow solid. Mp = 96.8-97.5 °C. R_f = 0.40 (hexane/EtOAc = 8/1). Yield = 63%, m = 82.9 mg.

^{1}H NMR (399.78 MHz, $CDCl_3$) δ 0.95 (t, J = 7.4 Hz, 3H), 1.63-1.72 (c, 2H), 2.63-2.67 (c, 2H), 7.44-7.49 (m, 3H), 7.52-7.57 (m, 3H), 7.64 (d, J = 7.8 Hz, 1H), 7.79 (c, 1H), 8.38-8.40 (c, 1H).

^{13}C NMR (100.53 MHz, $CDCl_3$) δ 14.1, 23.3, 28.9, 113.9, 121.2, 123.5, 127.8, 128.3, 129.1, 129.3, 129.9, 133.5, 134.6, 137.9, 151.6, 162.4.

IR (ATR) 3061 w, 2959 w, 2931 w, 2872 w, 1721 s, 1485 m, 1094 m, 763 m, 697 m.

MS: *m/z* (EI, relative intensity, %) 265 (17), 264 (81, M^+), 236 (13), 235 (70), 208 (6), 207 (100), 179 (15), 178 (28), 105 (16), 77 (32).

HRMS ($[M+H]^+$) Calcd for $C_{18}H_{17}O_2$: 265.12231; Found: 265.12208.

IV. Procedure for the Preparation of Nickelalactone 4

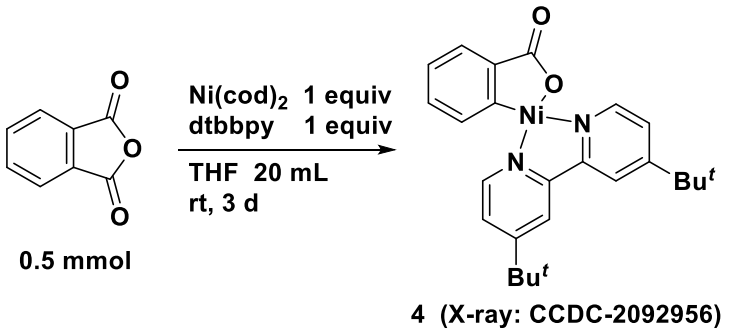

To an oven-dried 13.5 mL screw-capped vial in a glove box, $Ni(cod)_2$ (137.6mg, 0.5 mmol), dtbbpy (134.2 mg, 0.5 mmol), phthalic anhydride (77.4 mg, 0.5 mmol) and THF (4 mL) were added in sequential order. The mixture was stirred at rt for 3 days in the glove box. The nickelalactone precipitated as red microcrystals, which were collected on a Kiriyama funnel, washed with THF to afford the desired product **4** (33.8 mg, 15%) as a red solid. **^{1}H NMR** (399.78 MHz, CD_2Cl_2) δ 1.43 (d, J = 7.3 Hz, 18H), 7.08 (m , 2H), 7.17 (m, 2H), 7.46-7.48 (c, 1H), 7.57 (c, 1H), 7.84 (c, 1H), 7.93 (c, 1H), 8.73-8.76 (m, 2H)

V. The Reaction of the Complex 4 with Diphenylacetylene

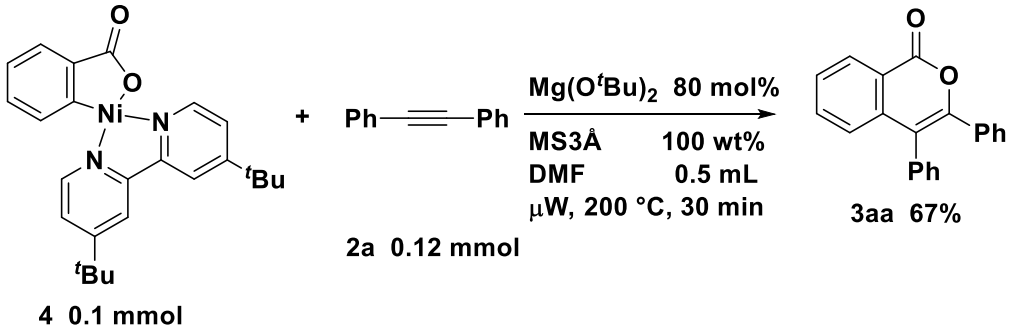

To an oven-dried 4 mL special microwave tube in a glove box, **4** (44.7mg, 0.01 mmol), $Mg(O^tBu)_2$ (13.6 mg, 0.08 mmol), diphenylacetylene (**2a**, 21.4 mg, 0.12 mmol), MS3Å (13.6 mg, 100 wt%), and DMF (0.5 mL) were added in sequential order. The mixture was stirred under microwave irradiation at 200 °C for 30 min and then allowed to cool to rt. The resulting mixture was washed with 1 M HCl aq. (5 mL) and extracted with EtOAc (30 mL). The organic layer was washed with water and filtered

through a silica pad. The filtrate was concentrated to dryness in vacuo and the residue was purified by MLPC (hexane/EtOAc = 8/1) to afford the desired product **3aa** (19.6 mg, 67%) as a white solid.

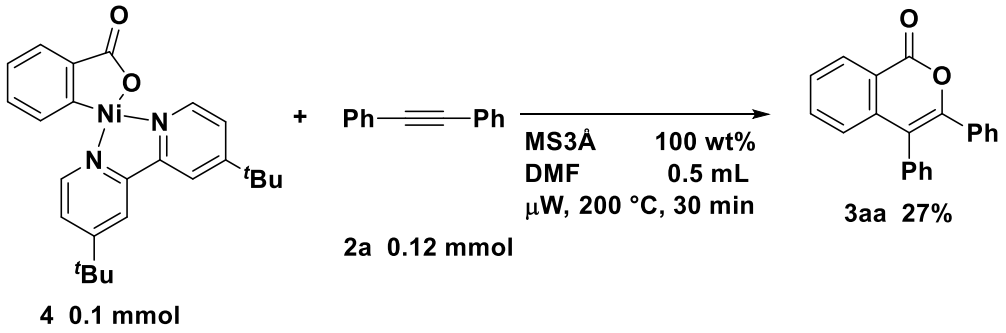

To an oven-dried 4 mL special microwave tube in a glove box, **4** (44.7mg, 0.01 mmol), diphenylacetylene (**2a**, 21.4 mg, 0.12 mmol), MS3Å (13.6 mg, 100 wt%), and DMF (0.5 mL) were added in sequential order. The mixture was stirred under microwave irradiation at 200 °C for 30 min and then allowed to cool to rt. The resulting mixture was washed with 1 M HCl aq. (5 mL) and extracted with EtOAc (30 mL). The organic layer was washed with water and filtered through a silica pad. The filtrate was concentrated and dried in vacuo to obtain the desired product in 27% NMR yield.

VI. The Use of Complex 4 in Catalytic Reaction

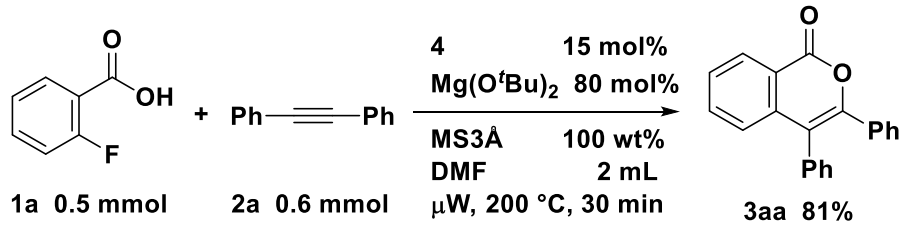

To an oven-dried 5 mL special microwave tube in a glove box, **4** (33.5mg, 0.075 mmol), $Mg(O^tBu)_2$ (68.2 mg, 0.4 mmol), 2-fluorobenzoic acid (**1a**, 104.1 mg, 0.5 mmol), diphenylacetylene (**2a**, 106.9 mg, 0.6 mmol), MS3Å (68.2 mg, 100 wt%), and DMF (2 mL) were added in sequential order. The mixture was stirred under microwave irradiation at 200 °C for 30 min and then allowed to cool to rt. The resulting mixture was washed with 1 M HCl aq. (5 mL) and extracted with EtOAc (30 mL). The organic layer was washed with water and filtered through a silica pad. The filtrate was concentrated to dryness in vacuo and the residue was purified by MLPC (hexane/EtOAc = 8/1) to afford the desired product **3aa** (121.1 mg, 81%) as a white solid.

VII. X-ray Crystallographic Data

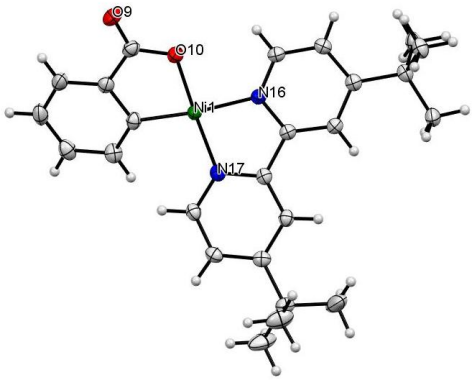

Plots are drawn at 50% probability level.

Crystal Data

Identification code	**4**
Empirical formula	$C_{25}H_{28}N_2NiO_2$
Formula weight	447.20
Temperature/K	123
Crystal system	orthorhombic
Space group	Pbca
a/Å	16.2551 (2)
b/Å	15.2146 (2)
c/Å	17.4643 (2)
α/°	90
β/°	90
γ/°	90
Volume/Å^3	4319.18 (9)
Z	8
ρcalcg/cm^3	1.375
μ/mm^{-1}	1.478
F(000)	1888.0
Crystal size/mm^3	0.122 × 0.069 × 0.051
Radiation	Cu Kα (λ = 1.54184)
2Θ range for data collection/°	9.436 to 148.562
Index ranges	$-20 \leq h \leq 19$, $-18 \leq k \leq 15$, $-21 \leq l \leq 21$
Reflections collected	24686
Independent reflections	4350 [R_{int} = 0.0450, R_{sigma} = 0.0377]

Data/restraints/parameters	4350/0/277
Goodness-of-fit on F^2	1.045
Final R indexes [I>=2σ (I)]	R_1 = 0.0378, wR2 =0.1055
Final R indexes [all data]	R_1 = 0.0414, wR2 = 0.1087
Largest diff. peak/hole / e $Å^{-3}$	0.52/-0.26

Experimental

Single crystals of $C_{25}H_{28}N_2NiO_2$ **4** were CCDC-2092956. A suitable crystal was selected and CCDC-2092956 on a Rigaku XtaLAB P200 diffractometer using multi-layer mirror monochromated Cu-Kα radiation. The crystal was kept at 123 K duringdata collection.Using Olex2,[13] the structure was solved with the SHELXT[14] structure solution programusingIntrinsic Phasingand refined with the SHELXL refinement package usingLeast Squaresminimisation.

1.5. References

(1) For selected recent reviews on transition metal-catalyzed directed C–H bond functionalization, see: (a) Sambiagio, C.; Schönbauer, D.; Blieck, R.; Dao-Huy, T.; Pototschnig, G.; Schaaf, P.; Wiesinger, T.; Zia, M. F.; Wencel-Delord, J.; Besset, T.; Maes, B. U. W.; Schnürch, M. *Chem. Soc. Rev.* **2018**, *47*, 6603–6743. (b) Dey, A.; Sinha, S. K.; Achar, T. K.; Maiti, D. *Angew. Chem. Int. Ed.* **2019**, *58*, 10820–10843. (c) Gandeepan, P.; Müller, T.; Zell, D.; Cera, G.; Warratz, S.; Ackermann, L. *Chem. Rev.* **2019**, *119*, 2192–2452. (d) Rej, S.; Ano, Y.; Chatani, N. Bidentate *Chem. Rev.* **2020**, *120*, 1788–1887. (e) Higham, J. I.; Bull, J. A. *Org. Biomol. Chem.* **2020**, *18*, 7291–7315.

(2) For recent selected papers on chelation-assisted C–O functionalization, see: (a) Cong, X.; Tang, H.; Zeng, X. *J. Am. Chem. Soc.* **2015**, *137*, 14367–14372. (b) Zhao, Y.; Snieckus, V. *Chem. Commun.* **2016**, *52*, 1681–1684. (c) Kondo, H.; Kochi, T.; Kakiuchi, F. *Org. Lett.* **2017**, *19*, 794–797. (d) Purohit, P.; Seth, K.; Kumar, A.; Chakraborti, A. K. *ACS Catal.* **2017**, *7*, 2452–2457. (e) Tang, J.; Liu, L. L.; Yang, S.; Cong, X.; Luo, M.; Zeng, X. *J. Am. Chem. Soc.* **2020**, *142*, 7715–7720. (f) Ambre, R.; Wang, T.-H.; Xian, A.; Chen, Y.-S.; Liang, Y.-F.; Jurca, T.; Zhao, L.; Ong, T.-G. *Chem. –Euro. J.* **2020**, *26*, 17021–17026. (g) Iyori, Y.; Ueno, R.; Morishige, A.; Chatani, N. *Chem. Sci.* **2021**, *12*, 1772–1777. (h) Iyori, Y.; Chatani, N. *Chem. Lett.* **2021**, *50*, 510–512.

(3) For recent selected papers on chelation-assisted C–N functionalization, see: (a) Cong, X.; Fan, F.; Ma, P.; Luo, M.; Chen, H.; Zeng, X. *J. Am. Chem. Soc.* **2017**, *139*, 15182–15190. (b) Zhao, Q.; Zhang, J.; Szostak, M. *ACS Catal.* **2019**, *9*, 8171–8177. (c) Xu, J.-X.; Zhao, F.; Yuan, Y.; Wu, X.-F. *Org. Lett.* **2020**, *22*, 2756–2760. (d) Tang, J.; Fan, F.; Cong, X.; Zhao, L.; Luo, M.; Zeng, X. *J. Am. Chem. Soc.* **2020**, *142*, 12834–12840.

(4) For reviews on C–F activation, see: (a) Ahrens, T.; Kohlmann, J.; Ahrens, M.; Braun, T. *Chem. Rev.* **2015**, *115*, 931–972. (b) Ahrens, T.; Kohlmann, J.; Ahrens, M.; Braun, T. *Chem. Rev.* **2015**, *115*, 931–972. (c) Fu, L.; Chen, Q.; Nishihara, Y. R *The Chem. Rec.* **2021**, *21*, 3394–3410. (d) Das, A.; Chatani, N. *ACS Catal.* **2021**, *11*, 12915–12930.

(5) For recent selected papers on chelation-assisted C–F functionalization, see: (a) Sun, A. D.; Leung, K.; Restivo, A. D.; LaBerge, N. A.; Takasaki, H.; Love, J. A. *Chem. –Euro. J.* **2014**, *20*, 3162–3168. (b) Guo, W.-H.; Min, Q.-Q.; Gu, J.-W.; Zhang, X. *Angew. Chem., Int. Ed.* **2015**, *54*, 9075–9078. (c) Capdevila, L.; Meyer, T. H.; Roldán-Gómez, S.; Luis, J. M.; Ackermann, L.; Ribas, X. *ACS Catal.* **2019**, *9*, 11074–11081. (d) Nohira, I.; Liu, S.; Bai, R.; Lan, Y.; Chatani, N. *J. Am. Chem. Soc.* **2020**, *142*, 17306–17311. (e) Nohira, I.; Chatani, N. *ACS Catal.* **2021**, *11*, 4644–4649. (f) Zhang, T.; Nohira, I.; Chatani, N. *Org. Chem. Front.* **2021**, *8*, 3783–3787. (g) Kawakami, H.; Nohira, I.; Chatani, N. *Synthesis* **2021**, *53*, 3075–3080.

(6) For recent reviews on the use of carboxylic acids as a directing group, see: (a) Pichette Drapeau, M.; Gooßen, L. J. *Chem. –Euro. J.* **2016**, *22*, 18654–18677. (b) Das, A.; Maji, B. *Chem. –Euro. J.* **2021**, *16*, 397–408. (c) Das, J.; Mal, D. K.; Maji, S.; Maiti, D. *ACS Catal.* **2021**, *11*, 4205–4229.

(7) (a) Subramanian, V.; Batchu, V. R.; Barange, D.; Pal, M. *J. Org. Chem.* **2005**, *70*, 4778–4783. (b) Kumar, M. R.; Irudayanathan, F. M.; Moon, J. H.; Lee, S. *Adv. Synth. Catal.* **2013**, *355*, 3221–3230. (c) Tyagi, A.; Reshi, N. U. D.; Daw, P.; Bera, J. K. *Dalton Trans.* **2020**, *49*, 15238–15248. (d) Kotora, M.; Ishikawa, M.; Tsai, F.-Y.; Takahashi, T. *Tetrahedron* **1999**, *55*, 4969–4978.

(8) Guo, X.-X. *J. Org. Chem.* **2013**, *78*, 1660–1664.

(9) A similar nickel complex ligated by bpy was prepared by an oxidative addition followed by decarbonylation of phthalic anhydride on $Ni(acac)_2$/bpy/Et_3Al or Ni(cod)(bpy). (a) Fischer, R.; Walther, D.; Braunlich, G.; Undeutsch, B.; Ludwig, W.; Bandmann, H. *J. Organomet. Chem.* **1992**, *427*, 395–407. (b) Langer, J.; Gärtner, M.; Görls, H.; Walther, D. *Synthesis* **2006**, *2006*, 2697–2706.

(10) Pd-catalyzed cross-coupling reactions of aryl fluorides bearing an *ortho*-carboxylate group had been previously reported. However, the substrates required an additional nitro group at the *para*-position to the C–F bond for the cross-coupling to occur. Bahmanyar, S.; Borer, B. C.; Kim, Y. M.; Kurtz, D. M.; Yu, S. *Org. Lett.* **2005**, *7*, 1011–1014.

(11) The present system was applicable to the activation of C–O bonds. Iyori, Y.; Ueno, R.; Morishige, A.; Chatani, N. *Chem. Sci.* **2021**, *12*, 1772–1777.

(12) Chu, H.; Cheng, J.; Yang, J.; Guo, Y.-L.; Zhang, J. *Angew. Chem., Int. Ed.* **2020**, *59*, 21991–21996.

(13) Dolomanov, O.V.; Bourhis, L.J.; Gildea, R.J; Howard, J.A.K.; Puschmann, H.; *J. Appl. Cryst.*, **2009**, *42*, 339.

(14) Sheldrick, G.M.; *Acta Cryst.*, **2015**, *A71*, 3.

Chapter 2

Nucleophilic aromatic substitution of non-activated aryl fluorides with aliphatic amides

2.1. Introduction

Nucleophilic aromatic substitution (S_NAr) reactions of aryl halides via the formation of a Meisenheimer complex is one of the classical and fundamental reactions in organic synthesis to achieve the ipso substitution of arenes.[1] While aryl fluorides have been extensively used as a substrate in S_NAr reactions,[2] the introduction of strong electron-withdrawing groups on the aryl fluoride is generally required to promote the reaction.[3] However, the number of examples of unusual S_NAr reactions which probably proceeds through a concerted S_NAr reaction mechanism are continuously increasing.[4,5] In fact, S_NAr reactions of unactivated aryl fluorides with heteroatom nucleophiles, such as oxygen,[6] nitrogen,[6,7] silicon,[8] and phosphorus atoms[9] have recently become subjects of interest. On the other hand, the use of carbon nucleophiles in S_NAr reactions of non-activated aryl fluorides continues to be rare. In 2000, Caron reported the S_NAr reaction of neutral- and non-activated aryl fluorides with secondary alkyl nitriles.[10] They also demonstrated that amides, esters, and ketones cannot be used in the reaction. In 2015, Cao reported the use of carbanions generated from diarylmethanes[11] and indenes[12] as carbon nucleophiles in S_NAr reactions of non-activated aryl fluorides. In 2017, Ichikawa extended Caron's work using π-extended aromatic fluorides as substrates, which are relatively more reactive than simple aryl fluorides.[13] In 2020, Ohmiya reported the S_NAr reaction of neutral aryl fluorides with tertiary carbanions which are generated from organoboronates with an alkoxide base.[14] While some examples have appeared, the use of carbon nucleophiles still remains an undeveloped area of research. In 2018, Pliego, on the basis of DFT calculations, proposed that the arylation of enolates with unactivated arenes would be possible if the solvent effect were to be reduced.[15] We wish to report herein an S_NAr reaction of electronically neutral aryl fluorides with aliphatic amides and lactams in non-polar solvent systems (Scheme 1).

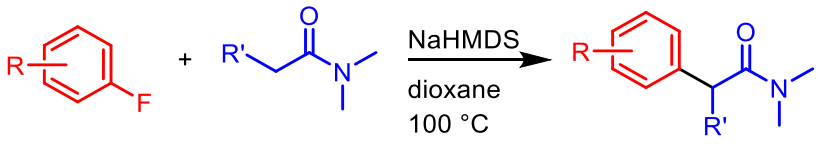

Scheme 1. Nucleophilic aromatic substation (S_NAr) reaction of aryl fluorides with amides.

2.2. Results and Discussion

We started our investigation by optimizing the reaction conditions using 4-fluoro-1,1'-biphenyl (**1a**) and *N*,*N*-dimethylpropionamide (**2a**) as model substrates and NaHMDS (sodium hexamethyldisilazide) as the base. Among the solvents (toluene, DMF, CPME, DME, and 1,4-dioxane)

that were examined, the best yield of the desired 2-([1,1'-biphenyl]-4-yl)-*N,N*-dimethylpropanamide (**3aa**) was 88% NMR yield when 1,4-dioxane was used as a solvent (Table 1, entries 1-4). Curiously, strong bases, such as KO^{t}Bu and NaO^{t}Bu were not effective (entries 5 and 6). After examining the molar ratios of **2a** and NaHMDS, 4 equivalents of **2a** and 2 equivalents of NaHMDS were found to be the optimal ratios (entries 8-10). It was found that the expected product **3aa** was formed in 87% yield, even when the reaction was carried out for 18 hours at 100 °C (entry 11), which is comparable to that obtained when 140 °C was used (entry 1). The addition of 15-crown-5 gave a complex mixture (entry 12). Finally, the reaction conditions shown in entry 11 were determined as the optimal conditions.

Table 1. Optimization of the reaction conditions

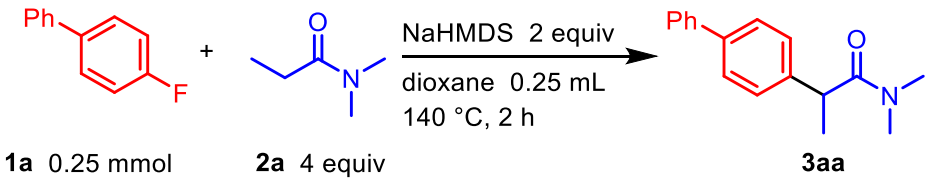

1a 0.25 mmol **2a** 4 equiv **3aa**

Entry	Deviations from the standard reaction conditions	NMR yields **3aa** (%)
1	-	88
2	DMF in place of dioxane	5
3	toluene in place of dioxane	84
4	DME in place of dioxane	78
5	KO^{t}Bu in place of NaHMDS	decomposition
6	NaO^{t}Bu in place of NaHMDS	no reaction
7	KHMDS in place of NaHMDS	77
8	**2a** 2 equiv.	77
9	NaHMDS 1 equiv.	75
10	**2a** 2 equiv., NaHMDS 1 equiv.	68
11	**100 °C, 18 h**	**87**
12	15-crown-5 (2 equiv) at 100 °C, 18 h	complex mixture

The scope of aryl fluorides was then examined (Scheme 2). The reaction of **1a** with **2a** under the optimal conditions (entry 12 in Table 1) gave **3aa** in 86% isolated yield. The reaction of 3-fluoro-1,1'-biphenyl (**1b**) also gave **3ba** as the sole product. On the other hand, a substrate **1c** that contains a phenyl group at the ortho-position gave a separable mixture of the desired product **3ca** in 36% yield and the unexpected product **3ba** in 5% yield. The undesired product **3ba** was likely formed through the formation of an aryne intermediate which is generated by the deprotonation of **1c** with NaHMDS because the nucleophilic attack is retarded by the steric congestion around the C–F bond in **1c**. Curiously, an electron-donating diphenylamino group gave the corresponding product **3da** in good yield. It was found that a boryl group also remained intact in the reaction to give **3ea** in 73% yield, which can be used for further elaboration. A pyridine-substituted phenyl fluoride **1f** also gave the corresponding product **3fa** in 90% yield. Only the one C–F bond participated in the reaction when the difluoro-substituted substrates **1h** and **1i** were reacted, affording **3ha** and **3ia**, respectively in which

the other C–F bond remained intact. In the reaction of **1i**, no meta-substitution occurred and **3ia** was obtained as a single product, unlike **1c**. The fluoropyridines **1k** and **1l** also gave the corresponding products **3ka** and **3la**, albeit in low yields. A substrate **1m** underwent double alkylation to give the expected **3ma** in 87% yield. The reaction of 4-fluorobenzotrifluoride resulted in a complex mixture at 100 °C. In the case of an ethyl ester, a complex mixture was also obtained, even at any position probably due to the cleavage of the ester group under the reaction conditions that were employed (see Experimental Section).

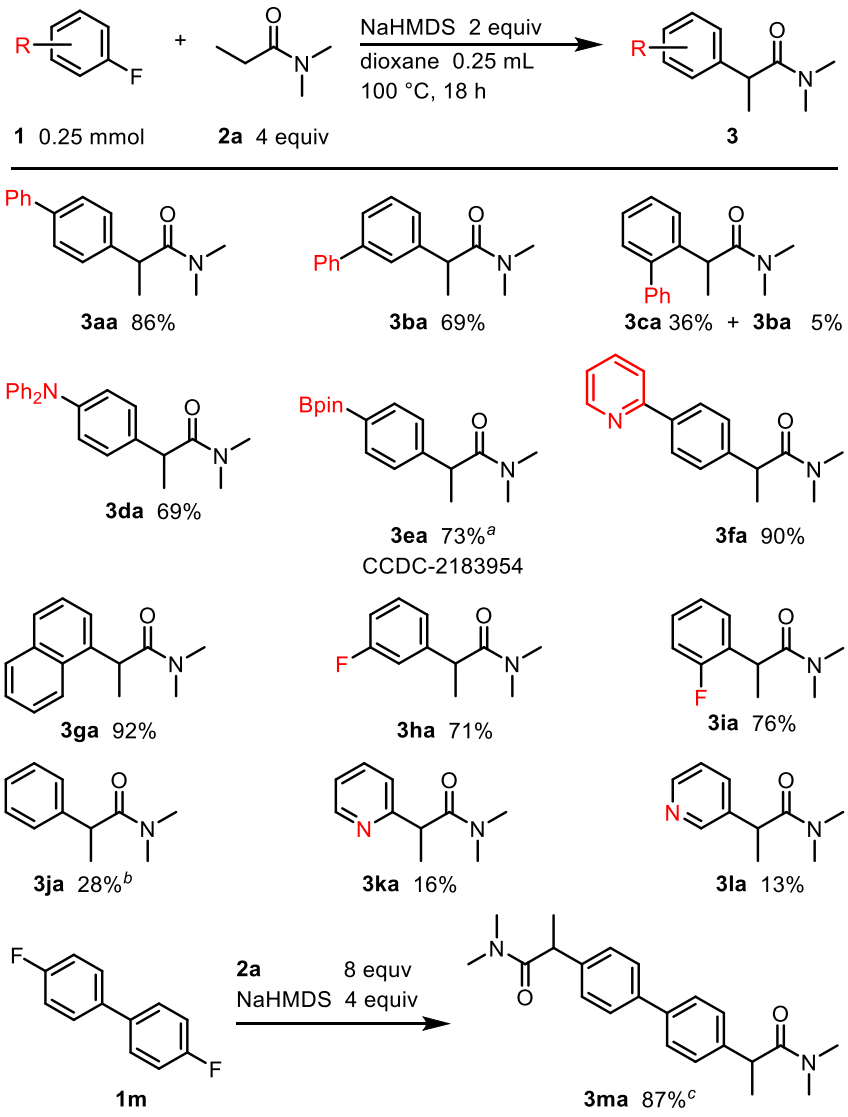

Scheme 2. Scope of aryl fluorides. [a] KHMDS was used in place of NaHMDS. [b] Reaction conditions: 1j (1.0 mmol), 2a (4.0 mmol), and NaHMDS (2.0 mmol), in 1,4-dioxane (0.25 mL) at 140 °C for 18 h. [c] Reaction conditions: 1m (0.25 mmol), 2a (2.0 mmol) and NaHMDS (1.0 mmol) in 1,4-dioxane (0.25 mL) at 100 °C for 18 h.

We next examined the scope of amide enolates (Scheme 3). Although the reaction of a long chain carboxamide **2c** under the optimal conditions gave only a trace amount of the corresponding product **3ac**, the reaction at 140 °C gave **3ac** in 69% yield. The phenylacetamide **2d** also gave the desired product **3ad** in 74% yield when the reaction was carried out at 140 °C. The reaction of acetamides **2e** and **2f** gave mono-arylation products as a single product and no bis-arylation was detected. The reaction of the five-membered lactam **2h** at 100 °C gave **3ah**, but the seven-membered lactam **2i** required a higher reaction temperature.

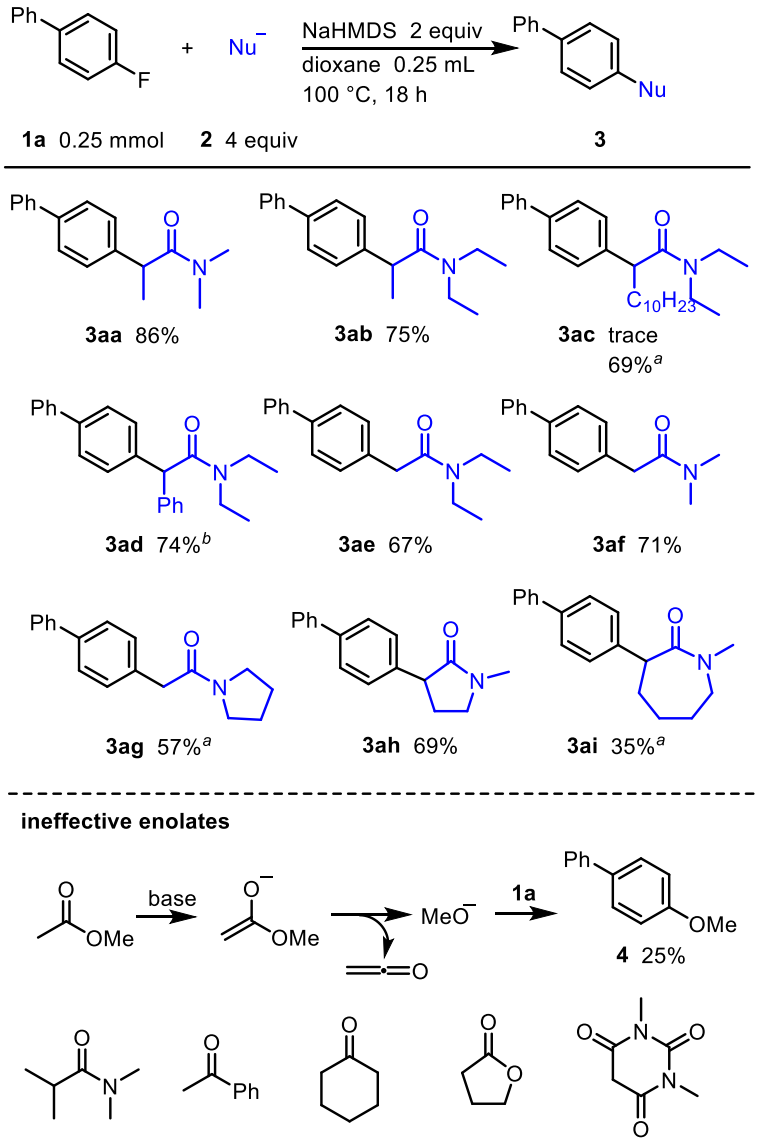

Scheme 3. Scope of enolates. [a] Reaction conditions: 1a (0.25 mmol), 2 (1.0 mmol) and NaHMDS (0.5 mmol) in 1,4-dioxane (0.25 mL) at 140 °C for 2 h. [b] Reaction conditions: 1a (0.25 mmol), 2d (1.0 mmol) and NaHMDS (0.5 mmol) in 1,4-dioxane (0.25 mL) at 140 °C for 4 h.

We next examined other nucleophiles. The reaction of **1a** with methyl acetate at 140 °C for 18 h did not give the expected product and, instead, a methoxy group was introduced at the ipso-position in the aromatic ring to give **4**, although an ester has a pKa value that is similar to that for an amide. A methoxy anion would be generated from an ester enolate along with the generation of ketene under the reaction conditions. It was found that *N,N*-dimethylisobutyramide, acetophenone, cyclohexanone, ketones, γ-butyrolactone, and 1,3-dimethylpyrimidine-2,4,6(1H,3H,5H)-trione were also ineffective substrates. It is well known that alkyl fluorides are not appropriate substrates for use in S_N2 reactions with carbon nucleophiles.[16] To the best of our knowledge, there is only one example of an S_N2 reaction of simple alkyl fluorides with a carbon nucleophile, which is derived from imine magnesium enolates.[17] Gratifyingly, the reaction of octyl fluoride (**5**) with **2a** gave **6** in 58% yield.

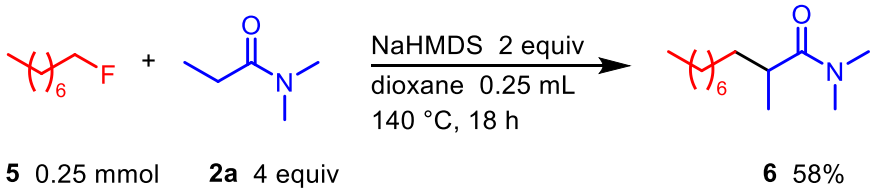

Scheme 4. The reaction of an alkyl fluoride.

To gain insight into the reaction intermediates that are produced, the reaction between **1a** and **2a** with NaHMDS as a base in toluene-d_8 was monitored by ^{1}H NMR spectroscopy. An unidentified singlet peak appeared at 2.1 ppm and the intensity of the peak increased with time when **2a** was treated with NaHMDS at 140 °C. However, the generation of an amide enolate could not be confirmed probably because of its instability. Thus, the enolate would be decomposed under the conditions or would participate in side reactions. We next performed preliminary DFT calculations in order to develop a better understanding of the reaction mechanism for the present reaction (See the Supplementary Information for details). The results of the DFT calculations indicate that the reaction proceeds through a concerted ipso substituent (**TS2**),[18] and not a stepwise pathway (**TS3**) (Scheme 5).

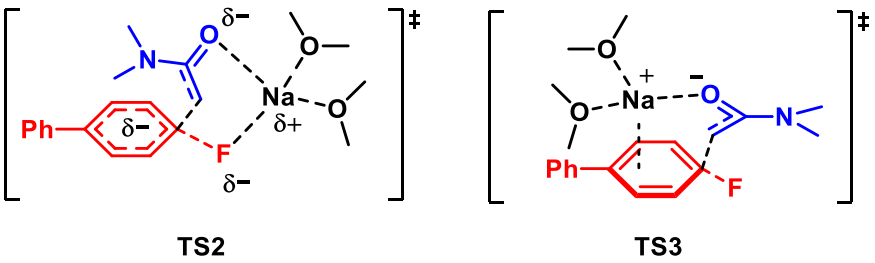

Scheme 5. Transition states (CPCM(THF)-M06-2X/def2SVP).

2.3. Conclusion

In summary, we report the development of an S_NAr reaction of non-activated aryl fluorides with amide enolates. Preliminary DFT calculations suggest that the reaction proceeds through a concerted S_NAr reaction pathway. However, the reaction appears to partially proceed via an aryne intermediate only when a sterically bulky aryl fluoride is used, but the aryne pathway is minor.

2.4. Experimental Section

I. General Information

^1H, ^{13}C and ^{19}F NMR spectra were recorded on a JEOL ECZ-400S spectrometer in $CDCl_3$ with tetramethylsilane as an internal reference standard. The chemical shifts in the ^1H NMR spectra were recorded relative to tetramethylsilane (δ: 0.0). The chemical shifts in ^{13}C NMR spectra were recorded relative to $CDCl_3$ (δ: 77.0). Data are given as follows: chemical shifts in ppm (δ), multiplicity (s = singlet, d = doublet, t = triplet, q = quartet, brs = broad singlet, brd = broad doublet, m = multiplet, c = complex), coupling constant (Hz), and integration. Infrared spectra (IR) were recorded on a JASCO FT/IR-4000 spectrometer using the ATR method. Absorption data are reported in reciprocal centimeters from 800 to 3500 cm^{-1} with the following relative intensities: s (strong), m (medium), or w (weak). Mass spectra were obtained using SHIMADZU QP-2010 or QP-2020 spectrometers with a quadrupole mass analyzer at 70 eV. Data were recorded as follows: mass/charge ratio and relative intensity to base peak at 100%. High-resolution mass spectra (HRMS) were obtained using a JEOL JMS-T100LP spectrometer with a time-of-flight mass analyzer. Melting points were determined on a Stanford Research Systems MPA100 apparatus equipped with a digital thermometer and are uncorrected. Medium-pressure liquid chromatography (MPLC) was performed with Biotage Isolera®.

II. Materials

Toluene (super dehydrated), 1,4-dioxane (super dehydrated), DMF (super dehydrated), DME (super dehydrated), NaHMDS, KHMDS, NaO^{t}Bu and KO^{t}Bu were purchased from commercial sources and were used as received. The aryl fluorides (**1a-1g, 1m**) and amide (**2d**) were purchased from commercial sources and recrystallized from hexane and EtOAc before use. The aryl fluorides (**1h-1l**), amide (**2a-2c, 2e-2i**) and alkyl fluorides (**5**) were purchased from commercial sources and used after bubbling with nitrogen.

III. Nucleophilic Aromatic Substitution of Non-activated Aryl Fluorides with Aliphatic Amides

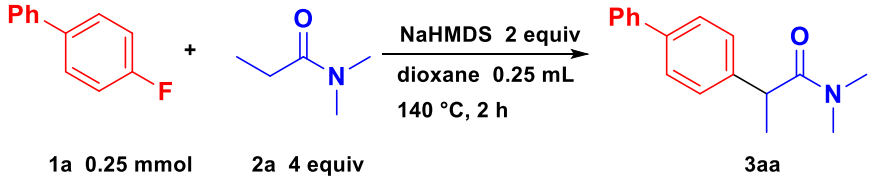

1a 0.25 mmol 2a 4 equiv 3aa

To an oven-dried 10 mL screw-capped vial in a glove box, NaHMDS (91.7 mg, 0.5 mmol), *N,N*-dimethylpropionamide (**2a**, 101.9 mg, 1.0 mmol), 4-fluorobiphenyl (**1a**, 43.1 mg, 0.25 mmol), and 1,4-dioxane (0.25 mL) were added in sequential order. The mixture was stirred at 100 °C for 18 h followed by cooling. The resulting mixture was washed with H_2O (10 mL) and extracted with EtOAc (30 mL). The organic layer filtered through a silica pad. The filtrate was concentrated to dryness in vacuo and the residue was purified by MPLC (hexane/EtOAc = 1/3) to afford the desired product.

2-[(1,1'-Biphenyl)-4-yl]-*N,N*-dimethylpropanamide (3aa) [CAS No. 675840-25-2]

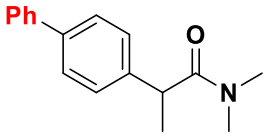

A white solid. Mp = 102.2-103.5 °C. R_f = 0.50 (hexane/EtOAc = 1/3). Yield = 86%, m = 53.8 mg.

^{1}H NMR (399.78 MHz, $CDCl_3$) δ 1.47 (d, *J* = 6.9 Hz, 3H), 2.93 (s, 3H), 2.97 (s, 3H), 3.93 (q, *J* = 6.9 Hz, 1H), 7.31-7.35 (c, 3H), 7.41-7.44 (m, 2H), 7.53-7.58 (c, 4H).

^{13}C NMR (100.53 MHz, $CDCl_3$) δ 20.7, 35.9, 37.2, 42.8, 127.0, 127.2, 127.5, 127.7, 128.7, 139.6, 140.7, 140.9, 173.6.

IR (ATR) 2970 w, 2930 w, 1644 s, 1422 m, 1147 m

MS: *m/z* (EI, relative intensity, %) 254 (11), 253 (52, M^+), 182 (16), 181 (100), 179 (1), 166 (23), 165 (24), 72 (70).

HRMS ($[M+H]^+$) Calcd for $C_{17}H_{20}NO$: 254.15394; Found: 254.15399.

2-[(1,1'-Biphenyl)-3-yl]-*N,N*-dimethylpropanamide (3ba)

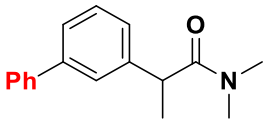

A white solid. Mp = 87.2-88.7 °C. R_f = 0.50 (hexane/EtOAc = 1/3). Yield = 69%, m = 41.3 mg.

^{1}H NMR (399.78 MHz, $CDCl_3$) δ 1.48 (d, *J* = 6.9 Hz, 3H), 2.92 (s, 3H), 2.95 (s, 3H), 3.94 (q, *J* = 6.8 Hz, 1H), 7.24-7.26 (m, 1H), 7.32-7.48 (c, 6H), 7.56-7.59 (m, 2H).

^{13}C NMR (100.53 MHz, $CDCl_3$) δ 20.8, 35.9, 37.2, 43.3, 125.5, 126.1, 126.2, 127.2, 127.3, 128.7,

129.2, 140.9, 141.7, 142.4, 173.5.

IR (ATR) 2973 w, 2930 w, 1644 s, 1476 m, 1394 m, 758 m, 704 m.

MS: *m/z* (EI, relative intensity, %) 253 (37, M^+), 181 (22), 166 (11), 165 (14), 72 (100).

HRMS ($[M+H]^+$) Calcd for $C_{17}H_{20}NO$: 254.15394; Found: 254.15407.

2-[(1,1'-Biphenyl)-2-yl]-*N*,*N*-dimethylpropanamide (3ca)

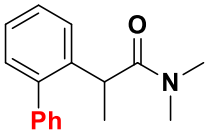

A colorless oil. R_f = 0.52 (hexane/EtOAc = 1/3). Yield = 36%, m = 22.1 mg. (**3ba**: Yield = 5%, m = 3.0 mg.)

^{1}H NMR (399.78 MHz, $CDCl_3$) δ 1.47 (d, *J* = 6.9 Hz, 3H), 2.48 (s, 3H), 2.85 (s, 3H), 3.87 (q, *J* = 6.8 Hz, 1H), 7.21-7.49 (c, 9H).

^{13}C NMR (100.53 MHz, $CDCl_3$) δ 20.7, 35.9, 36.6, 39.0, 126.6, 127.2, 127.3, 128.2, 128.3, 129.1, 130.0, 139.2, 140.8, 141.3, 174.2.

IR (ATR) 2977 w, 2931 w, 1647 s, 1479 m, 1394 m, 758 m, 207 m.

MS: *m/z* (EI, relative intensity, %) 253 (23, M^+), 208 (13), 182 (12), 181 (74), 179 (13), 166 (30), 165 (39), 72 (100).

HRMS ($[M+H]^+$) Calcd for $C_{17}H_{20}NO$: 254.15394; Found: 254.15383.

2-[4-(Diphenylamino)phenyl]-*N*,*N*-dimethylpropanamide (3da)

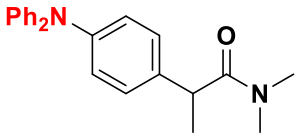

A yellow solid. Mp = 93.9-95.2 °C. R_f = 0.53 (hexane/EtOAc = 1/3). Yield = 69%, m = 55.3 mg.

^{1}H NMR (399.78 MHz, $CDCl_3$) δ 1.43 (d, *J* = 6.9 Hz, 3H), 2.95 (s, 3H), 2.97 (s, 3H), 3.85 (q, *J* = 6.9 Hz, 1H), 6.98-7.02 (c, 4H), 7.05-7.08 (c 4H), 7.11-7.14 (m, 2H), 7.21-7.26 (c, 5H).

^{13}C NMR (100.53 MHz, $CDCl_3$) δ 20.6, 35.9, 37.2, 42.3, 122.6, 124.1, 128.1, 129.1, 135.9, 146.3, 147.7, 173.8. One signal is obscured by overlap with other signals.

IR (ATR) 2970 w, 2929 w, 1644 s, 1588, 1489 s, 1275 s, 753 s, 697 s.

MS: *m/z* (EI, relative intensity, %) 344 (30, M^+), 273 (23), 272 (100).

HRMS ($[M+H]^+$) Calcd for $C_{23}H_{25}N_2O$: 345.19614; Found: 345.19608.

***N,N*-Dimethyl-2-[4-(4,4,5,5-tetramethyl-1,3,2-dioxaborolan-2-yl)phenyl]propenamide (3ea)**

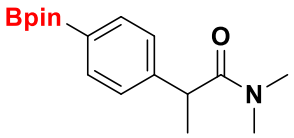

A white solid. Mp = 158.0-158.9 °C. R_f = 0.66 (hexane/EtOAc = 1/3). Yield = 73%, m = 60.2 mg.

^{1}H NMR (399.78 MHz, $CDCl_3$) δ 1.33 (s, 12H), 1.43 (d, *J* = 6.9 Hz, 3H), 2.85 (s, 3H), 2.94 (s, 3H), 3.88 (q, *J* = 6.9 Hz, 1H), 7.27 (d, *J* = 7.3 Hz, 2H), 7.77 (d, *J* = 7.5 Hz, 2H).

^{13}C NMR (100.53 MHz, $CDCl_3$) δ 20.7, 24.8, 24.8, 35.9, 37.1, 43.6, 83.7, 126.7, 135.3, 145.1, 173.3.

IR (ATR) 2978 m, 2931 m, 1648 m, 1360 s, 1145 m, 1092 m.

MS: *m/z* (EI, relative intensity, %) 303 (23, M^+), 231 (55), 230 (16), 132 (22), 131 (17), 116 (11), 83 (10), 72 (100).

HRMS ($[M+H]^+$) Calcd for $C_{17}H_{27}BNO_3$: 304.20785; Found: 304.20824.

***N,N*-Dimethyl-2-[4-(pyridin-2-yl)phenyl]propanamide (3fa)**

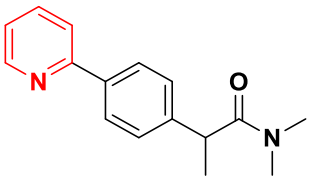

A white solid. Mp = 103.3-104.1 °C. R_f = 0.16 (hexane/EtOAc = 1/3). Yield = 90%, m = 56.3 mg.

^{1}H NMR (399.78 MHz, $CDCl_3$) δ 1.47 (d, *J* = 6.9 Hz, 3H), 2.90 (s, 3H), 2.97 (s, 3H), 3.94 (q, *J* = 6.8 Hz, 1H), 7.21-7.24 (m, 1H), 7.38 (d, *J* = 8.0 Hz, 2H), 7.70-7.77 (m, 2H), 7.94 (d, *J* = 8.0 Hz, 2H), 8.68 (dt, *J* = 4.8, 0.9 Hz, 1H).

^{13}C NMR (100.53 MHz, $CDCl_3$) δ 20.6, 35.9, 37.1, 43.1, 120.4, 122.0, 127.4, 127.7, 136.7, 137.9, 142.7, 149.6, 157.1, 173.4.

IR (ATR) 2975 w, 2930 w, 1643 s, 1466 m, 777 m.

MS: *m/z* (EI, relative intensity, %) 255 (10), 256 (54, M^+), 183 (15), 181 (100), 167 (38), 72 (91).

HRMS ($[M+H]^+$) Calcd for $C_{16}H_{19}NO$: 255.14919; Found: 255.14921.

***N,N*-Dimethyl-2-(naphthalen-2-yl)propanamide (3ga) [CAS No. 169770-80-3]**

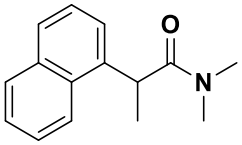

A white solid. Mp = 103.3-106.4 °C. R_f = 0.41 (hexane/EtOAc = 1/3). Yield = 92%, m = 67.1 mg.

^{1}H NMR (399.78 MHz, $CDCl_3$) δ 1.54 (d, *J* = 6.9 Hz, 3H), 2.67 (s, 3H), 3.00 (s, 3H), 4.59 (q, *J* = 6.9 Hz, 1H), 7.37 (dd, *J* = 7.2, 1.3 Hz, 1H), 7.42 (t, *J* = 7.5 Hz, 1H), 7.49-7.53 (m, 1H), 7.55-7.59 (m, 1H),

7.75 (d, J = 8.0 Hz, 1H), 7.89 (d, J = 7.8 Hz, 1H), 8.11 (d, J = 8.5 Hz, 1H).

^{13}C NMR (100.53 MHz, $CDCl_3$) δ 19.6, 35.9, 37.0, 39.3, 122.3, 124.0, 125.6, 125.9, 126.4, 127.3, 129.2, 130.5, 134.0, 138.1, 174.1.

IR (ATR) 2974 w, 2930 w, 1644 s, 1394 m, 777 s.

MS: *m/z* (EI, relative intensity, %) 228 (11), 227 (64, M^+), 156 (15), 155 (100), 153 (26), 152 (13), 128 (12), 127 (10), 72 (99).

HRMS ($[M+H]^+$) Calcd for $C15H_{18}NO$: 228.13829; Found: 228.13829.

2-(4-Fluorophenyl)-*N,N*-dimethylpropanamide (3ha) [CAS No. 2041088-95-1]

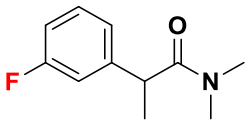

A yellow oil. R_f = 0.51 (hexane/EtOAc = 1/3). Yield = 71%, m = 64.9 mg.

^{1}H NMR (399.78 MHz, $CDCl_3$) δ 1.43 (d, J = 6.9 Hz, 3H), 2.91 (s, 3H), 2.96 (s, 3H), 3.90 (q, J = 6.9 Hz, 1H), 6.92 (tq, J = 8.5, 1.1 Hz, 1H), 6.98-7.02 (m, 1H), 7.04 (d, J = 7.8 Hz, 1H), 7.25-7.30 (m, 1H).

^{13}C NMR (100.53 MHz, $CDCl_3$) δ 20.5, 35.9, 37.1, 42.8, 113.7 (d, J = 21.2 Hz), 114.2 (d, J = 21.2 Hz), 123.0, 123.0, 130.2, 130.2, 144.3, 144.3, 163.0 (d, J = 246.6 Hz), 173.0.

^{19}F NMR (376.17 MHz, $CDCl_3$) δ -112.5.

IR (ATR): 2975 w, 2933 w, 1643 s, 1483 m.

MS: *m/z* (EI, relative intensity, %) 195 (15, M^+), 72 (100).

HRMS ($[M+H]^+$) Calcd for $C_{11}H_{15}NOF$: 196.11322; Found: 196.11310.

2-(2-Fluorophenyl)-*N,N*-dimethylpropanamide (3ia)

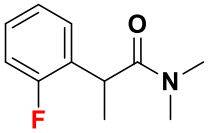

A yellow oil. R_f = 0.65 (hexane/EtOAc = 1/3). Yield = 76%, m = 69.9 mg.

^{1}H NMR (399.78 MHz, $CDCl_3$) δ 1.39 (d, J = 6.9 Hz, 3H), 2.86 (s, 3H), 2.92 (s, 3H), 4.24 (q, J = 6.9 Hz, 1H), 6.98-7.03 (m, 1H), 7.07 (td, J = 7.5, 1.2 Hz, 1H), 7.15-7.21 (m, 1H), 7.30 (td, J = 7.7, 1.8 Hz, 1H).

^{13}C NMR (100.53 MHz, $CDCl_3$) δ 19.0, 34.6, 35.8, 36.8, 115.1 (d, J = 22.2 Hz), 124.6 (d, J = 2.9 Hz), 128.3 (d, J = 15.4 Hz), 128.3 (d, J = 2.9 Hz) 128.5 (d, J = 15.4 Hz), 159.5 (d, J = 244.7 Hz), 173.1.

^{19}F NMR (376.17 MHz, $CDCl_3$) δ -120.1.

IR (ATR) 2978 w, 2934 w, 1650 s, 1396 m, 760 m.

MS: *m/z* (EI, relative intensity, %) 195 (31, M^+), 123 (14), 103 (13), 72 (100).

HRMS ($[M+H]^+$) Calcd for $C_{11}H_{15}NOF$: 196.11322; Found: 196.11294.

***N,N*-Dimethyl-2-phenylpropanamide (3ja) [CAS No. 41836-85-5]**

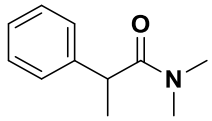

To an oven-dried 10 mL screw-capped vial in a glove box, NaHMDS (367.0 mg, 2.0 mmol), *N,N*-dimethylpropionamide (**2a**, 404.8 mg, 4.0 mmol), fluorobenzene (**1j**, 47.6 mg, 1.0 mmol), and 1,4-dioxane (0.25 mL) were added in sequential order. The mixture was stirred at 140 °C for 18 h.

A colorless oil. R_f = 0.66 (hexane/EtOAc = 1/3). Yield = 28%, m = 63.3 mg.

^{1}H NMR (399.78 MHz, $CDCl_3$) δ 1.44 (d, J = 6.9 Hz, 3H), 2.89 (s, 3H), 2.95 (s, 3H), 3.88 (q, J = 6.9 Hz, 1H), 7.21-7.33 (c, 5H).

^{13}C NMR (100.53 MHz, $CDCl_3$) δ 20.7, 35.8, 37.1, 43.2, 126.6, 127.2, 128.7, 141.8, 173.6.

IR (ATR) 2976 w, 2931 w, 1644 s, 1396 m, 1148 m, 759 m.

MS: *m/z* (EI, relative intensity, %) 177 (28, M^+), 105 (26), 72 (100).

HRMS ($[M+H]^+$) Calcd for $C_{11}H_{16}NO$: 178.12264; Found: 178.12260.

***N,N*-Dimethyl-2-(pyridin-2-yl)propanamide (3ka) [CAS No. 886193-93-7]**

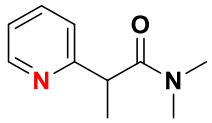

A colorless oil. R_f = 0.08 (hexane/EtOAc = 1/3). Yield = 16%, m = 7.2 mg.

^{1}H NMR (399.78 MHz, $CDCl_3$) δ 1.50 (d, J = 7.1 Hz, 3H), 2.96 (s, 3H), 2.98 (s, 3H), 4.19 (q, J = 6.9 Hz, 1H), 7.16 (ddd, J = 7.5, 5.0, 1.1 Hz, 1H), 7.34 (d, J = 7.8 Hz, 1H), 7.65 (td, J = 7.7, 1.8 Hz, 1H), 8.51 (dq, J = 5.0, 0.8 Hz, 1H).

^{13}C NMR (100.53 MHz, $CDCl_3$) δ 18.8, 35.9, 37.3, 45.9, 121.3, 121.8, 137.0, 149.1, 161.5, 173.0.

IR (ATR) 2931 w, 1646 m, 1472 w, 1397 w, 772 s.

MS: *m/z* (EI, relative intensity, %) 178 (7, M^+), 134 (15), 133 (12), 121 (50), 107 (37), 106 (100), 93 (18), 78 (17), 72 (66).

HRMS ($[M+H]^+$) Calcd for $C_{10}H_{15}N_2O$: 179.11789; Found: 179.11768.

***N,N*-Dimethyl-2-(pyridin-3-yl)propanamide (3la) [CAS No. 1881981-45-8]**

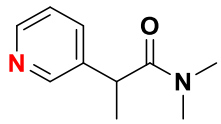

A colorless oil. R_f = 0.16 (hexane/EtOAc = 1/3). Yield = 13%, m = 6.5 mg.

^{1}H NMR (399.78 MHz, $CDCl_3$) δ 1.46 (d, J = 6.9 Hz, 3H), 2.95 (s, 3H), 2.96 (s, 3H), 3.95 (q, J = 6.9 Hz, 1H), 7.25-7.28 (c, 2H), 7.68 (dt, J = 8.0, 1.9 Hz, 1H), 8.49-8.52 (c, 2H).

^{13}C NMR (100.53 MHz, $CDCl_3$) δ 20.4, 36.0, 37.2, 40.3, 134.8, 148.4, 149.1, 172.8. two signals are obscured by overlap with other signals.

IR (ATR) 2975 w, 2929 w, 1643 s, 1398 m.

MS: *m/z* (EI, relative intensity, %) 178 (33, M^+), 106 (13), 72 (100).

HRMS ($[M+H]^+$) Calcd for $C_{10}H_{15}N_2O$: 179.11789; Found: 179.11760.

2,2'-[(1,1'-Biphenyl)-4,4'-diyl]bis(*N*,*N*-dimethylpropanamide) (3ma)

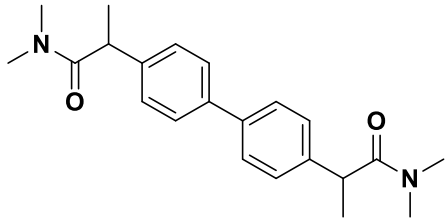

To an oven-dried 10 mL screw-capped vial in a glove box, NaHMDS (183.4 mg, 1.0 mmol), *N,N*-dimethylpropionamide (**2a**, 202.8 mg, 2.0 mmol), 4,4'-difluoro-1,1'-biphenyl (**1m**, 47.6 mg, 0.25 mmol), and 1,4-dioxane (0.25 mL) were added in sequential order.

A white solid. Mp = 156.5-157.8 °C. R_f = 0.41 (hexane/EtOAc = 0/1). Yield = 87%, m = 76.1 mg.

^{1}H NMR (399.78 MHz, $CDCl_3$) δ 1.47 (d, *J* = 6.9 Hz, 6H), 2.93 (s, 6H), 2.97 (s, 6H), 3.93 (q, *J* = 6.9 Hz, 2H), 7.33 (dt, *J* = 8.4, 1.8 Hz, 4H), 7.52 (dt, *J* = 8.5, 1.9 Hz, 4H).

^{13}C NMR (100.53 MHz, $CDCl_3$) δ 20.6, 35.9, 37.1, 42.8, 127.3, 127.7, 139.1, 140.8, 173.6.

IR (ATR) 2973 w, 2930 w, 1638 s, 1493 m, 1395 m.

MS: *m/z* (EI, relative intensity, %) 352 (21, M^+), 281 (20), 280 (100), 208 (36), 207 (13), 72 (43).

HRMS ($[M+H]^+$) Calcd for $C_{22}H_{29}N_2O_2$: 353.22235; Found: 353.22194.

2-[(1,1'-Biphenyl)-4-yl]-*N*,*N*-diethylpropanamide (3ab)

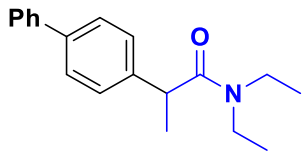

A colorless oil. R_f = 0.66 (hexane/EtOAc = 3/1). Yield = 75%, m =56.5 mg.

^{1}H NMR (399.78 MHz, $CDCl_3$) δ 1.03 (t, *J* = 7.1 Hz, 3H), 1.11 (t, *J* = 7.1 Hz, 3H), 1.48 (d, *J* = 6.9 Hz, 3H), 3.14 (td, *J* = 14.5, 7.3 Hz, 1H), 3.25 (td, *J* = 13.8, 6.8 Hz, 1H), 3.32-3.41 (m, 1H), 3.52 (td, *J* = 13.8, 7.0 Hz, 1H), 3.87 (q, *J* = 6.9 Hz, 1H), 7.30-7.37 (m, 3H), 7.40-7.44 (m, 2H), 7.52-7.59 (m, 4H).

^{13}C NMR (100.53 MHz, $CDCl_3$) δ 12.8, 14.3, 20.9, 40.3, 41.6, 42.6, 126.9, 127.1, 127.4, 127.6, 128.7, 139.5, 140.7, 141.4, 172.6.

IR (ATR): 2972 w, 2931 w, 1639 s, 1484 m, 1458 m, 1429 m, 762 m.

MS: *m/z* (EI, relative intensity, %): 281 (13, M^+), 180 (15), 100 (100), 72 (33).

HRMS ($[M+H]^+$) Calcd for $C_{19}H_{24}NO$: 282.18524; Found: 282.18560.

2-[(1,1'-Biphenyl)-4-yl]-*N*,*N*-diethyldodecanamide (3ac)

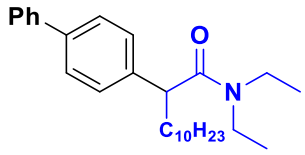

The mixture was stirred at 140 °C for 2 h.

A colorless oil. R_f = 0.75 (hexane/EtOAc = 1/3). Yield = 69%, m = 70.2 mg.

^{1}H NMR (399.78 MHz, $CDCl_3$) δ 0.87 (t, *J* = 6.9 Hz, 3H), 1.04-1.11 (m, 6H), 1.24-1.34 (m, 16H), 1.67-1.76 (m, 1H), 2.07-2.16 (m, 1H), 3.17 (td, *J* = 14.6, 7.3 Hz, 1H), 3.29 (td, *J* = 13.8, 6.9 Hz, 1H), 3.36-3.51 (m, 2H), 3.67 (t, *J* = 7.3 Hz, 1H), 7.30-7.35 (m, 1H), 7.38 (dd, *J* = 6.5, 1.7 Hz, 2H), 7.40-7.46 (m, 2H), 7.52-7.59 (c, 4H).

^{13}C NMR (100.53 MHz, $CDCl_3$) δ 12.9, 14.1, 14.6, 22.7, 28.0, 29.3, 29.5, 29.6, 29.6, 31.9, 35.5, 40.4, 41.7, 48.5, 126.9, 127.1, 127.2, 128.2, 128.7, 139.5, 140.0, 140.8, 172.2. One signal is obscured by overlap with other signals.

IR (ATR) 2924 s, 2853 m, 1641 s, 1484 m, 1458 m, 1429 m, 761 m.

MS: *m/z* (EI, relative intensity, %) 407 (5, M^+), 267 (41), 167 (44), 100 (100), 72 (25).

HRMS ($[M+H]^+$) Calcd for $C_{28}H_{42}NO$: 408.32609; Found: 408.32582.

2-[(1,1'-Biphenyl)-4-yl]-*N*,*N*-diethyl-2-phenylacetamide (3ad)

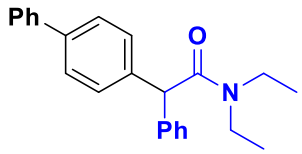

The mixture was stirred at 140 °C for 4 h.

A white solid. Mp = 99.6-100.7 °C. R_f = 0.33 (hexane/EtOAc = 3/1). Yield = 74%, m = 60.4 mg.

^{1}H NMR (399.78 MHz, $CDCl_3$) δ 1.12-1.25 (m, 6H), 3.28-3.51 (m, 4H), 5.19 (s, 1H), 7.23-7.28 (c, 1H), 7.29-7.36 (m, 7H), 7.39-7.43 (m, 2H), 7.51-7.57 (c, 3H).

^{13}C NMR (100.53 MHz, $CDCl_3$) δ 12.8, 14.7, 40.7, 42.1, 54.2, 127.0, 127.0, 127.1, 127.2, 128.6, 128.7, 128.9, 129.4, 139.0, 139.7, 140.8, 170.6. One signal is obscured by overlap with other signals.

IR (ATR) 2974 w, 2932 m, 1641 s, 1485 m, 1454 m, 1428 m, 1131 m, 759 s, 728 m, 697 s.

MS: *m/z* (EI, relative intensity, %) 343 (5, M^+), 243 (24), 100 (100), 72 (29).

HRMS ($[M+H]^+$) Calcd for $C_{24}H_{26}NO$: 344.20089; Found: 344.20178.

2-[(1,1'-Biphenyl)-4-yl]-*N*,*N*-diethylacetamide (3ae) [CAS No. 180728-35-2]

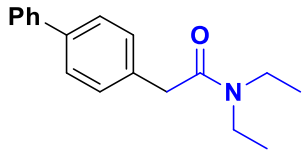

A colorless oil. R_f = 0.50 (hexane/EtOAc = 1/3). Yield = 67%, m = 48.3 mg.

^{1}H NMR (399.78 MHz, $CDCl_3$) δ 1.13 (td, *J* = 7.1, 5.3 Hz, 6H), 3.32 (q, *J* = 7.1 Hz, 2H), 3.40 (q, *J* = 7.1 Hz, 2H), 3.73 (s, 2H), 7.30-7.34 (m, 3H), 7.42 (td, *J* = 6.7, 1.5 Hz, 2H), 7.52-7.59 (m, 4H).

^{13}C NMR (100.53 MHz, $CDCl_3$) δ 12.9, 14.2, 40.1, 40.4, 42.3, 127.0, 127.1, 127.3, 128.7, 129.1, 134.5, 139.5, 140.8, 170.0

IR (ATR) 2947 w, 2933 w, 1639 s, 1485 m, 1458 m, 1428 m, 755 m.

MS: *m/z* (EI, relative intensity, %) 267 (22, M^+), 165 (13), 100 (100), 72 (43).

HRMS ($[M+H]^+$) Calcd for $C_{18}H_{22}NO$: 268.16959; Found: 268.16941.

2-[(1,1'-Biphenyl)-4-yl]-*N*,*N*-dimethylacetamide (3af) [CAS No. 180728-36-3]

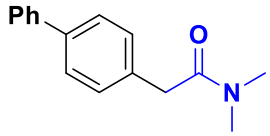

A white solid. Mp = 90.2-92.2 °C. R_f = 0.42 (hexane/EtOAc = 1/3). Yield = 71%, m = 44.6 mg.

^{1}H NMR (399.78 MHz, $CDCl_3$) δ 2.99 (s, 3H), 3.04 (d, *J* = 0.9 Hz, 3H), 3.76 (s, 2H), 7.32-7.35 (c, 3H), 7.41-7.45 (m, 2H), 7.54-7.59 (c, 4H).

^{13}C NMR (100.53 MHz, $CDCl_3$) δ 35.6, 37.7, 40.6, 127.0, 127.2, 127.3, 128.7, 129.2, 134.1, 139.6, 140.8, 170.9.

IR (ATR) 3028 w, 2930 w, 1639 s, 1486 m, 1393 m, 1130 m, 756 s, 698 m.

MS: *m/z* (EI, relative intensity, %) 239 (37, M^+), 167 (25), 165 (16), 72 (100).

HRMS ($[M+H]^+$) Calcd for $C_{16}H_{18}NO$: 240.13829; Found: 240.13818.

2-[(1,1'-Biphenyl)-4-yl]-1-(pyrrolidin-1-yl)ethan-1-one (3ag) [CAS No. 903761-18-2]

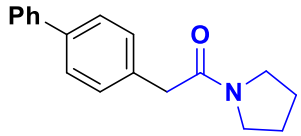

The mixture was stirred at 140 °C for 2 h.

A white solid. Mp = 88.2-89.1 °C. R_f = 0.51 (hexane/EtOAc = 1/3). Yield = 57%, m = 36.5 mg.

^{1}H NMR (399.78 MHz, $CDCl_3$) δ 1.81-1.88 (m, 2H), 1.90-1.97 (m, 2H), 3.46 (t, *J* = 6.7 Hz, 2H), 3.51 (t, *J* = 6.9 Hz, 2H), 3.69 (s, 2H), 7.31-7.37 (c, 3H), 7.41-7.44 (m, 2H), 7.51-7.59 (c, 4H).

^{13}C NMR (100.53 MHz, $CDCl_3$) δ 24.3, 26.1, 41.8, 45.9, 46.9, 127.0, 127.1, 127.3, 128.7, 129.4,

134.0, 139.6, 140.8, 169.4.

IR (ATR) 2970 w, 2873 w, 1637 s, 1428 m, 758 m, 698 m.

MS: *m/z* (EI, relative intensity, %) 265 (28, M^+), 167 (10), 165 (14), 98 (100), 179 (15), 56 (12), 55 (36).

HRMS ($[M+H]^+$) Calcd for $C_{18}H_{20}NO$: 266.15394; Found: 266.15401.

3-[(1,1'-Biphenyl)-4-yl]-1-methylpyrrolidin-2-one (3ah)

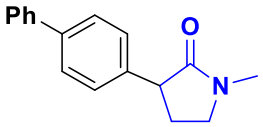

A colorless oil. R_f = 0.33 (hexane/EtOAc = 1/3). Yield = 69%, m = 41.4 mg.

^{1}H NMR (399.78 MHz, $CDCl_3$ δ 2.13-2.22 (m, 1H), 2.51-2.60 (m, 1H), 2.96 (s, 3H), 3.42-3.53 (m, 2H), 3.70 (t, *J* = 8.8 Hz, 1H), 7.31-7.35 (c, 3H), 7.43 (t, *J* = 7.7 Hz, 2H), 7.53-7.57 (c, 4H)

^{13}C NMR (100.53 MHz, $CDCl_3$) δ 28.0, 30.1, 47.7, 127.1, 127.1, 127.5, 128.3, 128.7, 139.0, 139.9, 140.9, 174.8. one signal is obscured by overlap with other signals.

IR (ATR) 3028 w, 2944 w, 2877 w, 1687 s, 765 m.

MS: *m/z* (EI, relative intensity, %) 252(19), 251 (100, M^+),195 (10), 194 (60), 193 (25), 179 (21), 178 (26), 165 (16), 117 (11).

HRMS ($[M+H]^+$) Calcd for $C_{17}H_{18}NO$: 252.13829; Found: 252.13922.

3-([1,1'-Biphenyl]-4-yl)-1-methylpyrrolidin-2-one (3ai)

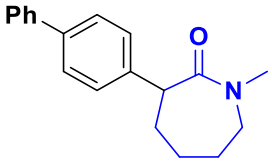

The mixture was stirred at 140 °C for 2 h.

A white solid. Mp = 97.2-102.1 °C. R_f = 0.58 (hexane/EtOAc = 8/1). Yield = 35%, m = 23.5 mg.

^{1}H NMR (399.78 MHz, $CDCl_3$) δ 1.51-1.88 (c, 3H), 2.02-2.08 (c, 3H), 3.04 (s, 3H), 3.27 (dd, *J* = 15.3, 5.0 Hz, 1H), 3.73 (dd, *J* = 15.3, 10.7 Hz, 1H), 3.91 (t, *J* = 6.1 Hz, 1H), 7.26-7.34 (c, 3H), 7.42 (t, *J* = 7.5 Hz, 2H), 7.55 (d, *J* = 8.2 Hz, 2H), 7.58 (dd, *J* = 8.1, 1.0 Hz, 2H)

^{13}C NMR (100.53 MHz, $CDCl_3$) δ 27.1, 28.9, 31.1, 36.2, 49.9, 50.6, 77.3, 126.9, 126.9, 127.1, 128.6, 128.8, 139.4, 140.8, 141.2, 175.3

IR (ATR) 3028 w, 2928 m, 2856 w, 1647 s, 1485 m, 763 m.

MS: *m/z* (EI, relative intensity, %) 280 (22), 279 (100, M^+), 222 (10), 221 (14), 220 (39), 205 (13), 194 (13), 193 (27), 180 (33), 179 (21), 178 (41), 167 (23), 165 (32), 154 (12), 152 (13), 98 (13), 73 (19), 72 (15), 70 (10), 44 (20).

HRMS ([M+H]$^+$) Calcd for $C_{19}H_{22}NO$: 280.16959; Found: 280.16968.

Ineffective aryl fluorides

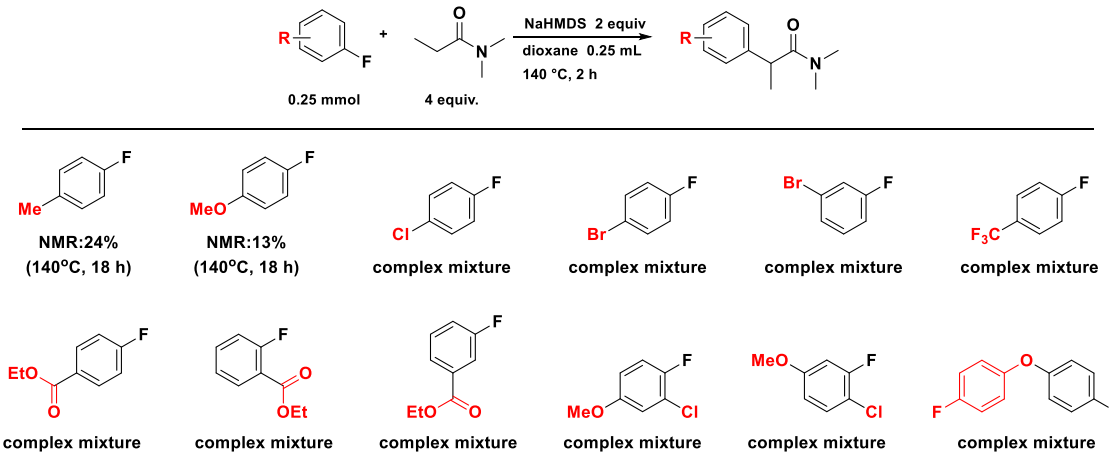

IV. S_N2 Reaction of Primary Alkyl Fluoride with Aliphatic Amide

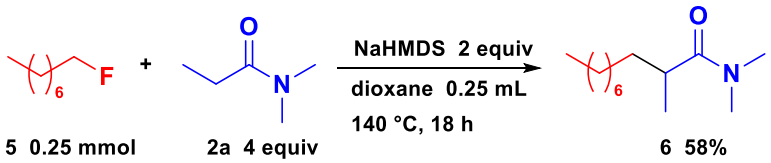

To an oven-dried 10 mL screw-capped vial in a glove box, NaHMDS (91.7 mg, 0.5 mmol), *N,N*-dimethylpropionamide (**2a**, 101.9 mg, 1.0 mmol), 1-fluorooctane (**1a**, 33.1 mg, 0.25 mmol), and 1,4-dioxane (0.25 mL) were added in sequential order. The mixture was stirred at 140 °C for 18 h followed by cooling. The resulting mixture was washed with H_2O (10 mL) and extracted with EtOAc (30 mL). The organic layer was washed with water and filtered through a silica pad. The filtrate was concentrated to dryness in vacuo and the residue was purified by MPLC (hexane/EtOAc = 1/3) to afford the desired product *N,N,*2-trimethyldecanamide (**6,** 26.3 mg, 58%).

A colorless oil. R_f = 0.25 (hexane/EtOAc = 3/1). Yield = 58%, m = 26.3 mg.

^{1}H NMR (399.78 MHz, $CDCl_3$) δ 0.87 (t, *J* = 6.9 Hz, 3H), 1.09 (d, *J* = 6.9 Hz, 3H), 1.25-1.39 (m, 13H), 1.64-1.70 (m, 1H), 2.65-2.73 (m, 1H), 2.96 (s, 3H), 3.05 (s, 3H)

^{13}C NMR (100.53 MHz, $CDCl_3$) δ 14.1, 17.4, 22.6, 27.5, 29.3, 29.5, 29.7, 31.8, 34.1, 35.5, 35.6, 37.2, 176.8

IR (ATR) 2928 s, 2855 m, 1646 s, 1464 m, 1397 m, 722 m.

MS: *m/z* (EI, relative intensity, %) 213 (1, M$^+$), 114 (14), 101 (100), 72 (35), 57 (14), 45 (23), 43 (14), 41 (11).

HRMS ([M+H]$^+$) Calcd for $C_{13}H_{28}ON$: 214.21654; Found: 214.21626.

V. Computational Studies

V.I General Information

All calculations of the geometory optimizations were performed by Gaussian 16 package[19]. The geometory optimizations and frequency calculations of all structures were conducted at the M06-2X functional[20] in conjunction with the def2SVP basis set[21] in the presence of two Me_2O models. The self-consistent reaction field (SCRF) method based on conductor-like polarizable continuum model (CPCM)[22] was adopted to evaluate the effects of solvent (THF). Each reported minimum has no imaginary frequency and each transition state structure has one imaginary frequency. Intrinsic reaction coordinate (IRC) analyses[23] from transition states to minima were used for confirming the reaction pathways. This level is denoted as CPCM(THF)-M06-2X/def2SVP. For describing energy diagram, the relative energies were corrected for the thermal free energies and given in kcal·mol^{-1}. The structures of intermediates and transition states were described by GaussView 6.0 package[24].

V.II DFT Studies on the Reaction Pathway

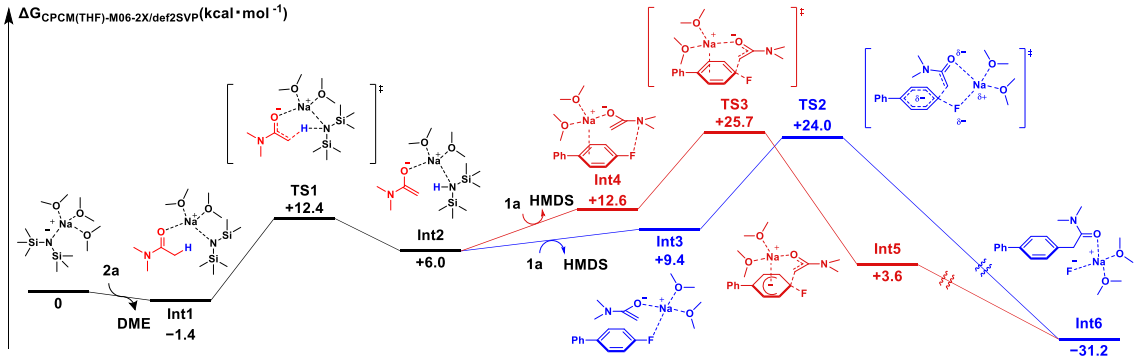

Figure S1. Energy diagram of the reaction pathway at CPCM(THF)-M06-2X/def2SVP level.

VI. X-ray Crystallographic Data

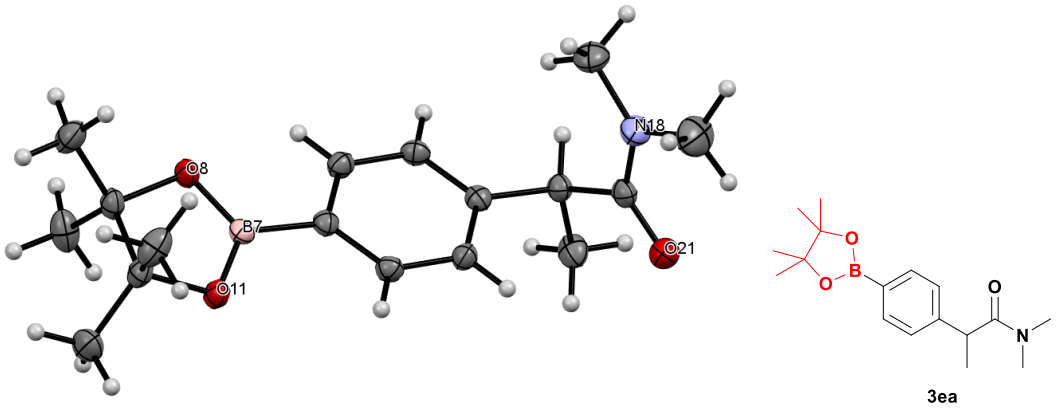

Figure S3. ORTEP plots of 3ea with thermal ellipsoids drawn at 50% probability level.

Table S1. Crystal data and structure refinement for 3ea

Identification code	3ea
Empirical formula	$C_{17}H_{26}BNO_3$
Formula weight	303.20
Temperature/K	123
Crystal system	triclinic
Space group	P-1
a/Å	6.4832(3)
b/Å	11.8496(6)
c/Å	11.9710(5)
α/°	70.722(4)
β/°	85.965(4)
γ/°	89.751(4)
Volume/Å^3	865.76(7)
Z	2
ρ_{calc}g/cm^3	1.163
μ/mm^{-1}	0.077
F (000)	328.0
Crystal size/mm^3	0.259 × 0.203 × 0.147
Radiation	Mo Kα (λ = 0.71073)
2Θ range for data collection/°	3.642 to 61.328
Index ranges	$-8 \le h \le 9$, $-14 \le k \le 16$, $-17 \le l \le 15$
Reflections collected	12100
Independent reflections	4253 [R_{int} = 0.0467, R_{sigma} = 0.0567]
Data/restraints/parameters	4253/0/206

Goodness-of-fit on F^2	1.053
Final R indexes [I>=2σ (I)]	R_1 = 0.0544, wR_2 = 0.1331
Final R indexes [all data]	R_1 = 0.0812, wR_2 = 0.1454
Largest diff. peak/hole / e $Å^{-3}$	0.33/-0.21

Experimental

Single crystals of $C_{17}H_{26}BNO_3$ 3ea were CCDC-2183954. A suitable crystal was selected and CCDC-2183954 on a Rigaku XtaLAB P200 diffractometer using multi-layer mirror monochromated Mo-Kα radiation. The crystal was kept at 123 K duringdata collection.Using Olex2[25], the structure was solved with the SHELXT[26] structure solution programusingIntrinsic Phasingand refined with the SHELXL refinement package usingLeast Squaresminimisation.

VII. ICP Analysis of Starting Materials and Product

ICP-AES (Inductively Coupled Plasma Emission Spectrometry) of NaHMDS

A sample was prepared by dissolving NaHMDS (1.0 g) neutralized with hydrochloric acid (5.0 mL) in pure water (1 or 5 wt%). An analysis was conducted on ICPS-8100(SHIMADZU). The Contents of Elements are shown in Table S2 and S3.

Table S2. 1wt% NaHMDS aq.

Order	Contents of NaHMDS
< 100 ppm	Na, Si
< 1 ppm	K
< 0.1 ppm	B, Al
0.1 ppm <	Mg, Ca, Fe, Zn, Sr, Ba

Table S3. 5wt% NaHMDS aq.

Order	Contents of NaHMDS
< 100 ppm	Na, Si
< 1 ppm	B, K
< 0.1 ppm	Al, Ca, Ba
0.1 ppm <	Mg, Fe, Zn, Sr

ICP-AES (Inductively Coupled Plasma Emission Spectrometry) of **1a**

A sample was prepared by dissolving **1a** (0.35 g) in EtOH (3.5 wt%). An analysis was conducted on ICPS-8100(SHIMADZU). The Contents of Elements are shown in Table S4.

Table S4. 3.5wt% **1a** aq.

Order	Contents of **1a**
< 1 ppm	-
< 0.1 ppm	Na, Si
0.1 ppm <	B, Mg, Ca, Cu, Zn

ICP-AES (Inductively Coupled Plasma Emission Spectrometry) of **2a**

A sample was prepared by dissolving **2a** (0.7 g) in EtOH (3.5 wt%). An analysis was conducted on ICPS-8100(SHIMADZU). The Contents of Elements are shown in Table S5.

Table S5. 3.5wt% **2a** aq.

Order	Contents of **2a**
< 1 ppm	-
< 0.1 ppm	Na, Si
0.1 ppm <	B, Mg, Ca, Cu, Zn

ICP-AES (Inductively Coupled Plasma Emission Spectrometry) of **3aa**

A sample was prepared by dissolving **3aa** (0.35 g) in EtOH (3.5 wt%). An analysis was conducted on ICPS-8100(SHIMADZU). The Contents of Elements are shown in Table S6.

Table S6. 3.5wt% **3aa** aq.

Order	Contents of **3aa**
< 10 ppm	-
< 1 ppm	Na, Si
< 0.1 ppm	B
0.1 ppm <	Mg, Ca, Cu, Zn

2.5. References

(1) For reviews on nucleophilic aromatic substitution (S_NAr) reactions, see: (a) Bunnett, J. F.; Zahler, R. E. *Chem. Rev.* **1951**, *49*, 273–412. (b) Terrier, F. *Modern Nucleophilic Aromatic Substitution*, Wiley-VCH Verlag GmbH & Co. KGaA, **2013**.

(2) Ai, H.-J.; Ma, X.; Song, Q.; Wu, X.-F. *Sci. China Chem.* **2021**, *64*, 1630–1659.

(3) For selected recent examples, see: (a) Yang, G.-H.; Liu, M.; Li, N.; Wu, R.; Chen, X.; Pan, L.-L.; Gao, S.; Huang, X.; Wang, C.; Yu, C.-M. *Eur. J. Org. Chem.* **2015**, *2015*, 616–624. (b) Podolan, G.; Jungk, P.; Lentz, D.; Zimmer, R.; Reissig, H.-U. *Adv. Synth. Catal.*, **2015**, *357*, 3215–3228. (c) Finck, L.; Oestreich, M. *Chem. – Eur. J.,* **2021**, *27*, 11061–11064.

(4) (a) Glukhovtsev, M. N.; Bach, R. D.; Laiter, S. *J. Org. Chem.* **1997**, *62*, 4036–4046. (b) Josefredo R. Pliego, J.; Piló-Veloso, D. *Phys. Chem. Chem. Phys.* **2008**, *10*, 1118–1124. (c) Kwan, E. E.; Zeng, Y.; Besser, H. A.; Jacobsen, E. N. *Nature Chem* **2018**, *10*, 917–923.

(5) For selected reviews on concerted S_NAr reactions, see: (a) Neumann, C. N.; Ritter, T. Facile *Acc. Chem. Res.* **2017**, *50*, 2822–2833. (b) Lennox, A. J. J. *Angew. Chem., Int. Ed.* **2018**, *57*, 14686–14688. (c) Rohrbach, S.; Smith, A. J.; Pang, J. H.; Poole, D. L.; Tuttle, T.; Chiba, S.; Murphy, J. A. *Angew. Chem., Int. Ed.* **2019**, *58*, 16368–16388.

(6) For recent selected examples, see: (a) Bizier, N. P.; Wackerly, J. Wm.; Braunstein, E. D.; Zhang, M.; Nodder, S. T.; Carlin, S. M.; Katz, J. L. *J. Org. Chem.* **2013**, *78*, 5987–5998. (b) Su, J.; Chen, Q.; Lu, L.; Ma, Y.; Auyoung, G. H. L.; Hua, R. *Tetrahedron* **2018**, *74*, 303–307.

(7) For selected recent examples, see: (a) Diness, F.; Fairlie, D. P. *Angew. Chem., Int. Ed.* **2012**, *51*, 8012–8016. (b) Meng, X.; Cai, Z.; Xiao, S.; Zhou, W. *J. Fluor. Chem.* **2013**, *146*, 70–75. (c) Lin, Y.; Li, M.; Ji, X.; Wu, J.; Cao, S. *Tetrahedron* **2017**, *73*, 1466–1472. (d) Iqbal, M. A.; Mehmood, H.; Lv, J.; Hua, R. *Molecules* **2019**, *24*, 1145. (e) Huang, H.; Lambert, T. H. *Angew. Chem., Int. Ed.* **2020**, *59*, 658–662. (f) Pistritto, V. A.; Schutzbach-Horton, M. E.; Nicewicz, D. A. *J. Am. Chem. Soc.* **2020**, *142*, 17187–17194.

(8) (a) Mallick, S.; Xu, P.; Würthwein, E.-U.; Studer, A. *Angew. Chem., Int. Ed.* **2019**, *58*, 283–287. (b) Liu, X.-W.; Zarate, C.; Martin, R. *Angew. Chem., Int. Ed.* **2019**, *58*, 2064–2068.

(9) You, Z.; Higashida, K.; Iwai, T.; Sawamura, M. *Angew. Chem., Int. Ed.* **2021**, *60*, 5778–5782.

(10) Caron, S.; Vazquez, E.; Wojcik, J. M. *J. Am. Chem. Soc.* **2000**, *122*, 712–713.

(11) Ji, X.; Huang, T.; Wu, W.; Liang, F.; Cao, S. *Org. Lett.* **2015**, *17*, 5096–5099.

(12) Ji, X.; Li, J.; Wu, M.; Cao, S. *ACS Omega* **2018**, *3*, 10099–10106.

(13) Fuchibe, K.; Imaoka, H.; Ichikawa, J. *Chem. –Asian J.* **2017**, *12*, 2359–2363.

(14) Takeda, M.; Nagao, K.; Ohmiya, H. *Angew. Chem., Int. Ed.* **2020**, *59*, 22460–22464.

(15) Silva, D. R.; Pliego, J. R. *Struct Chem* **2019**, *30*, 75–83.

(16) McMurry; J. *Organic Chemistry*, Brooks/Cole, New York, **2007**.

(17) Hatakeyama, T.; Ito, S.; Yamane, H.; Nakamura, M.; Nakamura, E. *Tetrahedron* **2007**, *63*, 8440–8448.

(18) For selected examples where, non-covalent interactions stabilized the transition state and/or intermediates by alkali cations, see: (a) Kennedy, C. R.; Lin, S.; Jacobsen, E. N. The *Angew. Chem., Int. Ed.* **2016**, *55*, 12596–12624. (b) Yamada, S. *Chem Rev* **2018**, *118* (23), 11353–11432. (c) D'Alterio, M. C.; Yuan, Y.-C.; Bruneau, C.; Talarico, G.; Gramage-Doria, R.; Poater, A. *Catal. Sci. Technol.* **2020**, *10*, 180–186. (d) Xu, L.-P.; Qian, S.; Zhuang, Z.; Yu, J.-Q.; Musaev, D. G. *Nat Commun* **2022**, *13*, 315.

(19) Gaussian16, Revision C.01, Frisch, M. J.; Trucks, G. W.; Schlegel, H. B.; Scuseria, G. E.; Robb, M. A.; Cheeseman, J. R.; Scalmani, G.; Barone, V.; Mennucci, B.; Petersson, G. A.; Nakatsuji, H.; Caricato, M.; Hratchian, X. Li, H. P.; Izmaylov, A. F.; Bloino, J.; Zheng, G.; Sonnenberg, J. L. Hada, M.; Ehara, M.; Toyota, K.; Fukuda, R.; Hasegawa, J.; Ishida, M.; Nakajima, T.; Honda, Y.; Kitao, O.; Nakai, H.; Vreven, T.; Montgomery, Jr., J. A.; Peralta, J. E.; Ogliaro, F.; Bearpark, M.; Heyd, J. J.; Brothers, E.; Kudin, K. N.; Staroverov, V. N.; Keith, T.; Kobayashi, R.; Normand, J.; Raghavachari, K.; Rendell, A.; Burant, J. C.; Iyengar, S. S.; Tomasi, J.; Cossi, M.; Rega, N.; Millam, J. M.; Klene, M.; Knox, J. E.; Cross, J. B.; Bakken, V.; Adamo, C.; Jaramillo, J.; Gomperts, R.; Stratmann, R. E.; Yazyev, O.; Austin, A. J.; Cammi, R.; Pomelli, C.; Ochterski, J.; Martin, W. R. L.; Morokuma, K.; Zakrzewski, V. G. G.; Voth, A.; Salvador, P.; Dannenberg, J. J.; Dapprich, S.; Daniels, A. D.; Farkas, O.; Foresman, J. B.; Ortiz, J. V.; Cioslowski, J. Fox, D. J. Gaussian, Inc., Wallingford CT, **2016**.

(20) Zhao, Y.; Truhlar, D. G. *Theor. Chem. Acc.* 2008, **120**, 215–241.

(21) (a) Weigend, F.; Ahlrichs, R.; *Phys. Chem. Chem. Phys.* 2005, **7**, 3297–3305; (b) Weigend, F.; *Phys. Chem. Chem. Phys.* **2006**, 8, 1057–1065.

(22) (a) Barone, V.; Cossi, M. *J. Phys. Chem. A* 1998, **102**, 1995–2001; (b) Cossi, M.; Rega, N.; Scalmani, G.; Barone, V. *J. Comput. Chem.* 2003, **24**, 669–681.

(23) (a) Mennucci, B.; Tomasi, J.; *J. Chem. Phys.*, **1997**, *106*, 5151–5158; (b) Fukui, K.; *Acc. Chem. Res.*, **1981**, *14*, 363–368; (c) Fukui, K. *J. Phys. Chem.* **1970**, *74*, 4161–4163.

(24) GaussView, Version 6.1, Dennington, R.; Keith, T. A.; Millam, J. M. Semichem Inc., Shawnee Mission, KS, **2016.**

(25) Dolomanov, O.V.; Bourhis, L.J.; Gildea, R. J.; Howard, J. A. K.; Puschmann, H. *J. Appl. Cryst.*, **2009**, *42*, 339.

(26) Sheldrick, G.M. *Acta Cryst.*, **2015**, *A71*, 3.

Chapter 3
Generation of Nickel Siloxycarbene Complexes from Acylsilanes for the Catalytic Synthesis of Silyl Enol Ethers

3.1. Introduction

Among the transition metal carbene complexes, Fischer carbene complexes, which are characterized by a coordinated carbene carbon bearing electronegative substituents, have held a prominent position in synthetic organic chemistry because of their unique reactivity profiles.[1,2] However, the generation of Fischer carbene complexes normally requires stoichiometric amounts of group 6 metal carbonyl complexes because heteroatom-substituted diazo compounds are unsuitable precursors due to their instability (**Scheme 1a**). This contrasts with other carbene complexes, which can be generated in situ from the corresponding diazo compounds, facilitating their use in numerous catalytic processes.[3,4] Recently, we reported that Fischer carbene complexes can be generated in situ from acylsilanes via palladium catalysis, enabling catalytic reactions involving Fischer carbene complexes, such as siloxycyclopropanation and β-lactam synthesis (**Scheme 1b**).[5] Although acylsilanes are known to isomerize to siloxycarbenes under visible-light irradiation or high-temperature conditions (>250 °C), [6] the short lifetime and nucleophilic nature of the resulting metal-free siloxycarbenes limit their applications.[7] Attempts to capture the photochemically generated siloxycarbene with transition metal complexes for the catalytic generation of Fischer carbene complexes have been made; however, this approach has met with limited success, presumably due to the challenge of capturing short-lived metal-free carbene species with a catalytic amount of metal complexes.[8] In this context, our palladium-catalyzed method provides an attractive alternative with potential application to an array of catalytic reactions because it depends solely on organometallic processes and avoids photoirradiation. To further expand the scope of this catalytic method, it is crucial to investigate whether the organometallic process involving the transformation of acylsilanes into siloxycarbene complexes can occur with metal species other than palladium. Herein, we report that nickel complexes can also mediate the generation of a siloxycarbene complex from acylsilanes (**Scheme 1c**). Importantly, this nickel-mediated organometallic process can be successfully applied not only to catalytic cyclopropanation and α-insertion reactions but also to the unusual catalytic addition to norbornene, which cannot be catalyzed by palladium. It should be noted that photochemical reactions of acylsilanes with external reagents to form silyl enol ethers have also been reported.[9]

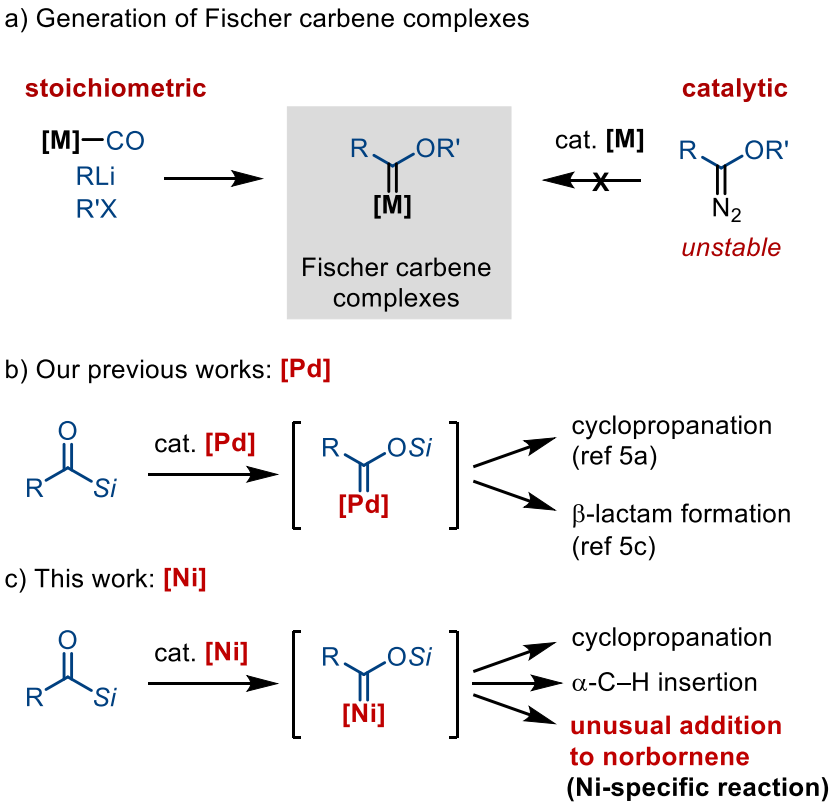

Scheme 1. Generation of Siloxycarbene-Metal Complexes from Acylsilanes.

3.2. Results and Discussion

We started our investigation by examining a cyclopropanation reaction using acylsilane **1a** and norbornene (**2a**) (Scheme 2). We previously reported that Pd–IPr and Pd–IPr* catalysts can efficiently promote this reaction, with the latter catalyst being more stereoselective (**Scheme 2a**). When the same reaction was conducted using $Ni(cod)_2$ (20 mol%) as a catalyst and IPr (20 mol%) as a ligand at 160 °C, cyclopropanated product **3a** was obtained in 3% yield (**Scheme 2b**). Although the major product was decarbonylation product **4a**,[10] the formation of **3a** clearly indicates that nickel can promote the generation of Fischer carbene complexes. When IPr was replaced with the bulkier ligand IPr*, the yield of **3a** increased to 55%. The yield was further improved to 79% by using norbornene as a limiting reagent (i.e., **1a**/**2a** = 2/1). Interestingly, the nickel catalyst afforded considerably better stereoselectivity than the palladium catalyst (24:1 for nickel vs. 6.5:1 for palladium), even though the nickel-catalyzed reactions required harsher conditions.

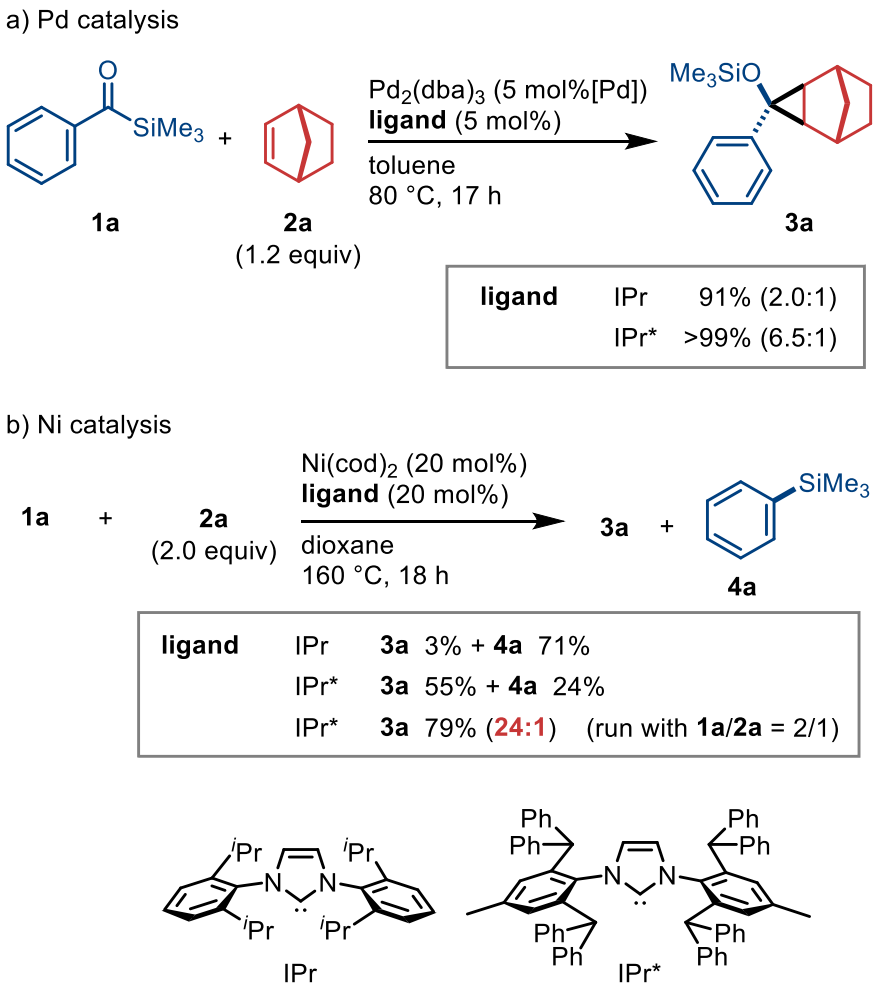

Scheme 2. Palladium- and Nickel-Catalyzed Cyclopropa-nation of **2a** with **1a**.

Next, we compared nickel and palladium catalysts in the reactions of acylsilanes with aliphatic substituents. When acylsilane **1b**, which bears a primary alkyl group, was reacted under the Pd–IPr*-catalyzed conditions, silyl enol ether **5b** was selectively obtained in 78% yield (**Scheme 3a**). Compound **5b** is presumably formed through an α-C–H insertion reaction of the postulated siloxycarbene complex, which is a common reaction pathway with carbene complexes bearing a β-hydrogen-containing alkyl substituent.[11] In contrast, the nickel-catalyzed reaction of **1b** exclusively yielded decarbonylation product **4b** in 80% yield. Next, acylsilane **1c**, which possesses a cyclohexyl group as a secondary alkyl substituent, was examined (**Scheme 3b**). In contrast to the reaction of **1b**, **1c** was converted into silyl enol ether **5c** under palladium- and nickel-catalyzed conditions without formation of decarbonylation product **4c**. Interestingly, nickel was a better catalyst than palladium with this specific substrate, as evidenced by the higher yield obtained with nickel (76% yield with nickel vs. 42% yield with palladium). Similarly, acylsilane **1d**, which also contains a secondary alkyl substituent, was also converted into silyl enol ether **5d** in quantitative yield by using a nickel catalyst. Acylsilane **1e** bearing a tertiary alkyl group failed to react irrespective of the catalyst, possibly due to its steric bulk inhibiting the initial oxidative addition of the C(acyl)–Si bond.

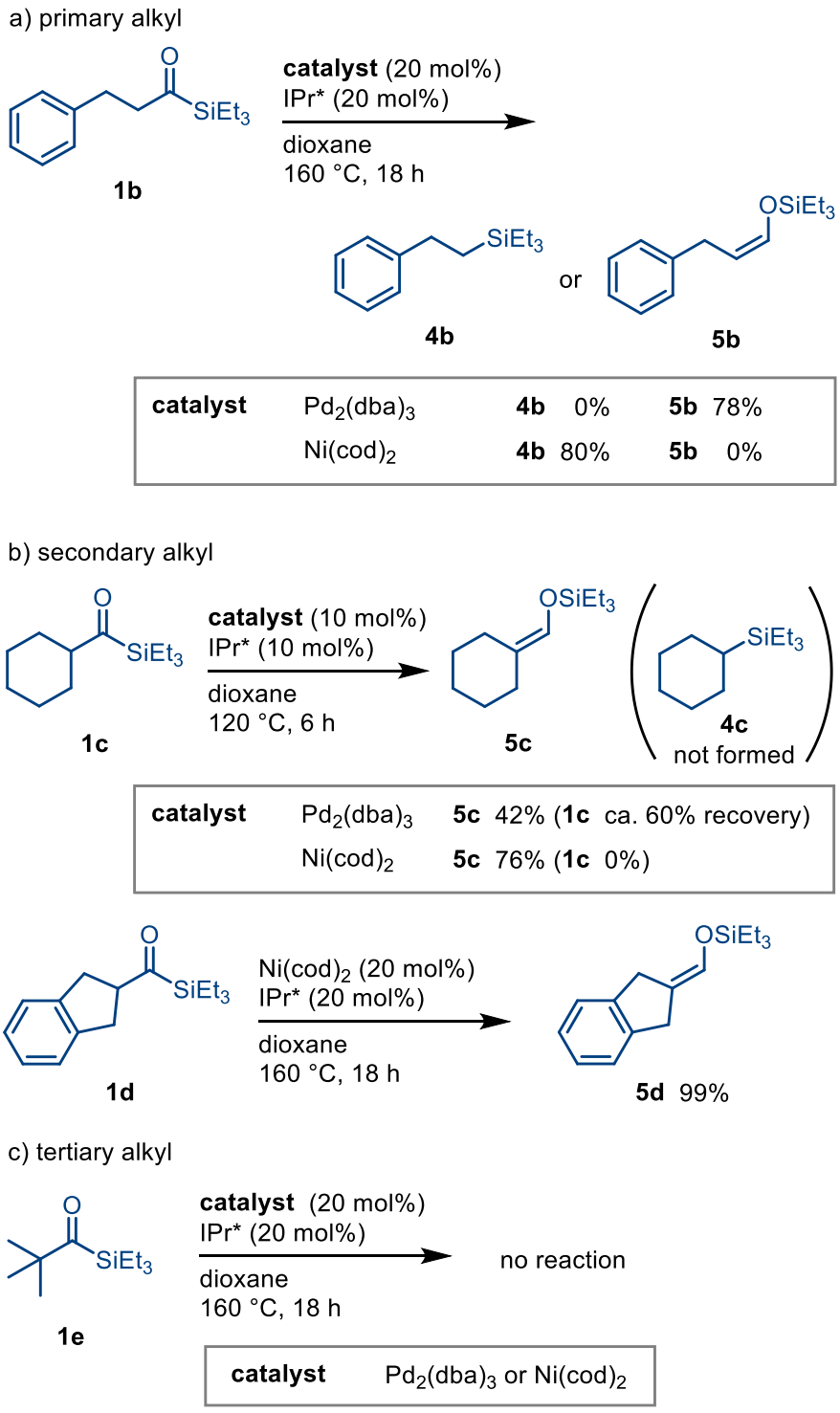

Scheme 3. Nickel-catalyzed α-Insertion of Aliphatic Acylsilanes

Next, we examined the reactions of aliphatic acylsilanes in the presence of **2a** to examine whether cyclopropanation occurs, as was observed for the reaction of aromatic acylsilane **1a**. The palladium-catalyzed reaction of **1b** with **2a** resulted in the selective formation of silyl enol ether **5b**, without incorporation of **2a** (**Scheme 4a**). In contrast, using nickel in place of palladium afforded silyl enol ether **6b** (56% isolated yield), in which **2a** was incorporated at the α-position of the siloxy group. It is noteworthy that the decarbonylation pathway was completely suppressed in the presence of **2a** (see **Scheme 3a**). The palladium and nickel catalysts were also compared in the reaction of secondary alkyl–substituted acylsilane **1c** with **2a** (**Scheme 4b**). As observed with **1b**,

1c afforded α-C–H insertion product **5c** using palladium, whereas addition to **2a** occurred to form **6c** in the case of nickel. The structure of **6c** was unambiguously determined by means of an X-ray crystallography analysis of the derivatized hydrazone **7c** (Scheme 4c). The nickel-catalyzed reaction of aliphatic acylsilanes with **2a** was found to be general, as evidenced by the formation of **6d** and **6f** from acylsilanes **1d** and **1f**, respectively. Meanwhile, using other alkenes instead of **2a**, such as 1-octene, styrene, vinyltrimethylsilane, *tert*-butyl acrylate, and acenaphthylene, did not afford the corresponding products under these nickel-catalyzed conditions.

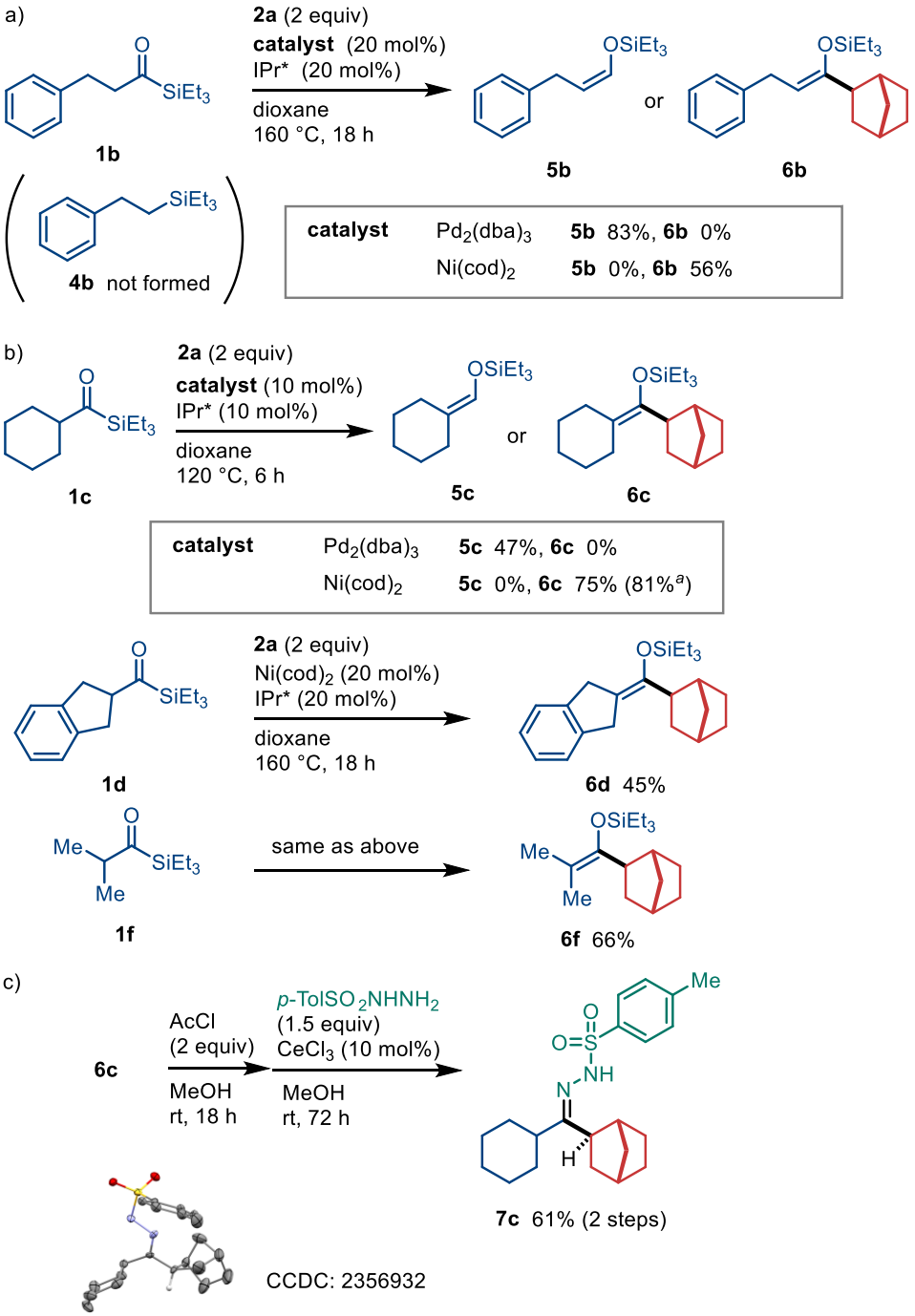

Scheme 4. Nickel-Catalyzed Synthesis of Silyl Enol Ethers from Alkanoylsilanes and **2a**
*a*Run with **2a** (3 equiv), Ni(cod)2 (20 mol%), and IPr* (20 mol%) at 160 °C for 18 h.

We conducted several mechanistic studies to obtain insights into the reaction mechanism. When silyl enol ether **5c** was reacted with **2a** under the standard nickel-catalyzed conditions, no reaction occurred (**Scheme 5a**), which allowed excluding **5c** as an intermediate for the formation of **6c**. Next, the reaction with labeled substrate **1c-*d***, in which the α-position of the acylsilane was deuterated (**Scheme 5b**), furnished silyl enol ether **6c-*d*** with the 98% of the deuterium being incorporated into the 3-position of the norbornane skeleton in a stereoselective manner.

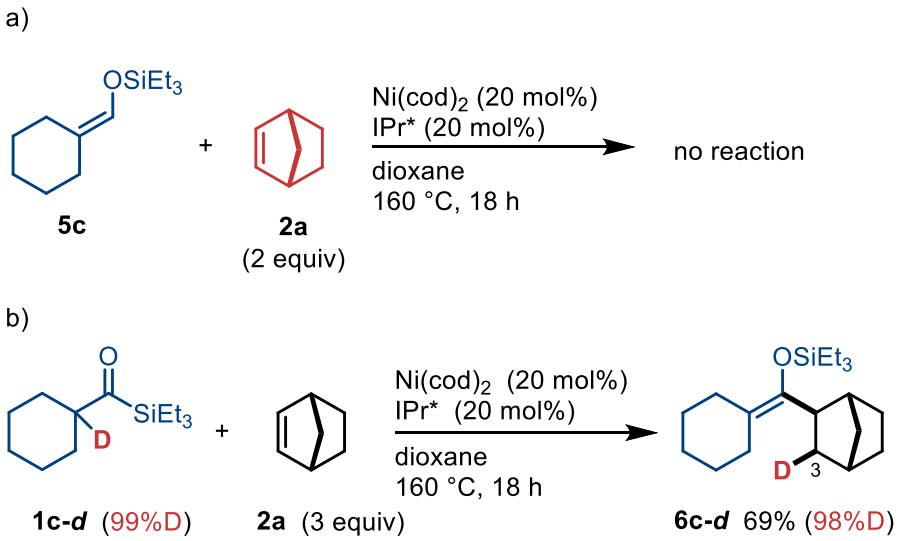

Scheme 5. Mechanistic Studies

We investigated computationally the origin of the different behaviors between palladium and nickel using density functional theory (DFT) calculations at the ωB97XD/SDD-6-311+G(d,p)-SDD//ωB97XD/LANL2DZ-6-31G(d,p)-SDD level of theory (**Scheme 6**). First, we examined the palladium-catalyzed reactions of primary alkyl–substituted acylsilane (Scheme 6a). The initial oxidative addition of the C(acyl)–Si bond was found to proceed with an activation barrier of 8.6 kcal/mol to form **INT1** (see SI for details). The oxidative addition complex **INT1** can then undergo two possible pathways. One is the extrusion of CO to form **INT2**; however, this is an unfavorable endergonic process (ΔG = +21.1 kcal/mol) with a high activation barrier of 26.2 kcal/mol. In contrast, 1,3-migration of a silyl group in **INT1** to form siloxycarbene complex **INT3** would occur in an exergonic manner (ΔG = −1.0 kcal/mol) with a lower activation barrier (22.3 kcal/mol), which renders this pathway more favored than decarbonylation. Subsequently, **INT3** undergoes insertion into an α-C–H bond via **TS3** to form **INT4**. Similarly, in the case of a secondary alkyl–substituted substrate, the activation barrier for decarbonylation from the corresponding oxidative addition complex **INT5**[12] was substantially higher than that required for the α-insertion reaction.[13] These results are in agreement with the experimental observation that alkyl-substituted acylsilanes led exclusively to α-insertion products rather than decarbonylation products (Scheme 3a, b).

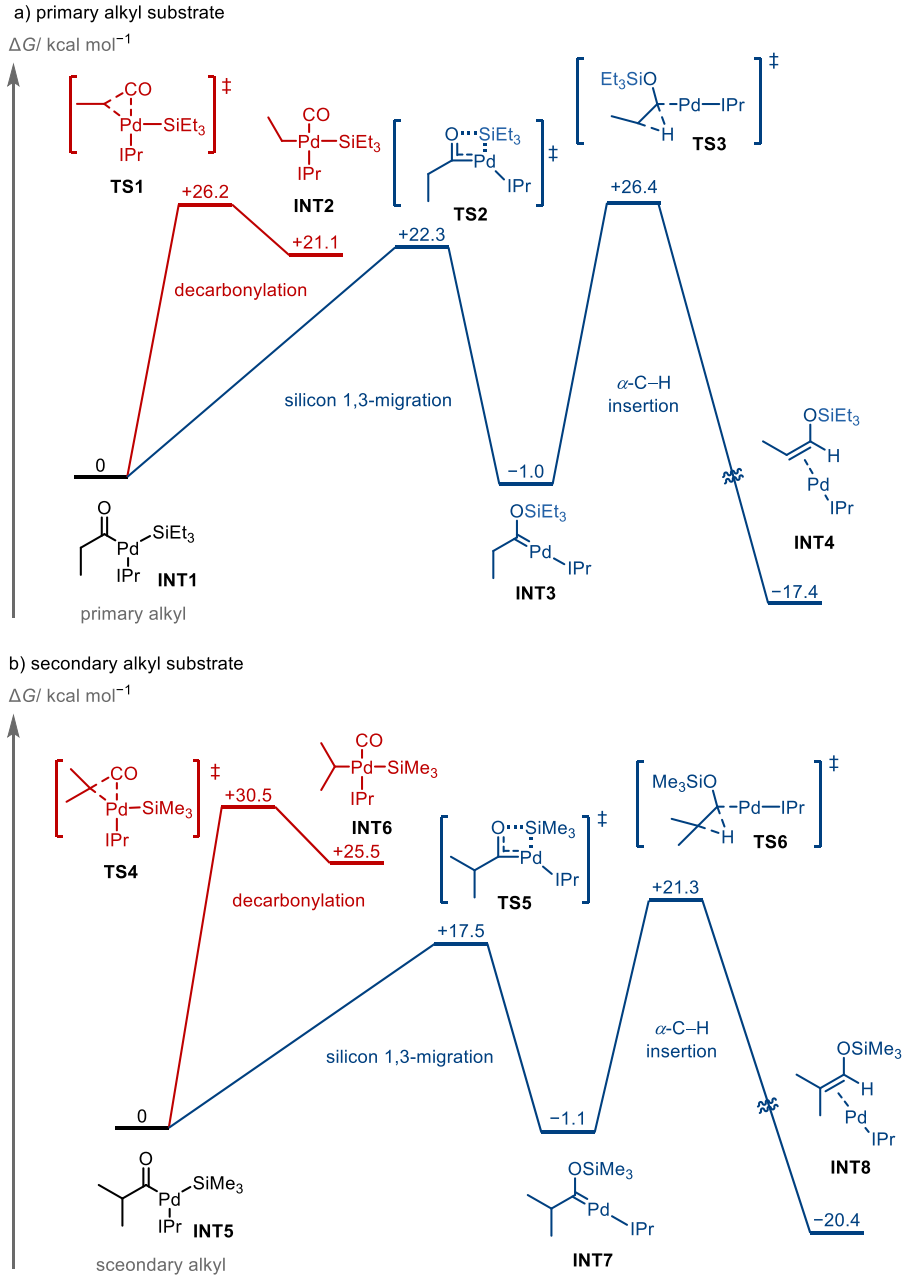

Scheme 6. Plausible Reaction Pathways for the Palladium-Catalyzed System[a]
[a]DFT calculations were conducted at the ωB97XD/6-311+G(d,p)-SDD//ωB97XD/6-31G(d,p)-LanI2DZ level of theory. Red: decarbonylation; blue: α-insertion via a siloxycarbene-palladium complex.

A similar comparison was also performed for the nickel-catalyzed system (**Scheme 7**). In the case of primary alkyl–substituted acylsilanes, the activation barrier for decarbonylation from oxidative addition complex **INT9**[14] was considerably lower (9.8 kcal/mol, **TS7**) than that required with the Pd catalyst (26.2 kcal/mol, **TS1** in Scheme 6).[15] Meanwhile, the activation barriers for the formation of the silyl enol ether via siloxycarbene-nickel complex **INT11** were comparable to those calculated for the palladium catalyst (19.0 kcal/mol for **TS8** and 25.1 kcal/mol for **TS9**). These results are consistent with the experimental observation that decarbonylation occurred with the nickel catalyst when primary alkyl–substituted acylsilanes were used (Scheme 3a). In the case of secondary alkyl–substituted substrates, the activation barrier required for decarbonylation from oxidative addition complex **INT14**[16] increased to 22.0 kcal/mol (i.e., **TS11**), possibly due to the increased steric demand for C–C bond activation, which makes the α-C–H insertion pathway more energetically feasible, as was experimentally observed

(Scheme 3b). It should be noted that the mechanism for the α-insertion from siloxycarbene-nickel complexes (*i.e.*, **INT11** or **INT16**) differs from that involving the palladium catalyst. While siloxycarbene-palladium complexes undergo α-C–H insertion in a concerted manner without any intermediate (**Scheme 6**), a β-hydrogen elimination/reductive elimination sequence occurs in the case of siloxycarbene-nickel complexes via a nickel-hydride intermediate (i.e., **INT12** or **INT17**) to form α-insertion products.

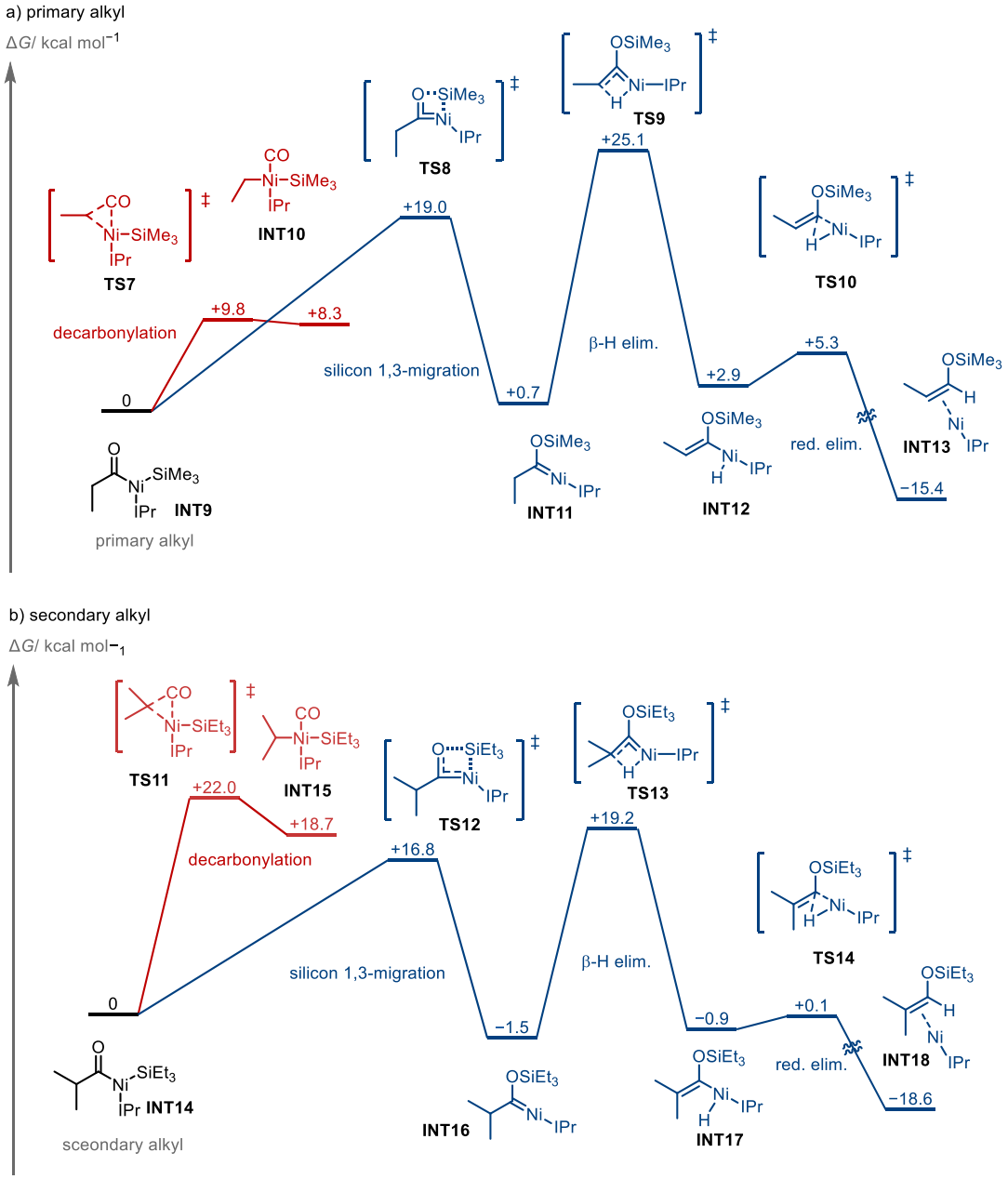

Scheme 7. Plausible Reaction Pathways for the Nickel-Catalyzed System[a]
[a]DFT calculations were conducted at the ωB97XD/6-311+G(d,p)-SDD//ωB97XD/6-31G(d,p)-LanI2DZ level of theory. Red: decarbonylation; blue: α-insertion via a siloxycarbene-palladium complex.

Finally, we investigated the mechanism for the nickel-catalyzed reaction of aliphatic acylsilanes with norbornene via DFT calculations using the reaction of isopropyl-substituted acylsilane with ethylene catalyzed by a Ni–IPr complex as a model reaction (**Scheme 8**). The oxidative addition of the C(acyl)–Si bond to the Ni–IPr complex was revealed to proceed via three-centered transition state **TS15** with an activation barrier of 18.2 kcal/mol, leading to the formation of oxidative addition complex **INT20**. Intermediate **INT20** can isomerize through

migration of the silyl group to the oxygen atom of the acyl ligand via **TS16** with a feasible energetic barrier (20.4 kcal/mol), furnishing siloxycarbene-nickel complex **INT21**. Upon addition of ethylene, **INT21** forms a more stable three-coordinate complex, i.e., **INT22**, which subsequently undergoes a concerted α-C–H insertion through transition state **TS15** to produce silyl enol ether–ligated nickel complex **INT23**. This α-C–H insertion process, which requires the highest activation barrier (30.3 kcal/mol) during the reaction pathway, is the turnover-limiting step. Subsequently, **INT23** undergoes ligand-to-ligand hydrogen transfer (LLHT)[17] via **TS18** (3.4 kcal/mol) to form **INT24**. The resulting intermediate **INT24** affords the silyl enol ether product via reductive elimination.

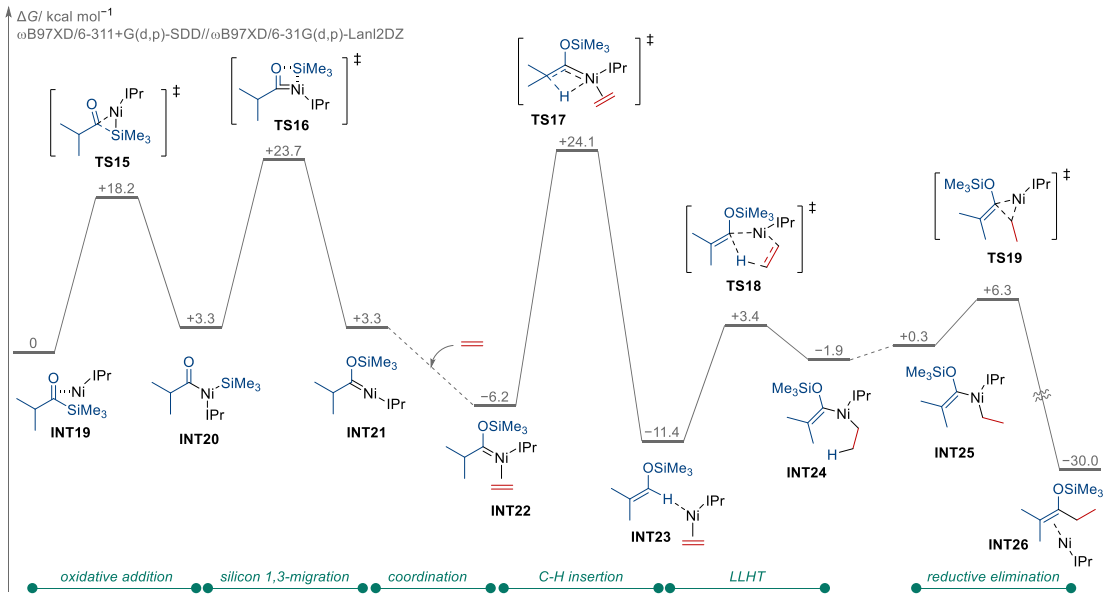

Scheme 8. DFT-Computed Energy Profile for the Nickel-Catalyzed Reaction of Aliphatic Acylsilanes with Ethylene to Form Silyl Enol Ethers

Scheme 8. DFT-Computed Energy Profile for the Nickel-Catalyzed Reaction of Aliphatic Acylsilanes with Ethylene to Form Silyl Enol Ethers

According to the experimental and theoretical studies discussed above, a plausible mechanism for the nickel-catalyzed reactions of aliphatic acylsilanes is depicted in Scheme 9. First, the C(acyl)–Si bond of the acylsilane substrate is oxidatively added to the nickel catalyst to form **A**, which can then undergo two possible pathways. When a primary alkyl–substituted acylsilane is used in the absence of **2a**, complex **A** predominantly undergoes decarbonylation. This decarbonylation pathway can be suppressed by adding **2a**, presumably because it occupies a vacant coordination site that is required for the decarbonylation, or by using bulkier secondary alkyl–substituted acylsilane substrates. In these cases, the silicon group in **A** migrates to the oxygen atom to form siloxycarbene-nickel complex **B**. Carbene complex **B** undergoes α-C–H insertion via nickel-hydride **C** to furnish a silyl enol ether when secondary alkyl–substituted acylsilanes are reacted in the absence of **2a**. Meanwhile, in the presence of **2a**, carbene complex **B** undergoes α-C–H insertion in a concerted manner to form enol ether complex **E**,[18] which immediately forms alkenyl-nickel species **F** via LLHT. Subsequent reductive elimination from **F** affords two-component coupling product **G**.

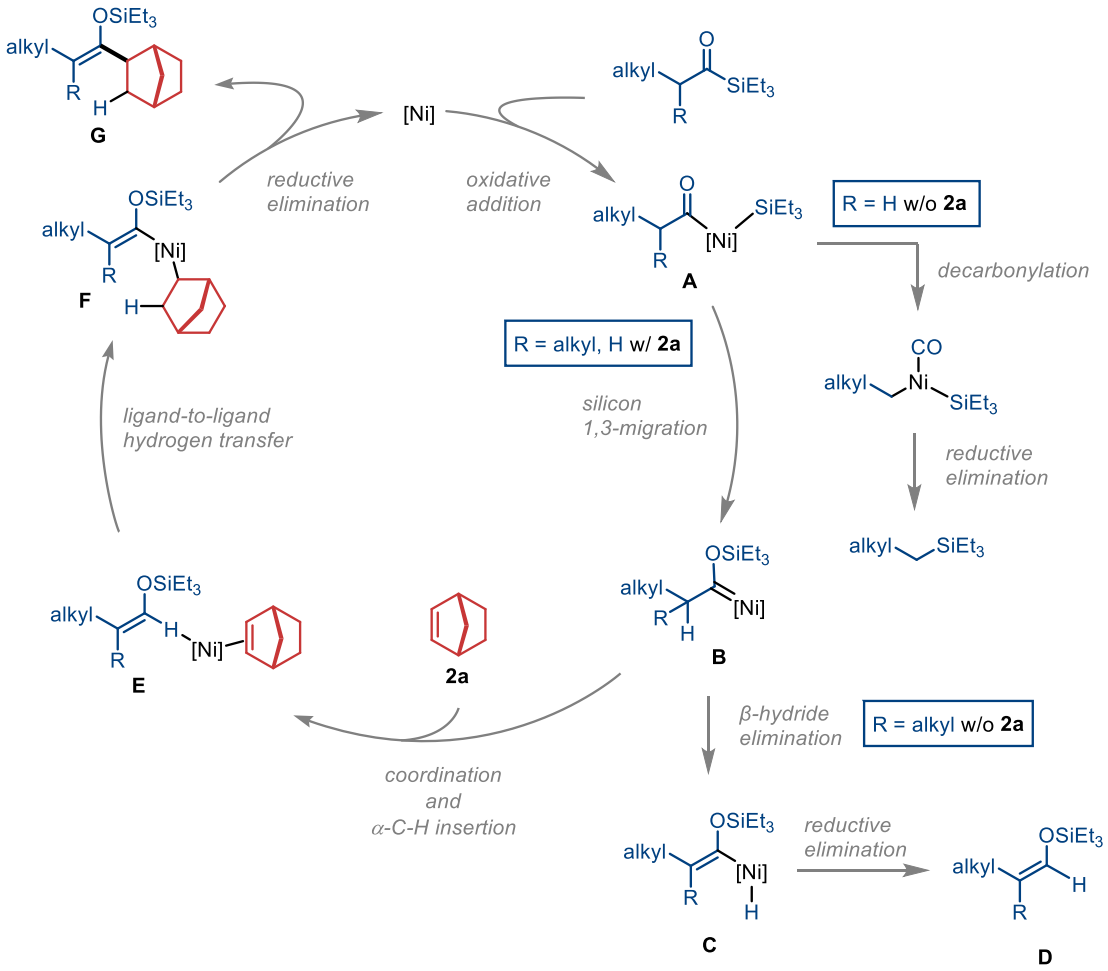

Scheme 9. Plausible Mechanism for the Nickel-Catalyzed Reactions of Aliphatic Acylsilanes

3.3. Conclusion

In summary, we have demonstrated that generation of siloxycarbene complexes from acylsilanes via oxidative addition of a C–Si bond followed by 1,3-silicon migration is not limited to palladium but can be also catalyzed by nickel. This protocol enables the generation of otherwise inaccessible Fischer carbene complexes of nickel. When aromatic acylsilanes are used, the resulting siloxycarbene-nickel intermediate undergoes cyclopropanation with alkenes, as in the case of palladium. Nickel-catalyzed reactions of aliphatic acylsilanes follow two distinct pathways depending on the bulkiness of the acyl substituents: primary alkyl–substituted acylsilanes afford decarbonylation products, whereas substrates with secondary alkyl groups form silyl enol ethers via α-C–H insertion from a siloxycarbene-nickel intermediate. These results contrast sharply with those obtained using the palladium-catalyzed system, which uniformly provides silyl enol ethers from aliphatic acylsilanes. Most notably, nickel-catalyzed reactions of aliphatic acylsilanes with norbornene furnish two-component coupling products, in which a C–H bond of the silyl enol ethers adds across norbornene. These findings underscore that the reactivity of siloxycarbene complexes is markedly influenced by the nature of the metal center, enabling new catalytic transformations using acylsilanes. Studies on further applications of siloxycarbene-Pd and -Ni complexes, as well as exploration of other late transition metals, are currently underway in our laboratory.

3.4. Experimental Section

I. General Information

^{1}H, ^{13}C and ^{19}F NMR spectra were recorded on a JEOL ECS-400 spectrometer in $CDCl_3$ or C_6D_6. The chemical shifts in ^{1}H NMR spectra were recorded relative to $CHCl_3$ (δ 7.26) or C_6H_6 (δ 7.15). The chemical shifts in ^{13}C NMR spectra were recorded relative to $CDCl_3$ (δ 77.00) or C_6D_6 (δ 128.00). Data are given as follows: chemical shifts in ppm (δ), multiplicity (s = singlet, d = doublet, t = triplet, q = quartet, brs = broad singlet, brd = broad doublet, m = multiplet, c = complex), coupling constant (Hz), and integration. Infrared spectra (IR) were recorded on a JASCO FT/IR-4200 spectrometer using the ATR method. Absorption data are reported in reciprocal centimeters from 800 to 3500 cm^{-1} with the following relative intensities: s (strong), m (medium), or w (weak). Mass spectra and high-resolution mass spectra (HRMS) were obtained on a JEOL JMS-700 or JMS-T100LP (DART TOF & ESI-TOF) spectrometer. Analytical gas chromatography (GC) was carried out on a Shimadzu GC-2014 gas chromatograph, equipped with a flame ionization detector. Column chromatography was performed with SiO_2 (Silica Gel 60 N (spherical, neutral) (40-50 Pm), (KANTO CHEMICAL CO., INC.). Medium-pressure liquid chromatography (MPLC) was performed with Biotage Isolera®. Preparative gel permeation chromatography (GPC) was carried out on a JAI LC-5060 equipped with two JAIGEL-2HR columns connected in series or two JAIGEL-2HR-40 columns connected in series.

For safety considerations, high-temperature reactions were conducted in pressure-resistant, screw-capped vials (purchased from ACE GLASS), with the surrounding area shielded by explosion-proof plates during the reaction.

II. Materials

Toluene (super dehydrated), 1,4-dioxane (super dehydrated), $Ni(cod)_2$, $Pd_2(dba)_3$ and 2-indancarboxylic acid were purchased and used as received. IPr* [CAS: 1262284-06-9] was prepared according to the literature method. [19] Acylsilanes **1a** ([5908-41-8]),[20] **1b** ([591768-00-2]), **1c** ([136578-54-6]), **1e** ([461051-97-8]), **1f** ([461051-96-7]), and **1g** ([461051-97-8]) were prepared according to the literature method. [21]

III. Synthesis of Acylsilanes 1c

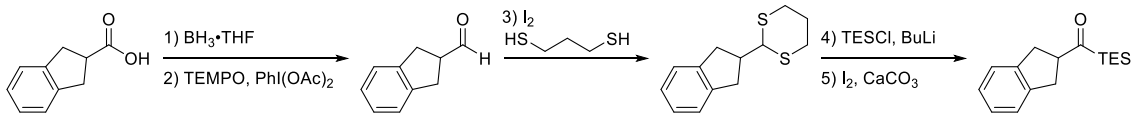

The acylsilane **1c** was prepared from 2-indancarboxylic acid via the following five steps.

Step1)

To a 50 mL round-bottom flask with a magnetic stir bar, 2-indancarboxylic acid (2.0g, 12.4 mmol) and THF (16 mL) were added. After the mixture was cooled to 0 °C, BF_3-THF complex (1.0 M in THF, 13.5 mmol, 1.1 equiv) was added dropwise to the solution via syringe. The reaction was stirred at rt for 18 h. The resulting mixture was quenched with MeOH (10 mL) and filtered through a pad of silica gel. The filtrate was concentrated in vacuo. The crude alcohol product was used in the next reaction without further purification.

Step2)

To a dry 200 mL round-bottom flask with a magnetic stir bar, the alcohol (ca. 10 mmol), TEMPO (156 mg, 1.0 mmol, 10 mol%), $PhI(OAc)_2$ (6.5g, 20 mmol, 2.0 equiv) and EtOAc (85 mL) were added. The mixture was stirred at rt under N_2 for 18 h. The resulting mixture was washed with sat. $NaHCO_3$ aq and the aqueous layer was extracted with EtOAc (150 mL). The combined organic extracts were dried over $MgSO_4$, filtered and concentrated in vacuo. The residue was passed through a short pad of silica gel to remove a remaining alcohol. The filtrate was concentrated in vacuo to give a crude aldehyde product, which was used in the next reaction without further purification.

Step3)

To a 300 mL round-bottom flask with a magnetic stir bar, the aldehyde (ca. 10 mmol), iodine (0.26g, 1.0 mmol, 10 mol%), 1,3-propanedithiol (1.15 mL, 11 mmol, 1.1equiv) and $CHCl_3$ (100 mL) were added. The mixture was stirred at rt for 18 h. The resulting mixture was quenched with sat. $Na_2S_2O_4$ aq, and $CHCl_3$ was removed in vacuo. The mixture was extracted with EtOAc (100 mL), and the organic extract was washed 10 wt% NaOH aq and H_2O. The organic extracts were dried over $MgSO_4$, filtered and concentrated in vacuo. The crude dithiane product was used in the next reaction without further purification.

Step4)

To a dry 100 mL round-bottom flask with a magnetic stir bar, the dithiane (ca. 5.9 mmol) was added. THF (17 mL) and TMEDA (1.06 mL, 7.1 mmol, 1.2equiv) were then added via syringe. The resulting solution was cooled to –40 °C under N_2, and *n*-BuLi (1.6 M in hexanes, 7.1 mmol, 1.2 equiv) was added dropwise to the solution via syringe. After the reaction was stirred at –40 °C for 2 h, Et_3SiCl (4.6 mL, 7.1 mmol, 1.2 equiv) was added dropwise via syringe at –78 °C. The reaction was stirred at –78 °C for 2 h and then quenched with sat. NH_4Cl aq. The organic layer was separated and washed with H_2O, and the aqueous layer was extracted with Et_2O (100 mL). The combined organic extracts were dried over $MgSO_4$, filtered and concentrated to dryness in vacuo. The crude silylated dithiane product was used in the next reaction without further purification.

Step5)

To a 100 mL round-bottom flask with a magnetic stir bar, the silylated dithiane (ca. 5.9 mmol) and $CaCO_3$ (4.77g, 47.2 mmol, 8 equiv), iodine (9.09g, 35.4 mmol, 6 equiv), THF (33 mL) and H_2O (8.2 mL) were added. The mixture was stirred at rt for 18 h. After the resulting mixture was quenched with sat. $Na_2S_2O_4$ aq, the mixture was extracted with EtOAc (200 mL). The organic layer was washed with H_2O, dried over $MgSO_4$, and filtered through a pad of silica gel. The filtrate was concentrated in vacuo. The residue was purified by GPC to afford the desired product as a light yellow oil (890 mg, 28% for 5 steps).

$\boldsymbol{R_f}$ 0.25 (hexane/EtOAc = 1/10).

^{1}H NMR (399.78 MHz, chloroform-*d*) δ 0.78-0.85 (m, 6H), 1.01 (t, J = 7.8 Hz, 9H), 3.05 (dd, J = 15.6, 9.2 Hz, 2H), 3.20 (q, J = 7.8 Hz, 2H), 3.68-3.77 (m, 1H), 7.15 (dt, J = 9.3, 3.4 Hz, 2H), 7.20 (dt, J = 8.7, 3.4 Hz, 2H)

^{13}C NMR (100.53 MHz, chloroform-*d*) δ 2.5, 7.3, 33.0, 56.4, 124.4, 126.5, 141.5, 246.5.

IR (ATR) 2953 w, 2911 w, 2975 w, 1635 m, 1459 m, 1003 m, 734 s, 694 s, 416 m.

MS: *m/z* (EI, relative intensity, %) 260 (2.4, M^+), 129 (17), 117 (10), 116 (34), 115 (100), 103 (18), 87 (84), 59 (32).

HRMS ($[M+H]^+$) Calcd for $C_{16}H_{24}OSi$: 260.1596; Found: 260.1599.

IV. Synthesis of (cyclohexyl-1-*d*)(triethylsilyl)methanone (1c-*d*)

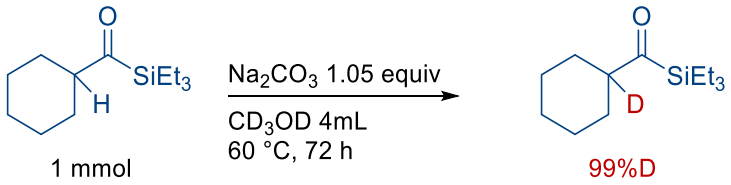

To an oven-dried 10 mL screw-capped vial, (cyclohexyl)(triethylsilyl)methanone (**1c**, 226 mg, 1.0 mmol), Na_2CO_3 (0.112 g, 1.05 mmol), and MeOH-d_4 (4.0 mL) were added. The mixture was stirred at 60 °C for 72 h, followed by cooling. The resulting mixture was washed with H_2O (10 mL) and extracted with Et_2O (30 mL). The organic layer was filtered and concentrated to dryness in vacuo and the residue was purified by MPLC (hexane/EtOAc = 1/9) to afford the desired product as a colorless oil (205 mg, 91%).

***R*f** 0.80 (hexane/EtOAc = 1/10)

^{1}H NMR (399.78 MHz, benzene-d_6) δ 0.61–0.70 (m, 6H), 0.89–0.96 (m, 8H), 1.03–1.18 (m, 4H), 1.29 (t, J = 12.4 Hz, 2H), 1.48–1.51 (m, 1H), 1.62–1.66 (m, 2H), 1.72 (d, J = 13.3 Hz, 2H).

^{2}D NMR (399.78 MHz, benzene) δ 2.69 (s, 1D)

^{13}C NMR (100.53 MHz, benzene-d_6) δ 2.9, 7.6, 26.0, 26.1, 26.7 55.7 (t, J = 19.5 Hz), 247.6.

IR (ATR) 2953 m, 2929 s, 2876 m, 2854 m, 1704 s, 1630 m, 1009 m, 734 s, 696 m.

MS: *m/z* (EI, relative intensity, %) 227 (0.37, M^+), 143 (69), 117 (13), 116 (46), 115 (100), 103 (22), 88 (25), 87 (100), 75 (19), 59 (75), 58 (14).

HRMS ($[M+H]^+$) Calcd for $C_{13}H_{26}DOSi$: 228.1889; Found: 228.1891.

V. Ni-Catalyzed Cyclopropanation of Norbornene with Acylsilanes

Trimethyl((3-phenyltricyclo[3.2.1.0^{2,4}]octan-3-yl)oxy)silane (3a: 2757322-85-1).

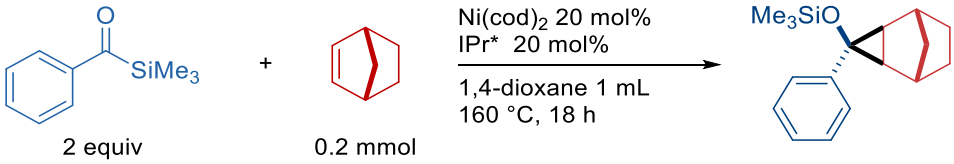

In a glove box, to an oven-dried 10 mL screw-capped vial, $Ni(cod)_2$ (11.0 mg, 0.040 mmol), IPr* (36.6 mg, 0.040 mmol), phenyl(trimethylsilyl)methanone (**1a**, 77.4 mg, 0.40 mmol), norbornene (**2a**, 19.3 mg, 0.20 mmol), and 1,4-dioxane (1.0 mL) were added. The cap was closed and the resulting mixture was stirred at 160 °C for 18 h. After cooling to rt, the resulting mixture was filtered through a celite pad. The filtrate was concentrated to dryness in vacuo and the residue was purified by MPLC (hexane to hexane/EtOAc = 1/9) to afford the desired product (colorless oil, R_f = 0.33 (hexane:EtOAc = 10:1), yield = 79%, m = 43.7 mg).

^{1}H NMR (399.78 MHz, benzene-d_6) δ –0.01 (s, 9H), 0.76 (d, J = 9.6 Hz, 1H), 1.04 (s, 2H), 1.16–1.19 (m, 2H), 1.42–1.44 (m, 2H), 2.41 (dt, J = 9.3, 2.1 Hz, 1H), 2.59 (s, 2H), 7.01–7.05 (m, 1H), 7.09–7.13 (m, 2H), 7.35–7.38 (m, 2H).

^{13}C NMR (100.53 MHz, benzene-d_6) δ 0.8, 30.4, 31.4, 31.5, 37.7, 65.6, 127.2, 127.8, 127.9, 128.0, 128 .2, 128.3, 145.6.

HRMS ($[M+H]^+$) Calcd for $C_{17}H_{25}OSi$: 273.1669; Found: 273.1670.

VI. Pd- and Ni-Catalyzed a-Insertion of Aliphatic Acylsilanes

(*Z*)-Triethyl((3-phenylprop-1-en-1-yl)oxy)silane (5b: 52341-10-3).

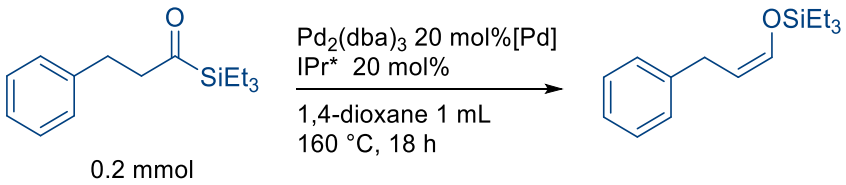

0.2 mmol

In a glove box, to an oven-dried 10 mL screw-capped vial, $Pd_2(dba)_3$ (18.3 mg, 0.020 mmol), IPr* (36.6 mg, 0.040 mmol), 3-phenyl-1-(triethylsilyl)propan-1-one (**1b**, 49.7 mg, 0.20 mmol), and 1,4-dioxane (1.0 mL) were added. The cap was closed and the resulting mixture was stirred at 160 °C for 18 h. After cooling to rt, the resulting mixture was filtered through a celite pad. The filtrate was concentrated to dryness in vacuo and the residue was purified by MPLC (hexane to hexane/EtOAc = 1/9) to afford the desired product (colorless oil, R_f = 0.20 (hexane), yield = 78%, m = 30.4 mg).

^{1}H NMR (399.78 MHz, benzene-d_6) δ 0.55 (q, J = 7.9 Hz, 6H), 0.94 (t, J = 8.0 Hz, 9H), 3.61 (d, J = 7.3 Hz, 2H), 4.69–4.76 (m, 1H), 6.26 (dt, J = 5.8, 1.5 Hz, 1H), 7.06 (t, J = 7.1 Hz, 1H), 7.16–7.20 (m, 2H), 7.22–7.27 (m, 2H)

^{13}C NMR (100.53 MHz, benzene-d_6) δ 4.7, 6.7, 30.4, 109.6, 126.0, 128.6, 128.7, 139.2, 142.2.

HRMS (M^+) Calcd for $C_{15}H_{25}OSi^+$: 249.16692; Found: 249.16670.

Triethyl(phenethyl)silane (4b: 14355-62-57).

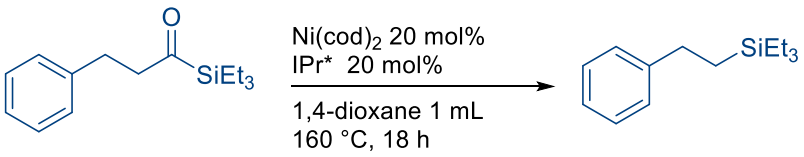

0.2 mmol

In a glove box, to an oven-dried 10 mL screw-capped vial, $Ni(cod)_2$ (11.0 mg, 0.040 mmol), IPr* (36.6 mg, 0.040 mmol), 3-phenyl-1-(triethylsilyl)propan-1-one (**1b**, 49.7 mg, 0.20 mmol), and 1,4-dioxane (1.0 mL) were added. The cap was closed and the resulting mixture was stirred at 160 °C for 18 h. After cooling to rt, the resulting mixture was filtered through a celite pad. The filtrate was concentrated to dryness in vacuo and the residue was purified by MPLC (hexane to hexane/EtOAc = 1/9) to afford the desired product (colorless oil, R_f = 0.78 (hexane), yield = 80%, m = 39.6 mg).

^{1}H NMR (399.78 MHz, benzene-d_6) δ 0.44 (q, J = 7.9 Hz, 6H), 0.78–0.82 (m, 2H), 0.89 (t, J = 8.0 Hz, 9H), 2.49–2.54 (m, 2H), 7.03–7.17 (m, 5H).

^{13}C NMR (100.53 MHz, benzene-d_6) δ 3.5, 7.7, 13.9, 30.4, 125.9, 128.1, 128.6, 145.6.

HRMS (M^+) Calcd for $C_{14}H_{24}Si^+$: 220.1642; Found: 220.1640.

(Cyclohexylidenemethoxy)triethylsilane (4c: 7030-75-3).

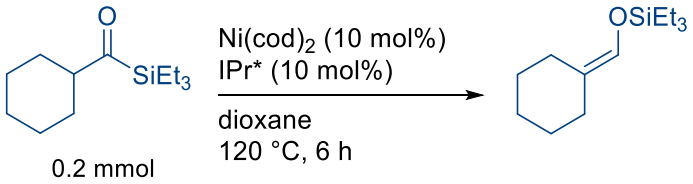

0.2 mmol

In a glove box, to an oven-dried 10 mL screw-capped vial, $Ni(cod)_2$ (11.0 mg, 0.040 mmol), IPr* (36.6 mg, 0.040 mmol), cyclohexyl(triethylsilyl)methanone (**1c**, 45.3 mg, 0.20 mmol), and 1,4-dioxane (1.0 mL) were added. The cap was closed and the resulting mixture was stirred at 120 °C for 6 h. After cooling to rt, the resulting mixture was filtered through a celite pad. The filtrate was concentrated to dryness in vacuo and the residue was purified by MPLC (hexane to hexane/EtOAc = 1/9) to afford the desired product (colorless oil, R_f = 0.13 (hexane), yield = 76%, m = 34.8 mg).

^{1}H NMR (399.78 MHz, benzene-d_6) δ 0.61 (q, J = 7.9 Hz, 6H), 0.98 (t, J = 8.0 Hz, 9H), 1.46–1.54 (m, 6H), 1.97 (t, J = 5.3 Hz, 2H), 2.39–2.42 (m, 2H), 6.20 (t, J = 1.1 Hz, 1H).

^{13}C NMR (100.53 MHz, benzene-d_6) δ 4.8, 6.8, 25.8, 27.4, 27.4, 28.9, 30.9, 121.2, 131.2.

HRMS (M^+) Calcd for $C_{13}H_{27}OSi^+$: 227.18257; Found: 227.18162.

((1,3-Dihydro-2*H*-inden-2-ylidene)methoxy)triethylsilane (5d).

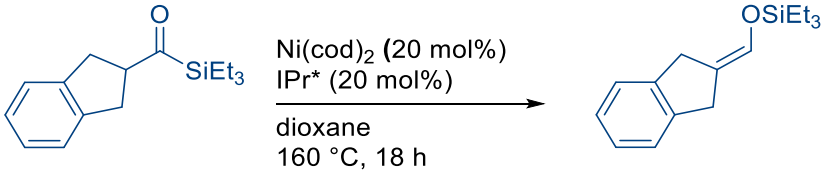

0.2 mmol

To an oven-dried 10 mL screw-capped vial in a glove box, $Ni(cod)_2$ (18.3 mg, 0.020 mmol), IPr* (36.6 mg, 0.040 mmol), (2,3-dihydro-1*H*-inden-2-yl)(triethylsilyl)methanone (**1d**, 52.1 mg, 0.20 mmol), and 1,4-dioxane (1.0 mL) were added in sequential order. The cap was closed and the resulting mixture was stirred at 160 °C for 18 h. After cooling to rt, the resulting mixture was filtered through a celite pad. The filtrate was concentrated to dryness in vacuo and the residue was purified by MPLC (hexane to hexane/EtOAc = 1/9) to afford the desired product (colorless oil, R_f = 0.20 (hexane), yield = 99%, m = 49.5 mg).

^{1}H NMR (399.78 MHz, benzene-d_6) δ 0.66 (q, J = 7.9 Hz, 6H), 1.04 (t, J = 7.8 Hz, 9H), 3.61 (s, 2H), 3.91 (q, J = 1.2 Hz, 2H), 6.42–6.44 (m, 1H), 7.14–7.21 (m, 4H).

^{13}C NMR (100.53 MHz, benzene-d_6) 4.9, 6.8, 34.9, 35.0, 119.9, 124.8, 125.2, 126.6, 127.8, 127.9, 133.5, 142.4.

IR (ATR) 2993 w, 2956w, 1770 m, 1758 m, 1449 w, 1375 w, 1243 s, 1059 m, 744 w.

MS: *m/z* (EI, relative intensity, %) 260 (31, M^+), 231 (26), 130 (12), 129 (100), 128 (21), 117 (24), 115 (13), 103 (36), 87 (19), 75 (18), 59 (23).

HRMS (M^+) Calcd for $C_{16}H_{24}OSi^+$: 260.15964; Found: 260.1589

VII. Nickel-Catalyzed Synthesis of Silyl Enol Ethers from Alkanoylsilanes with Norbornene

(*Z*)-((1-(Bicyclo[2.2.1]heptan-2-yl)-3-phenylprop-1-en-1-yl)oxy)triethylsilane (6b).

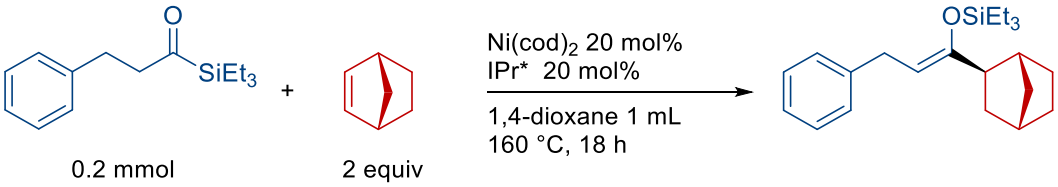

In a glove box, to an oven-dried 10 mL screw-capped vial, $Ni(cod)_2$ (11.0 mg, 0.040 mmol), IPr* (36.6 mg, 0.040 mmol), 3-phenyl-1-(triethylsilyl)propan-1-one (**1b**, 49.7 mg, 0.20 mmol), norbornene (**2a**, 38.8 mg, 0.40 mmol), and 1,4-dioxane (1.0 mL) were added. The cap was closed and the resulting mixture was stirred at 160 °C for 18 h. After cooling to rt, the resulting mixture was filtered through a celite pad. The filtrate was concentrated to dryness in vacuo and the residue was purified by MPLC (hexane to hexane/EtOAc = 1/9) to afford the desired product (colorless oil, R_f = 0.23 (hexane), yield = 56%, m = 38.2 mg).

^{1}H NMR (399.78 MHz, benzene-d_6) δ 0.68 (q, J = 8.1 Hz, 6H), 1.02 (t, J = 7.8 Hz, 10H), 1.09–1.18 (m, 2H), 1.37-1.60 (m, 4H), 1.56-1.62 (m, 1H), 2.10 (d, J = 10.1 Hz, 2H), 2.40 (d, J = 3.7 Hz, 1H), 3.55 (q, J = 3.4 Hz, 2H), 4.75 (td, J = 7.0, 1.1 Hz, 1H), 7.07 (t, J = 7.3 Hz, 1H), 7.19 (t, J = 7.6 Hz, 2H), 7.27 (d, J = 7.8 Hz, 2H).

^{13}C NMR (100.53 MHz, benzene-d_6) δ 6.1, 7.1, 29.4, 30.1, 32.1, 36.0, 36.1, 36.7, 40.7, 48.6, 104.8, 126.0, 128.6, 128.7, 142.6, 154.9.

IR (ATR) 2985 w, 2960 w, 1769 w, 1738 s, 1449 w, 1373 m, 1240 s, 1046 m, 846 w, 607 w.

MS: *m/z* (EI, relative intensity, %) 343 (12), 342 (43, M^+), 313 (30), 251 (33), 248 (22), 247 (100), 135 (23), 115 (73), 103 (71), 95 (14), 91 (36), 87 (68), 75 (43), 59 (62).

HRMS ($[M+H]^+$) Calcd for $C_{22}H_{35}OSi$: 343.2452; Found: 343.2453.

NOESY

The stereochemistry of the double bond was determined by NOESY.

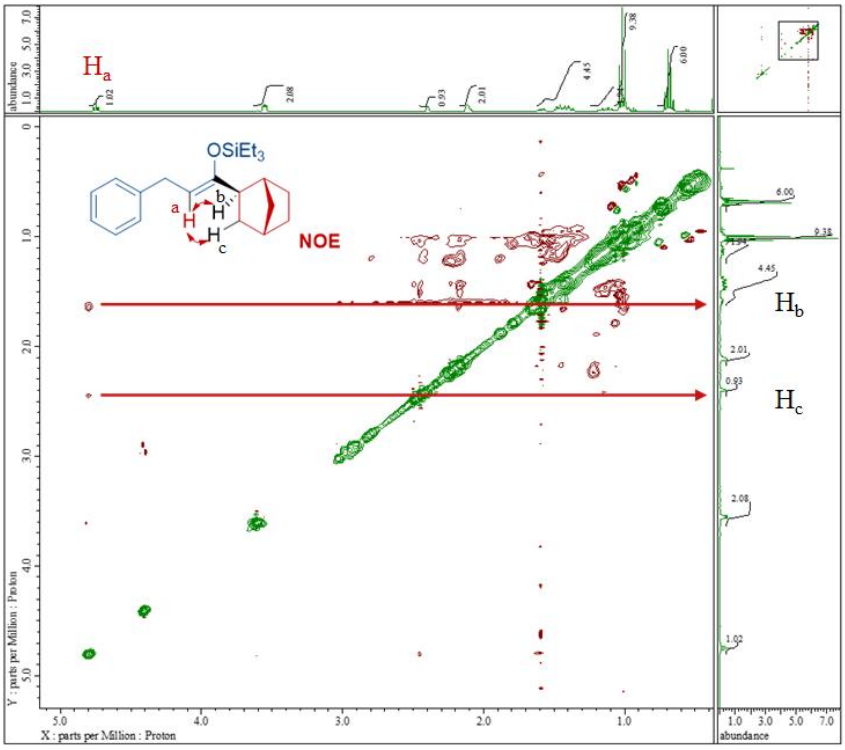

(Bicyclo[2.2.1]heptan-2-yl(cyclohexylidene)methoxy)triethylsilane (6c).

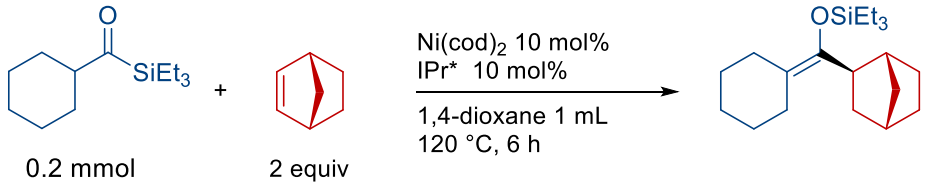

Condition A: In a glove box, to an oven-dried 10 mL screw-capped vial, $Ni(cod)_2$ (5.6 mg, 0.020 mmol), IPr* (18.3 mg, 0.040 mmol), 3-phenyl-1-(triethylsilyl)propan-1-one (**1c**, 49.7 mg, 0.20 mmol), norbornene (**2a**, 38.8 mg, 0.40 mmol), and 1,4-dioxane (1.0 mL) were added. The cap was closed and the resulting mixture was stirred at 120 °C for 6 h. After cooling to rt, the resulting mixture was filtered through a celite pad. The filtrate was concentrated to dryness in vacuo and the residue was purified by MPLC (hexane to hexane/EtOAc = 1/9) to afford the desired product (colorless oil, R_f = 0.63 (hexane), yield = 75%, m = 45.6 mg).

Condition B: In a glove box, to an oven-dried 10 mL screw-capped vial, $Ni(cod)_2$ (11.0 mg, 0.04 mmol), IPr* (36.6 mg, 0.040 mmol), cyclohexyl(triethylsilyl)methanone (**1c**, 45.3 mg, 0.20 mmol), norbornene (**2a**, 38.8 mg, 0.40 mmol), and 1,4-dioxane (1.0 mL) were added. The cap was closed and the resulting mixture was stirred at 160 °C for 18 h. After cooling to rt, the resulting mixture filtered through a celite pad. The same purification procedure as in Condition A was used to afford the desired product (colorless oil, yield = 81%, m = 52.1 mg).

^{1}H NMR (399.78 MHz, benzene-d_6) δ 2.56 (dd, J = 8.7, 6.0 Hz, 1H), 2.25 (m, 4H), 2.15–2.13 (m, 2H), 1.77 (m, 2H), 1.50–1.39 (m, 9H), 1.18–1.12 (m, 3H), 1.04 (t, J = 7.8 Hz, 9H), 0.77 (q, J = 7.9 Hz, 6H).

^{13}C NMR (100.53 MHz, benzene-d_6) δ 147.1, 115.5, 43.1, 43.0, 37.6, 37.3, 36.5, 30.8, 30.1, 29.2, 28.9, 28.3, 27.8, 27.3, 7.3, 6.3.

IR (ATR) 2981 s, 2953 m, 2925 m, 1769 m, 1744 s, 1373 w, 1240 s, 1050 m, 737 s.

MS: *m/z* (EI, relative intensity, %) 321 (16), 320 (62, M^+), 292 (23), 291 (81), 253 (46), 237 (20), 225 (30), 115 (63), 103 (100), 95 (15), 87 (80), 75 (60) 59 (68).

HRMS ($[M+H]^+$) Calcd for $C_{20}H_{37}OSi$: 320.2614; Found: 321.2615.

(((1*R*,2*R*,4*S*)-Bicyclo[2.2.1]heptan-2-yl)(1,3-dihydro-2*H*-inden-2-ylidene)methoxy)triethylsilane (6d).

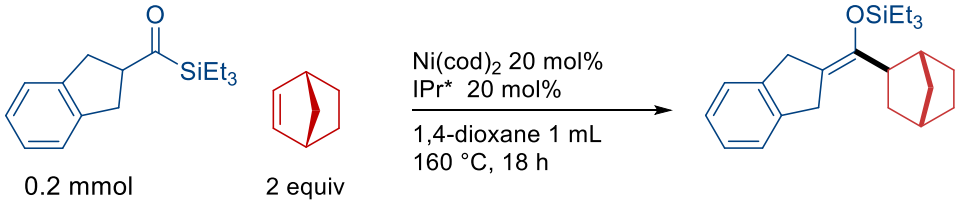

In a glove box, to an oven-dried 10 mL screw-capped vial, $Ni(cod)_2$ (11.0 mg, 0.040 mmol), IPr* (36.6 mg, 0.040 mmol), (2,3-dihydro-1*H*-inden-2-yl)(triethylsilyl)methanone (**1d**, 52.1 mg, 0.20 mmol), norbornene (**2a**, 38.8 mg, 0.40 mmol), and 1,4-dioxane (1.0 mL) were added. The cap was closed and the resulting mixture was stirred at 160 °C for 18 h. After cooling to rt, the resulting mixture was filtered through a celite pad. The filtrate was concentrated to dryness in vacuo and the residue was purified by MPLC (hexane to hexane/EtOAc = 1/9) to afford the desired product (colorless oil, R_f = 0.48 (hexane), yield = 45%, m = 30.8 mg).

^{1}H NMR (399.78 MHz, benzene-d_6) δ 0.77 (q, J = 7.8 Hz, 6H), 1.03 (t, J = 8.0 Hz, 9H), 1.08–1.21 (m, 3H), 1.42–1.49 (m, 3H), 1.75–1.82 (m, 2H), 2.25 (s, 1H), 2.30 (d, J = 1.4 Hz, 1H), 2.35 (dd, J = 8.2, 6.4 Hz, 1H), 3.62 (d, J =

2.3 Hz, 2H), 3.81 (d, J = 6.9 Hz, 2H), 7.10–7.17 (m, 4H)

^{13}C NMR (100.53 MHz, benzene-d_6) δ 6.5, 7.3, 29.1, 31.2, 35.7, 36.4, 36.9, 37.2, 37.4, 42.1, 45.4, 113.9, 124.9, 125.0, 126.6, 126.7, 142.3, 142.6, 149.2.

IR (ATR) 3395 w, 3339 w, 2954 s, 2872 s, 1704 m, 1645 m, 1556 w, 1180 w, 742 m.

MS: *m/z* (EI, relative intensity, %) 354 (10, M^+), 260 (23), 259 (100), 206 (11), 115 (37), 103 (10), 87 (35), 75 (10), 59 (25).

HRMS ($[M+H]^+$) Calcd for $C_{23}H_{35}OSi$: 354.2379; Found: 354.2380.

((1-(Bicyclo[2.2.1]heptan-2-yl)-2-methylprop-1-en-1-yl)oxy)triethylsilane (6f).

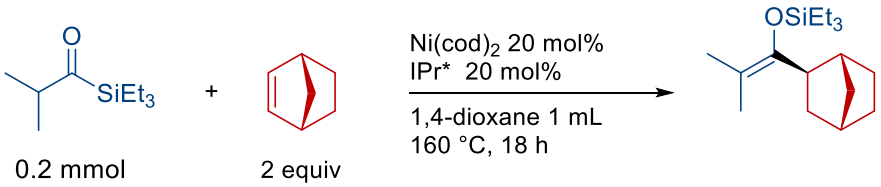

In a glove box, to an oven-dried 10 mL screw-capped vial, $Ni(cod)_2$ (11.0 mg, 0.040 mmol), IPr* (36.6 mg, 0.040 mmol), 2-methyl-1-(triethylsilyl)propan-1-one (**1f**, 37.3 mg, 0.20 mmol), norbornene (**2a**, 38.8 mg, 0.40 mmol), and 1,4-dioxane (1.0 mL) were added. The cap was closed and the resulting mixture was stirred at 160 °C for 18 h. After cooling to rt, the resulting mixture was filtered through a celite pad. The filtrate was concentrated to dryness in vacuo and the residue was purified by MPLC (hexane to hexane/EtOAc = 1/9) to afford the desired product (colorless oil, R_f = 0.60 (hexane), yield = 66%, m = 38.1 mg).

^{1}H NMR (399.78 MHz, benzene-d_6) δ 0.75 (q, J = 8.1 Hz, 6H), 1.03 (t, J = 8.0 Hz, 9H), 1.11–1.18 (m, 3H), 1.40–1.45 (m, 3H), 1.62 (s, 3H), 1.68 (s, 3H), 1.70–1.80 (m, 2H), 2.22 (s, 1H), 2.26 (d, J = 1.4 Hz, 1H), 2.52 (dd, J = 8.5, 6.2 Hz, 1H).

^{13}C NMR (100.53 MHz, benzene-d_6) δ 6.3, 7.3, 19.5, 29.1, 30.9, 36.5, 36.6, 37.5, 42.6, 43.5, 106.8, 149.7. One signal is overlapped with other signals.

IR (ATR) 2951 m, 2913 m, 2874 m, 1741 s, 1660 w, 1372 m, 1238 s, 1186 s, 1048 s, 830 w, 736 s.

MS: *m/z* (EI, relative intensity, %) 281 (14), 280 (59, M^+), 252 (23), 251 (100), 237 (15), 213 (32), 119 (15), 115 (53), 105 (10), 103 (81), 87 (50), 75 (42), 59 (36).

HRMS ($[M+H]^+$) Calcd for $C_{17}H_{33}OSi$: 281.2295; Found: 281.2297.

((Bicyclo[2.2.1]heptan-2-yl-3-d)(cyclohexylidene)methoxy)triethylsilane (6c-*d*).

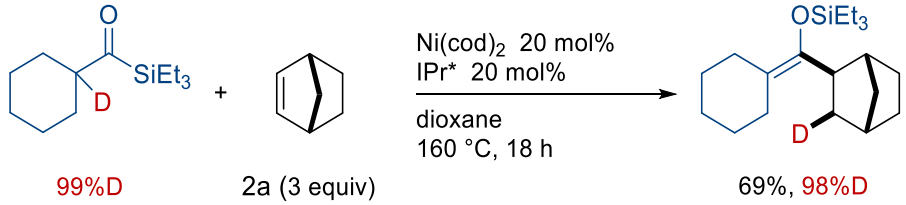

In a glove box, to an oven-dried 10 mL screw-capped vial, $Ni(cod)_2$ (11.0 mg, 0.040 mmol), IPr* (36.6 mg, 0.040 mmol), (cyclohexyl-1-*d*)(triethylsilyl)methanone (**1c-*d***, 35.2 mg, 0.123 mmol), norbornene (**2a**, 58.2 mg, 0.60 mmol), and 1,4-dioxane (1.0 mL) were added. The cap was closed and the resulting mixture was stirred at 160 °C

for 18 h. After cooling to rt, the resulting mixture was filtered through a celite pad. The filtrate was concentrated to dryness in vacuo and the residue was purified by MPLC (hexane to hexane/EtOAc = 1/9) to afford the desired product (colorless oil, R_f = 0.63 (hexane), yield = 69%, m =42.1 mg).

^{1}H NMR (399.78 MHz, benzene-d_6) δ 0.77 (q, J = 7.9 Hz, 6H), 1.04 (t, J = 7.8 Hz, 9H), 1.12–1.18 (m, 3H), 1.39–1.50 (m, 9H), 1.77 (dt, J = 9.6, 1.8 Hz, 1H), 2.14 (t, J = 4.8 Hz, 2H), 2.22–2.27 (m, 4H), 2.55 (d, J = 9.2 Hz, 1H).

^{2}D NMR (61.36 MHz, benzene) δ 1.72 (s, 1D).

^{13}C NMR (100.53 MHz, benzene d_6) δ 6.3, 7.3, 27.3, 27.8, 28.4, 28.9, 29.2, 30.1, 30.8, 36.9 (t, J = 20.1 Hz) 36.4, 37.6, 43.0, 115.5, 147.1. One signal is overlapped with other signals.

IR (ATR) 2984 w, 1737 s, 1373 m, 1235 s, 1044 s, 846 w, 682 w, 634 w, 607.

MS: *m/z* (EI, relative intensity, %) 322 (21), 321 (75, M^+), 293 (30), 292 (100), 254 (59), 238 (21), 225 (36), 115 (63), 103 (96), 87 (71), 75 (49), 53 (53).

HRMS ($[M+H]^+$) Calcd for $C_{20}H_{36}DOSi$: 322.2671; Found: 322.2672.

The relative configuration of the deuterium was determined by comparison of COSY and NOESY spectra with those of a non-deuterated product.

COSY

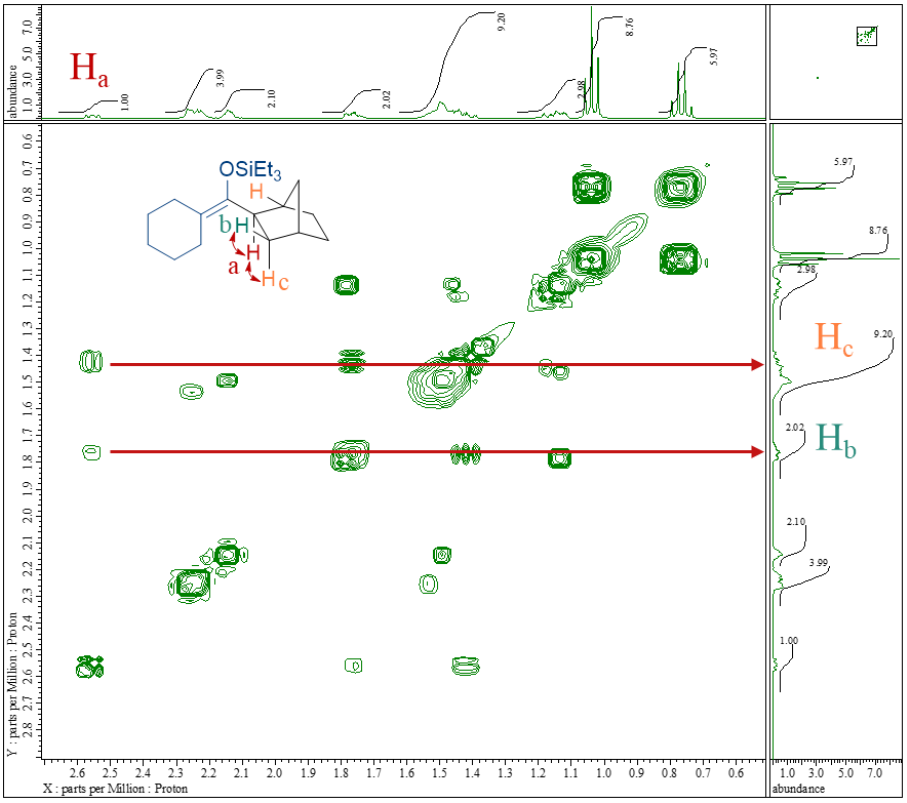
Ha
OSiEt3
H
bH
H
a
Hc
Hc
Hb
X : parts per Million : Proton
Y : parts per Million : Proton
abundance

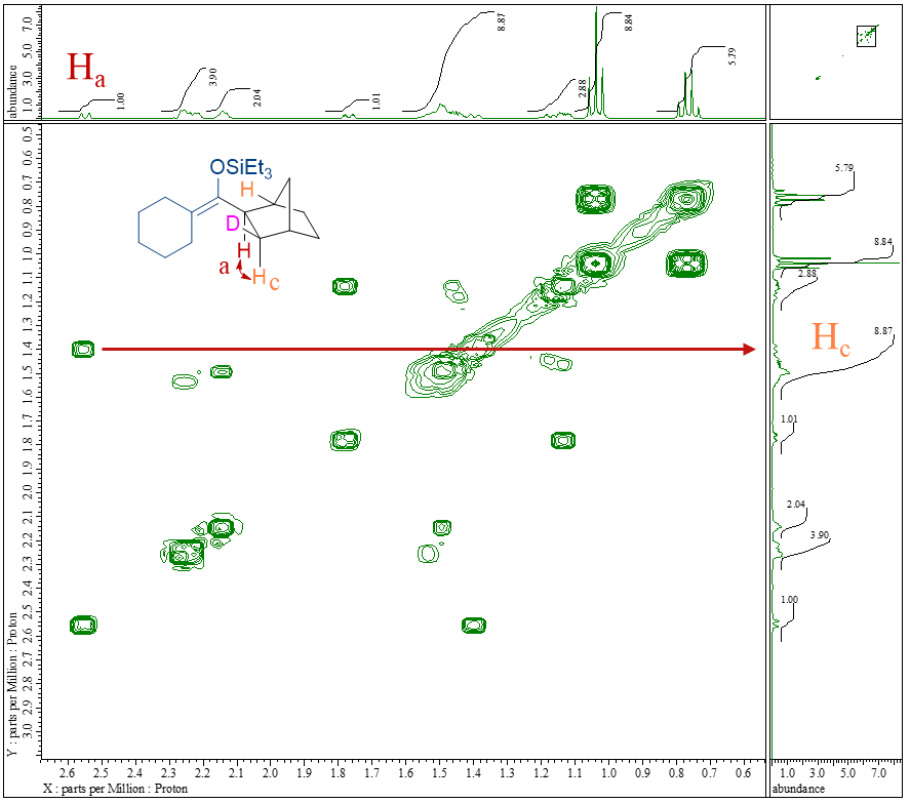
Ha
OSiEt3
H
D
H
a
Hc
Hc
X : parts per Million : Proton
Y : parts per Million : Proton
abundance

NOESY

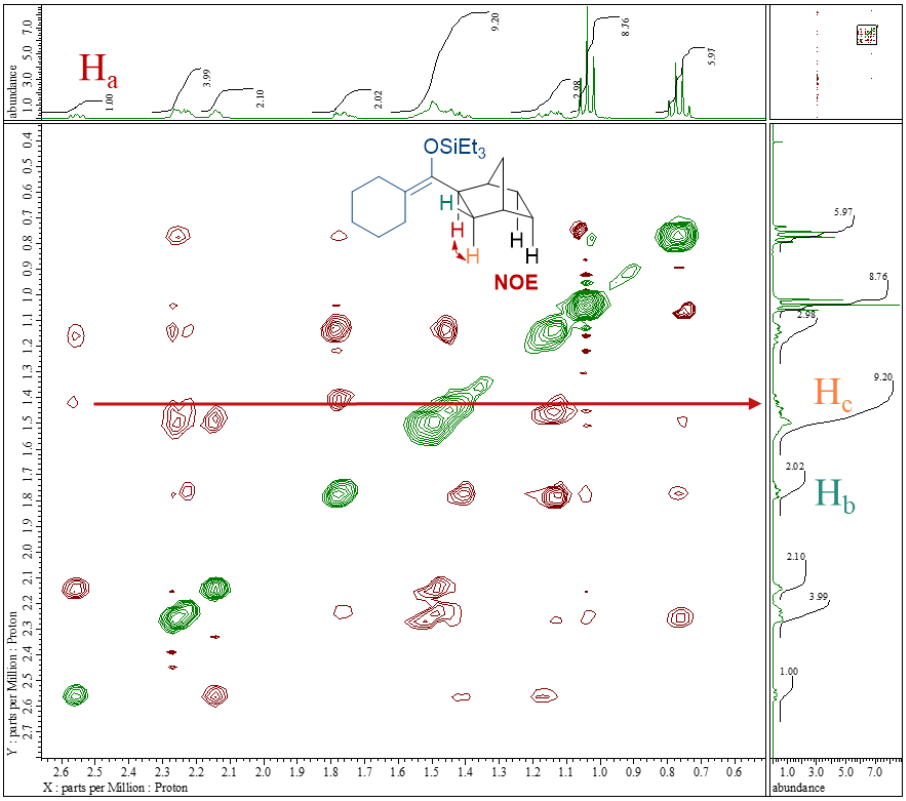
Ha
OSiEt3
H
H
H
H
H
NOE
Hc
Hb
9.20
8.76
5.97
2.98
2.02
2.10
3.99
1.00
abundance
Y : parts per Million : Proton
X : parts per Million : Proton

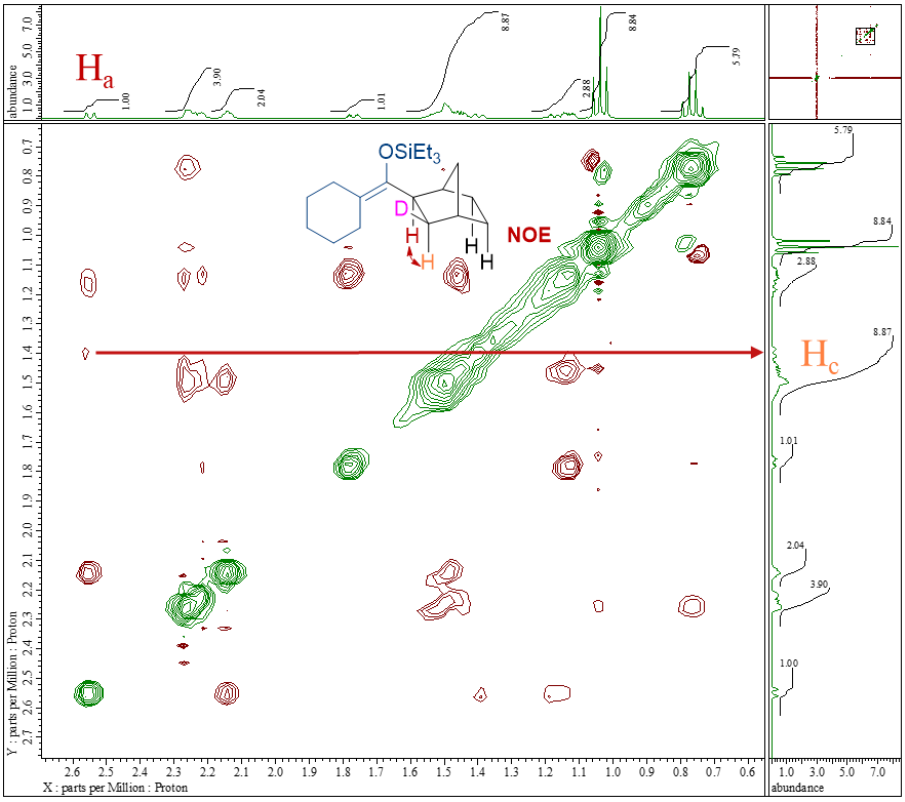
Ha
OSiEt3
D
H
H
H
NOE
Hc
8.87
8.84
5.79
2.88
1.01
2.04
3.90
1.00
abundance
Y : parts per Million : Proton
X : parts per Million : Proton

List of unsuccessful alkenes.

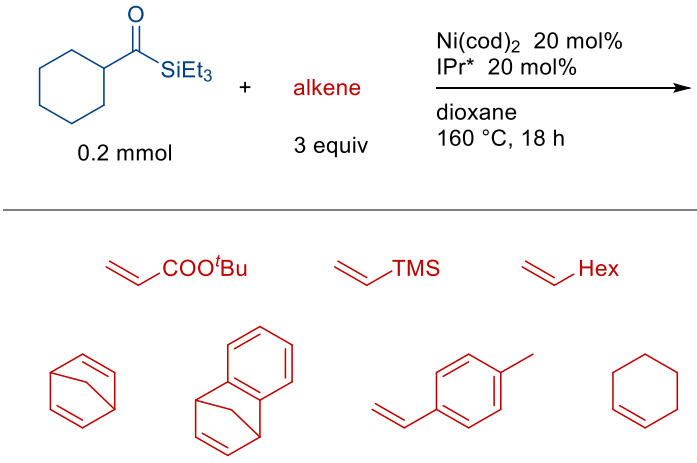

VIII. Attempted Ni-Catalyzed Synthesis of β-Lactam Derivatives

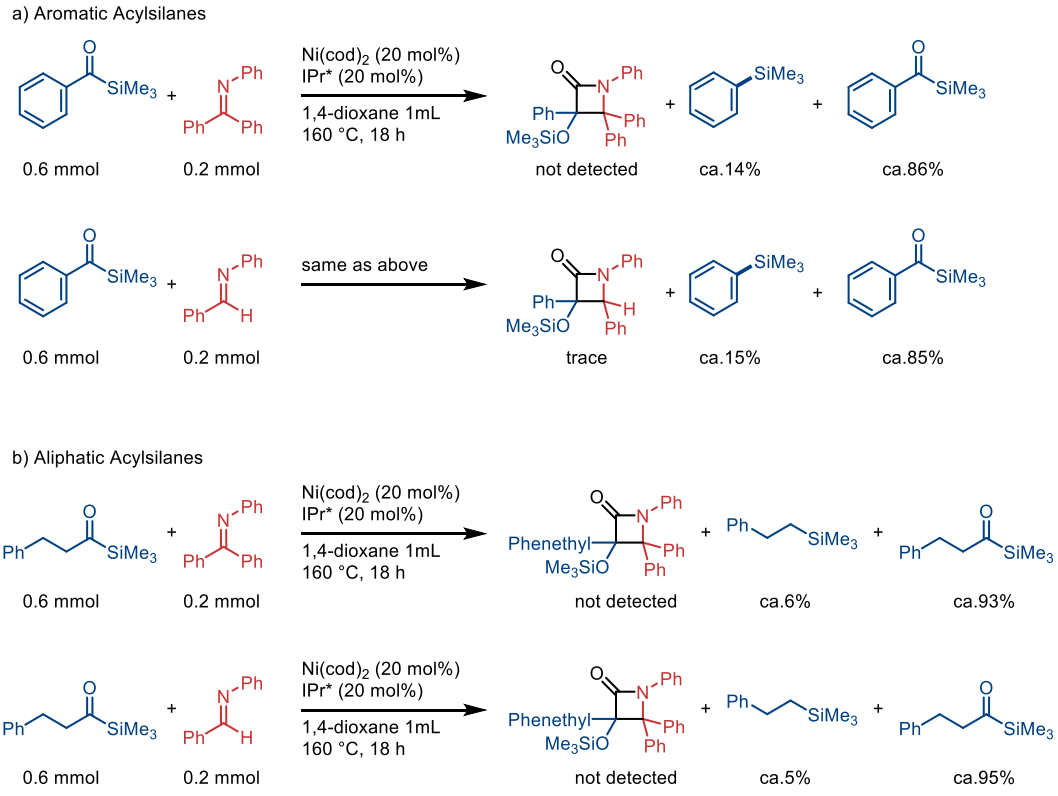

IX. Attempts to Observe Nickel Siloxycarbene Complexes

TNI* was synthesized based on reference 22.

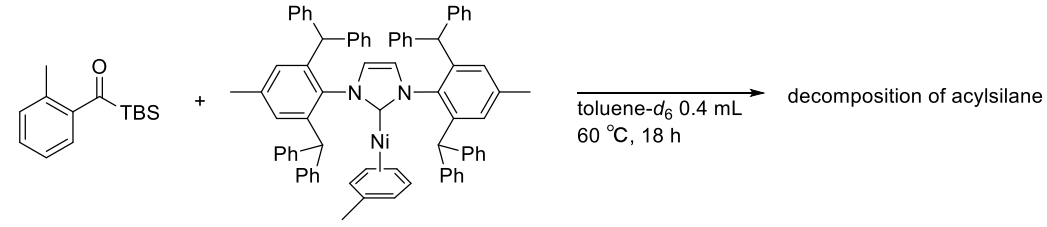

0.02 mmol **TNI*** 0.02 mmol

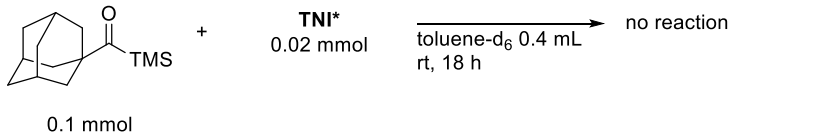

0.1 mmol

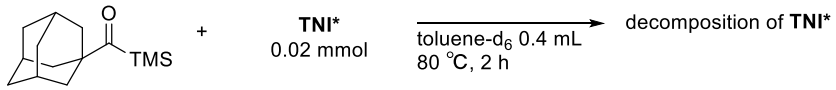

0.1 mmol

X. Reaction of Silyl Enol Ether 5c with 2a under the TNI*-Catalyzed Conditions

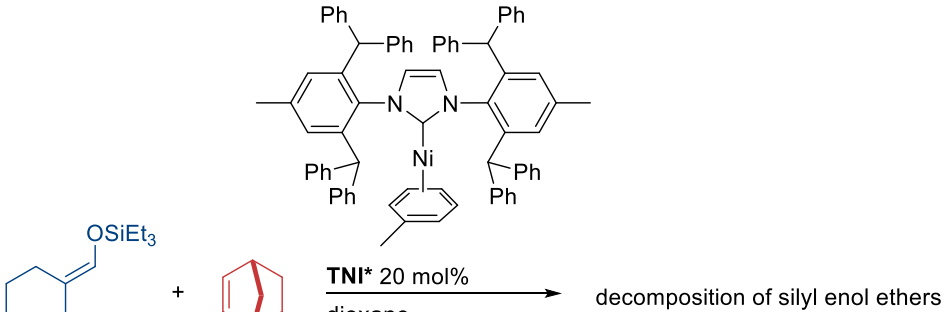

5c + **2a** (2 equiv)

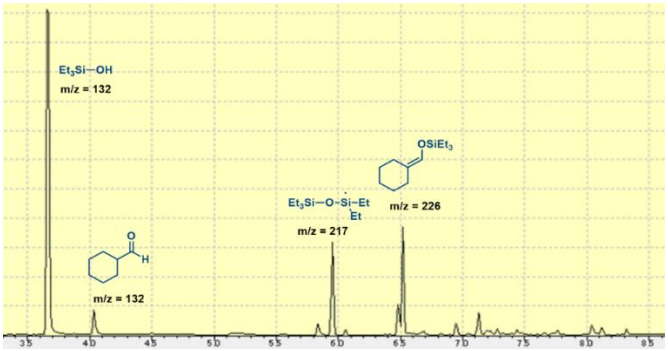

GC/MS trace of the reaction

We also tested the reaction of enol ether **5c** with norbornene using the η^6-(toluene)-coordinated nickel complex **TNI***, which is known for its rapid ligand exchange capabilities. However, no addition to norbornene was observed under these conditions. These findings imply that unfavorable ligand exchange is not the sole factor preventing the reaction between the silyl enol ether and norbornene.

XI. Derivatization of 6c to Crystalline Compound 7c

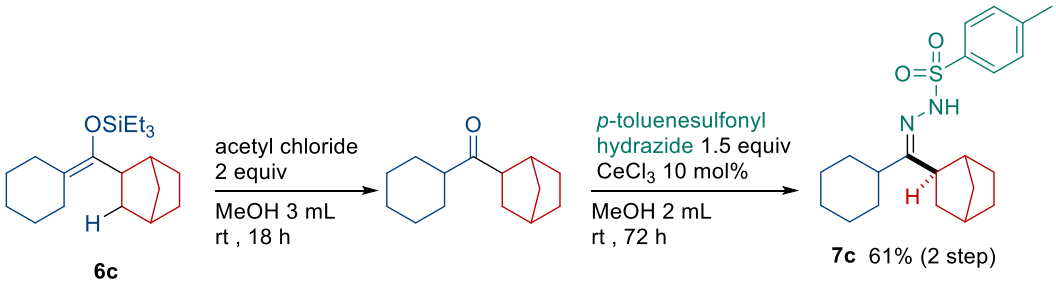

To a stirred solution of **6c** (47.1 mg, 0.15 mmol) in MeOH (3.0 mL), acetyl chloride (22 μL, 0.3 mmol) was added in one portion at rt under a N_2. The resulting mixture was stirred for 18 h. The mixture was then quenched with saturated aqueous solution of Na_2CO_3, and the resulting mixture was extracted with EtOAc (30 mL × 2). The combined organic extracts were washed with brine (100 mL) and dried over $MgSO_4$. It was then concentrated to afford the crude ketone (R_f=0.7 (hexane/EtOAc = 1/10)), which was used directly for the next step.

To a stirred solution of the ketone in MeOH (2.0 mL), *p*-toluenesulfonyl hydrazide (41.9 mg, 0.225 mmol) and $CeCl_3$ (3.7 mg, 0.015 mmol) were added. The mixture was stirred at rt for 72 h. The solution was then concentrated. The residue was purified by by MPLC (hexane/EtOAc = 1/0 to 1/1) to afford the desired product (white solid, Mp = 129.2–129.9 °C, R_f = 0.50 (hexane/EtOAc = 1/1), yield = 61%, m = 36.1 mg).

^{1}H NMR (399.78 MHz, benzene-d_6) δ 0.88–1.68 (m, 16H), 1.75 (d, J = 9.6 Hz, 1H), 1.83–1.89 (m, 4H), 1.99–2.19 (m, 3H), 2.51–2.57 (m, 1H), 6.75–6.83 (m, 2H), 8.10–8.18 (m, 2H), 8.64 (s, 1H).

^{13}C NMR (100.53 MHz, benzene-d_6) δ 21.1, 25.8, 26.0, 29.0, 29.1, 29.3, 30.2, 36.0, 36.6, 39.2, 41.7, 44.4, 127.9, 128.5, 128.7, 129.5, 136.9, 143.4, 166.6.

IR (ATR) 3216 w, 2929 s, 2864 m, 1701 w, 1450 m, 1335 s, 1165 s, 812 m, 669 s, 592 s, 548 m.

MS: *m/z* (EI, relative intensity, %) 139 (11), 123 (23), 95 (100), 83 (32), 67 (17), 55 (19), 41 (12).

HRMS ([M+H]$^+$) Calcd for $C_{21}H_{31}N_2O_2S$: 375.2101; Found: 375.2094.

XII. Crystallographic Information

X-ray crystal analyses were performed on a Rigaku/XtaLABPro P200 Hybrid Photon Counting diffractometer (Cu-Kα, λ = 1.54184 Å). The structures were solved with olex2.solve 1.5 and refined with SHELXL−2018/3.

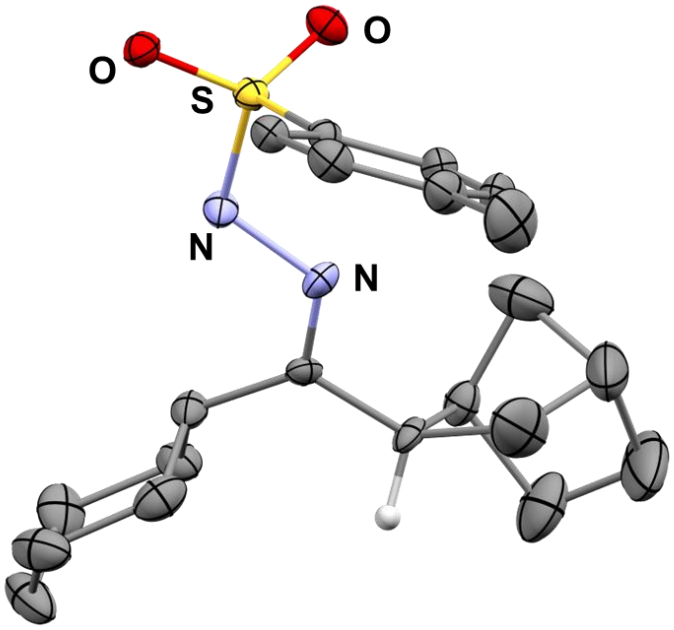

Figure S1 ORTEP drawings of **7c** depicted at the 30% probability level.[a]

[a]Crystal data for **7c**, monoclinic, space group $P\ 2_1/n$ (no. 14), a = 14.1925(5) Å, b = 6.7488(2) Å, c = 21.4579(7) Å, α = 90°, β = 104.815(4)°, γ = 90°, V = 1986.96(12) Å^3, T = 123 K, Z = 4, $R1$ ($wR2$) = 0.0682 (0.1889) for 285 parameters and 3948 unique reflections, GOF = 1.043, CCDC 2356932.

XIII. Computational Studies

XIII.I General Information

Calculations were performed with the Gaussian 09 (G09RevD.01) program.[23] Geometry optimizations and frequency calculations for all reported structures were performed using the ωB97XD functional[24] with a basis set consisting of the LANL2DZ basis set for metallic atoms (Pd) and 6-31G(d,p) for the rest. Single-point calculations on optimized geometries were separately calculated using the ωB97XD functional with a basis set consisting of the SDD basis set for metallic atoms (Ni) and 6-311+G(d,p) for the rest. Each reported minimum has zero imaginary frequency and each transition state (TS) structure has only one imaginary frequency. [25] From TSs, reaction paths were traced by the intrinsic reaction coordinate (IRC) method[26] to obtain the energy-minimum geometries. Energy changes were shown by the use of Gibbs free energies (T = 298.15 K and P = 1 atm). The structures of intermediates and transition states were described by GaussView 6.1 package. [27]

XIII.II DFT Studies on the Reaction Pathway

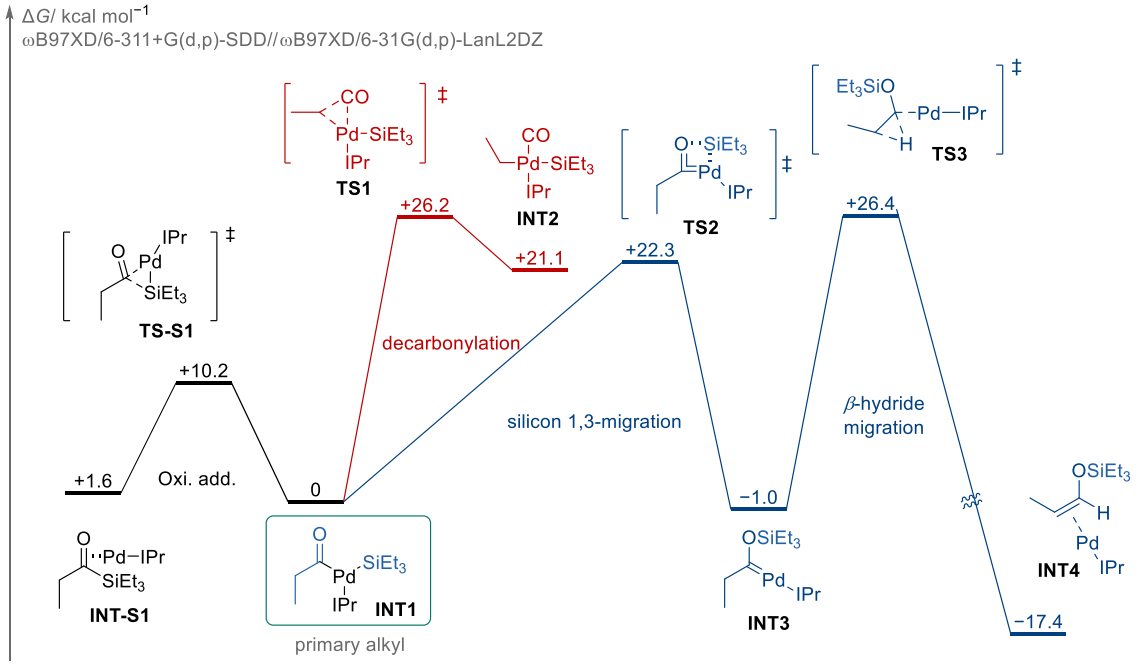

Figure S2 Energy diagram of palladium-catalyzed reactions of primary alkyl-substituted acylsilane at the wB97XD/6-311+G(d,p)-SDD// wB97XD/6-31G(d,p)-LanL2DZ.

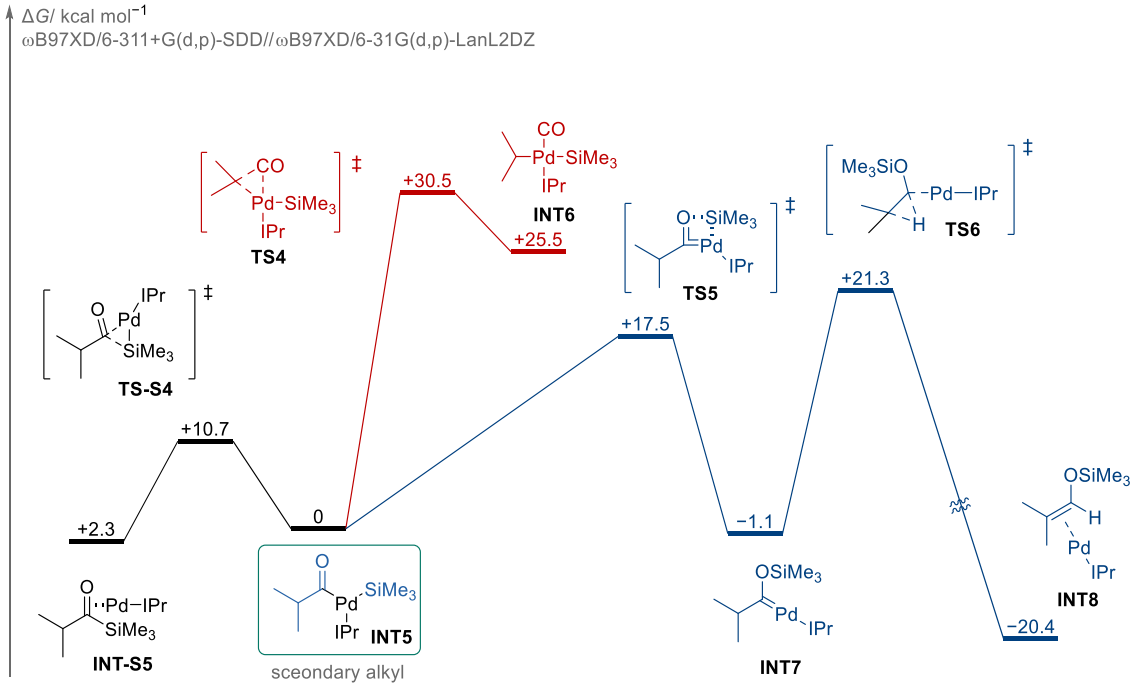

Figure S3 Energy diagram of palladium-catalyzed reactions of secondary alkyl-substituted acylsilane at the wB97XD/6-311+G(d,p)-SDD// wB97XD/6-31G(d,p)-LanL2DZ.

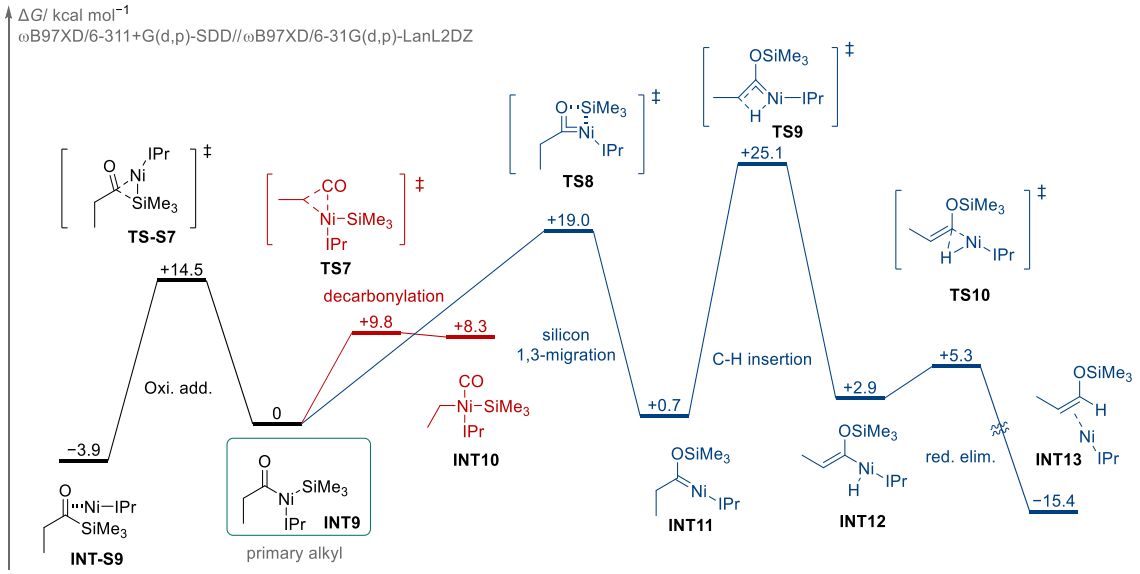

Figure S4 Energy diagram of nickel-catalyzed reactions of primary alkyl-substituted acylsilane at the wB97XD/6-311+G(d,p)-SDD// wB97XD/6-31G(d,p)-LanL2DZ.

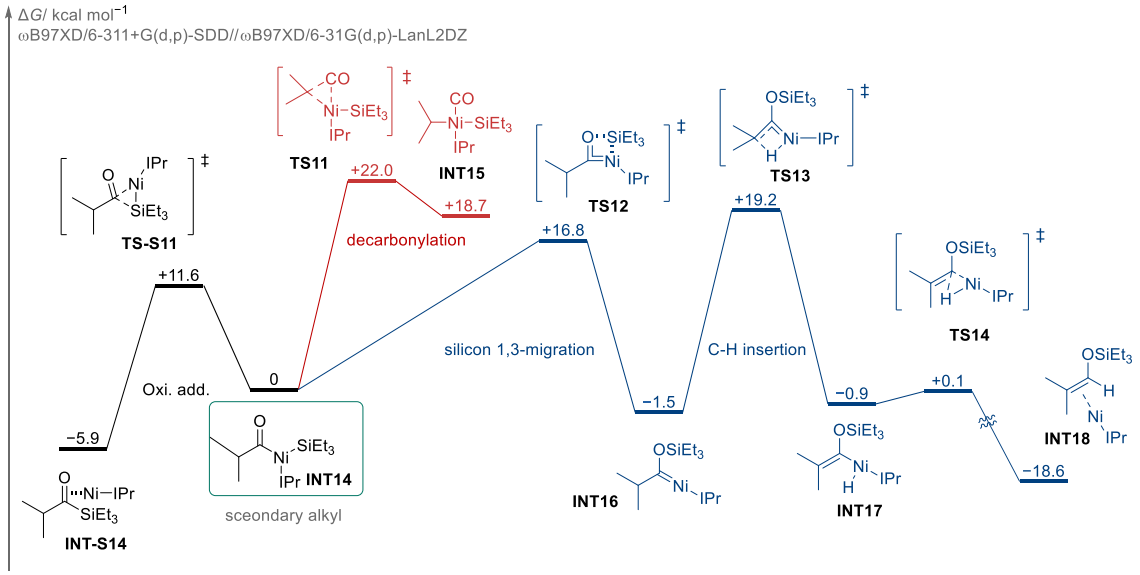

Figure S5 Energy diagram of nickel-catalyzed reactions of secondary alkyl-substituted acylsilane at the wB97XD/6-311+G(d,p)-SDD// wB97XD/6-31G(d,p)-LanL2DZ.

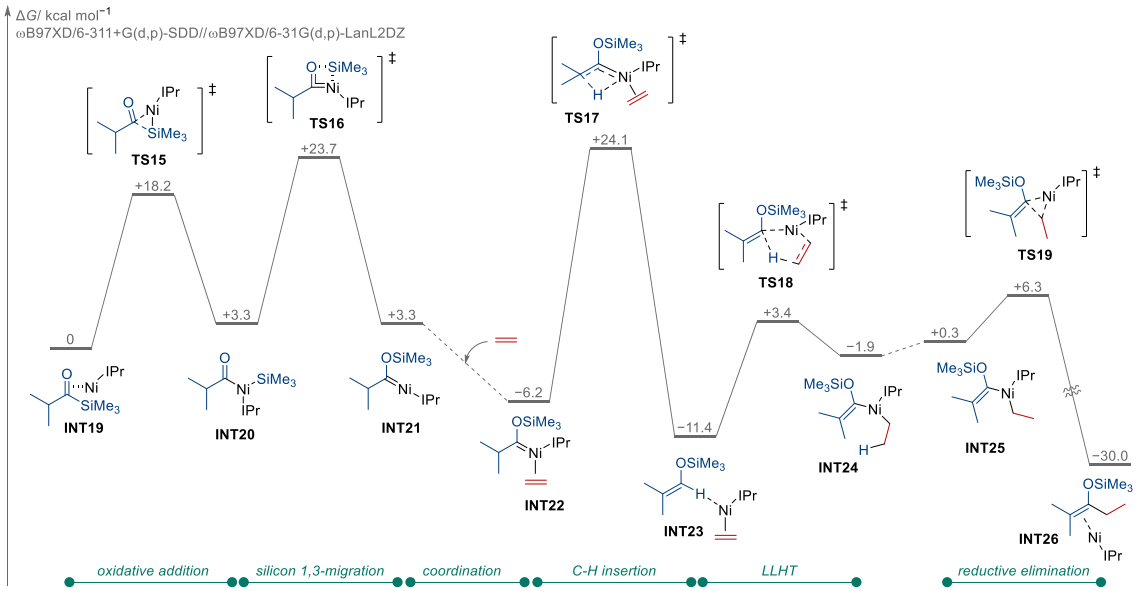

Figure S6 A DFT-computed energy profile for the nickel-catalyzed reaction of aliphatic acylsilanes with ethylene to form silyl enol ethers at the wB97XD/6-311+G(d,p)-SDD// wB97XD/6-31G(d,p)-LanL2DZ.

XIII.III Stability Comparison of INT23

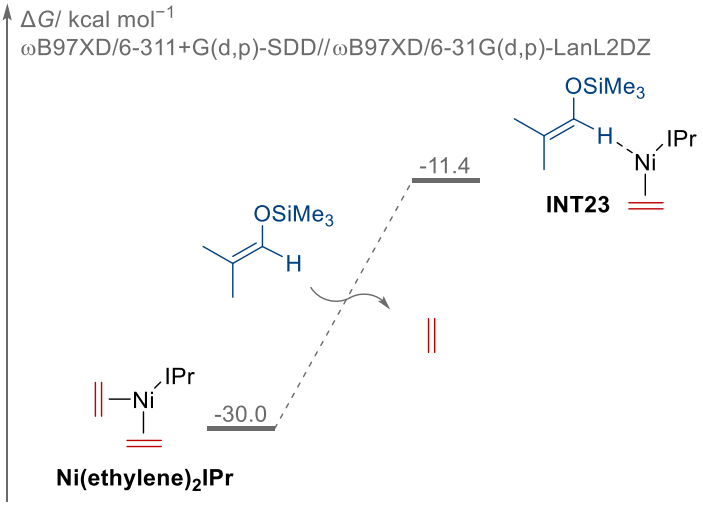

Figure S7 A DFT-computed energy profile for the ligand exchange of the the diethylene IPr nickel complex at the wB97XD/6-311+G(d,p)-SDD// wB97XD/6-31G(d,p)-LanL2DZ.

The likely reason the reaction did not proceed when using silyl enol ether as a starting material is the relative instability of **INT23** compared to Ni(cod)IPr, making the ligand exchange process unfavorable. Calculations revealed that the ligand exchange of the $Ni(ethylene)_2IPr$ complex to **INT23** is endergonic by 18.6 kcal/mol.

XIII.IV Stability Comparison of INT23´

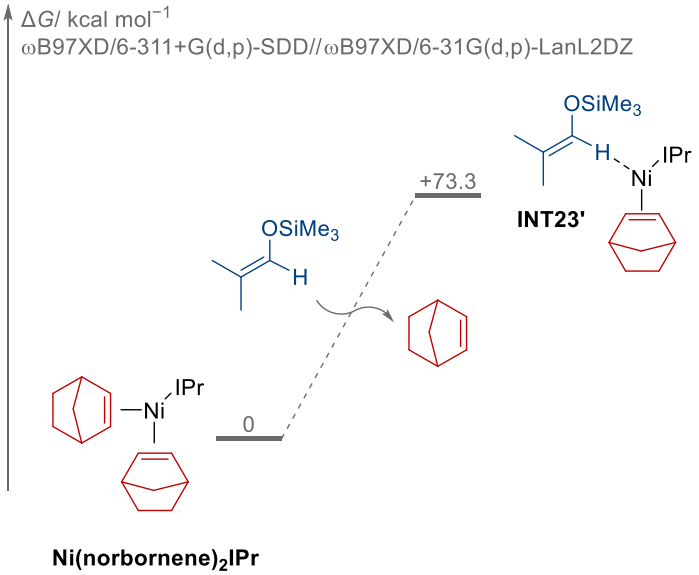

Figure S8 A DFT-computed energy profile for the ligand exchange of the the diethylene IPr nickel complex at the wB97XD/6-311+G(d,p)-SDD// wB97XD/6-31G(d,p)-LanL2DZ.

To further clarify the results in Scheme **5a**—specifically, why the silyl enol ether did not react with norbornene under the nickel-catalyzed conditions—we performed additional DFT calculations to assess the ligand exchange between Ni(norbornene)$_2$(IPr) and the silyl enol ether. This species is more likely to be the dominant nickel species under the conditions of Scheme **5a**. Our calculations indicate that this ligand exchange is highly endergonic, with an energy difference of 73.3 kcal/mol, which is considerably higher than that observed for Ni(ethylene)$_2$(IPr). This increased endergonicity likely arises from the stronger binding affinity and higher steric demands of norbornene relative to ethylene. Although these results do not directly reveal the kinetic barrier, the substantially endergonic nature of the ligand exchange suggests that it is disfavored under the reaction conditions in Scheme **5a**.

XIII.V Attempts to explore Brook rearrangement-type mechanism

We explored a mechanism analogous to the Brook rearrangement using DFT calculations (ωB97XD/6-311+G(d,p)-SDD//ωB97XD/6-31G(d,p)-Lanl2DZ). However, when attempting to locate the proposed transition state (**TS1'**), it consistently converged to the transition state for the concerted oxidative addition process (**TS3'**). These findings suggest that a Brook-like rearrangement mechanism is energetically less favorable compared to oxidative addition.

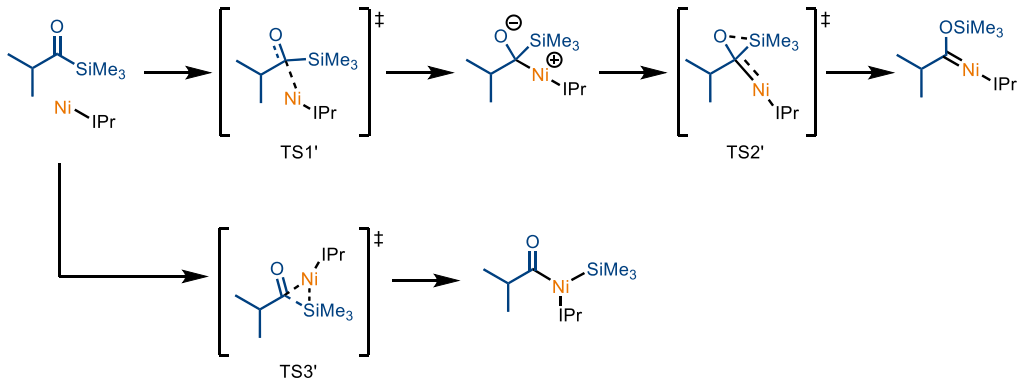

3.5. References

(1) Fischer, E. O.; Maasböl, *Angew. Chem. Int. Ed.* **1964**, *3*, 580–581.

(2) (a) Dötz, K. H. *Angew. Chem. Int. Ed.* **1984**, *23*, 587–608. (b) de Meijere, A.; Schirmer, H.; Duetsch, M. *Angew. Chem. Int. Ed.* **2000**, *39*, 3964–4002. (c) Gómez-Gallego, M.; Mancheño, M. J.; Sierra, M. A. *Acc. Chem. Res.* **2005**, *38*, 44–53. (d) Dötz, K. H.; Stendel, J. Jr. *Chem. Rev.* **2009**, *109*, 3227–3274. (e) Raubenheimer, H. G. *Dalton Trans.* **2014**, *43*, 16959–16973. (f) Feliciano, A.; Vázquez, J. L.; Benítez-Puebla, L. J.; Velazco-Cabral, I.; Cruz Cruz, D.; Delgado, F.; Vázquez, M. A. *Chem. Eur. J.* **2021**, *27*, 8233–8251. (g) Zhou, G.; Guo, Z.; Shen, X. *Angew. Chem. Int. Ed.* **2023**, *62*, e202217189.

(3) He, Y.; Huang, Z.; Wu, K.; Ma, J.; Zhou, Y.-G.; Yu, Z. *Chem. Soc. Rev.* **2022**, *51*, 2759–2852.

(4) While N-heterocyclic carbene and related complexes have been reported, these carbene ligands typically serve as supporting ligands and do not exhibit reactivity typical of Fischer carbenes, such as cyclopropanation or C-H insertion. For example, see: Kremzow, D.; Seidel, G.; Lehmann, C. W.; Fürstner, A., *Chem.–Eur. J.* **2005**, *11*, 1833-1853.

(5) (a) Sakurai, S.; Inagaki, T.; Kodama, T.; Yamanaka, M.; Tobisu, M. P. *J. Am. Chem. Soc.* **2022**, *144*, 1099–1105. (b) Sakurai, S.; Inagaki, T.; Kodama, T.; Yamanaka, M.; Tobisu, M. *Trends in Chemistry* **2022**, *4*, 1161–1162. (c) Inagaki, T.; Kodama, T.; Tobisu, M. *Nat. Catal.* **2024**, 1–7. (d) Inagaki, T.; Akita, Y.; Tobisu, M. *Org. Lett.* **2024**, *26*, 2141–2145.

(6) Brook, A. G. *J. Am. Chem. Soc.* **1957**, *79*, 4373–4375.

(7) (a) Zhao, Q.; Geng, Q.; Li, Y.; Li, J.; Liu, Z. *Org. Chem. Front.* **2023**. (b) Hong, W. P.; Lim, H. N.; Shin, I. *Org. Chem. Front.* **2023**, *10*, 819–836. (c) Guo, Y.; Zhou, G.; Shen, X. *Chin. J. Chem.* **2024**, *42*, 887–902.

(8) (a) Takeuchi, T.; Aoyama, T.; Orihara, K.; Ishida, K.; Kusama, H. *Org. Lett.* **2021**, *23*, 9490–9494. (b) Ueda, Y.; Masuda, Y.; Iwai, T.; Imaeda, K.; Takeuchi, H.; Ueno, K.; Gao, M.; Hasegawa, J.; Sawamura, M. *J. Am. Chem. Soc.* **2022**, *144*, 2218–2224. (c) Zheng, L.; Guo, X.; Li, Y.-C.; Wu, Y.; Xue, X.-S.; Wang, P. *Angew. Chem., Int. Ed.* **2022**, anie.202216373. (d) Zheng, L.; Li, Y.-C.; Wu, Y.; Wang, P. *ChemRxiv* January 2, 2024: 10.26434/chemrxiv-2024-6x3q7.

(9) (a) Fang, X.; Wen, S.; Jin, P.; Bao, W.; Liu, S.; Cong, H.; Shen, X. *ACS Catal.* **2022**, *12*, 2150–2157. (b) Zhou, G.; Guo, Z.; Liu, S.; Shen, X. *J. Am. Chem. Soc.* **2024**, *146*, 4026–4035. (c) Liu, Y.; Zhu, Z.; Zhang, Y.; Zhang, Y.; Liu, S.; Shen, X. *Org. Lett.* **2024**, *26*, 5911–5916.

(10) Nakatani, S.; Ito, Y.; Sakurai, S.; Kodama, T.; Tobisu, M. *J. Org. Chem.* **2020**, *85*, 7588–7594.

(11) (a) Taber, D. F.; Hennessy, M. J.; Louey, J. P. *J. Org. Chem.* **1992**, *57*, 436–441. (b) Taber, D. F.; Hoerrner, R. S. *J. Org. Chem.* **1992**, *57*, 441–447. (c) Muthusamy, S.; Gunanathan, C.; Babu, S. A. *Synthesis* **2002**, *2002*, 471–474. d) Solé, D.; Amenta, A.; Mariani, F.; Bennasar, M.-L.; Fernández, I. *Adv. Synth. Catal.* **2017**, *359*, 3654–3664. (e) Polukeev, A. V.; Wendt, O. F. *Organometallics* **2017**, *36*, 639–649.

(12) The activation barrier for the oxidative addition of isopropyl-substituted acylsilane catalyzed by Pd–IPr to form **INT5** was +8.4 kcal/mol. See SI for details.

(13) DeAngelis, A.; Dmitrenko, O.; Fox, J. M. *J. Am. Chem. Soc.* **2012**, *134*, 11035–11043.

(14) The activation barrier for the oxidative addition of ethyl-substituted acylsilane catalyzed by Ni-IPr to form **INT9** was +18.4 kcal/mol. See SI for details.

(15) A similar behavior was also observed in the catalytic decarbonylative cross-coupling of phenyl esters, in which nickel exhibits superior activity than palladium: (a) Amaike, K.; Muto, K.; Yamaguchi, J.; Itami, K. *J. Am. Chem.*

Soc. **2012**, *134*, 13573–13576. (b) Ben Halima, T.; Zhang, W.; Yalaoui, I.; Hong, X.; Yang, Y.-F.; Houk, K. N.; *J. Am. Chem. Soc.* **2017**, *139*, 1311–1318. (c) Liu, C.; Li, G.; Shi, S.; Meng, G.; Lalancette, R.; Szostak, R.; Szostak, M. *ACS Catal.* **2018**, *8*, 9131–9139. (d) Li, R.; Xu, H.; Zhao, N.; Jin, X.; Dang, Y. *J. Org. Chem.* **2020**, *85*, 833–840. (e) Liu, J.; Ling, M.; Xie, H. *Theor. Chem.* **2020**, *1185*, 112889.

(16) The activation barrier for the oxidative addition of acylsilane by Ni–IPr to form **INT14** was +17.5 kcal/mol. See SI for details.

(17) Guihaumé, J.; Halbert, S.; Eisenstein, O.; Perutz, R. N. *Organometallics* **2012**, *31*, 1300–1314.

(18) The reaction did not proceed when using silyl enol ether as a starting material (Scheme 5a) most likely due to the relative instability of complex **E** compared with Ni(cod)IPr, which makes the ligand exchange process unfavorable. Calculations revealed that the ligand exchange of the Ni(norbornene)$_2$IPr complex to the corresponding enol ether–bound complex similar to **E** is endergonic by 73.3 kcal/mol. See SI for details.

(19) Gómez-Suárez, A., Ramón, R. S., Songis, O., Slawin, A. M. Z., Cazin, C. S. J. Nolan, S. P. Influence of a Very Bulky N-Heterocyclic Carbene in Gold-Mediated Catalysis. *Organometallics* **2011**, *30*, 5463–5470.

(20) Capaldo, L.; Riccardi, R.; Ravelli, D.; Fagnoni, M. *ACS Catal.* **2018**, *8*, 304–309.

(21) (a) Yu, C.-J.; Li, R.; Gu, P. Intermolecular Schmidt Reaction of Alkyl Azides with Acyl Silanes. *Tetrahedron Lett.* **2016**, *57*, 3568–3570. (b) Linghu, X.; Nicewicz, D. A.; Johnson, J. S. *Org. Lett.* **2002**, *4*, 2957–2960.

(22) Y. Hoshimoto, Y. Hayashi, H. Suzuki, M. Ohashi, and S. Ogoshi, *Organometallics* **2014**, *33*, 1276-1282.

(23) Frisch, M. J.; Trucks, G. W.; Schlegel, H. B.; Scuseria, G. E.; Robb, M. A.; Cheeseman, J. R.; Scalmani, G.; Barone, V.; Mennucci, B.; Petersson, G. A.; Nakatsuji, H.; Caricato, M.; Li, X.; Hratchian, H. P.; Izmaylov, A. F.; Bloino, J.; Zheng, G.; Sonnenberg, J. L.; Hada, M.; Ehara, M.; Toyota, K.; Fukuda, R.; Hasegawa, J.; Ishida, M.; Nakajima, T.; Honda, Y.; Kitao, O.; Nakai, H.; Vreven, T.; Montgomery, J. A., Jr.; Peralta, J. E.; Ogliaro, F.; Bearpark, M.; Heyd, J. J.; Brothers, E.; S82 Kudin, K. N.; Staroverov, V. N.; Keith, T.; Kobayashi, R.; Normand, J.; Raghavachari, K.; Rendell, A.; Burant, J. C.; Iyengar, S. S.; Tomasi, J.; Cossi, M.; Rega, N.; Millam, N. J.; Klene, M.; Knox, J. E.; Cross, J. B.; Bakken, V.; Adamo, C.; Jaramillo, J.; Gomperts, R.; Stratmann, R. E.; Yazyev, O.; Austin, A. J.; Cammi, R.; Pomelli, C.; Ochterski, J. W.; Martin, R. L.; Morokuma, K.; Zakrzewski, V. G.; Voth, G. A.; Salvador, P.; Dannenberg, J. J.; Dapprich, S.; Daniels, A. D.; Farkas, Ö .; Foresman, J. B.; Ortiz, J. V.; Cioslowski, J.; Fox, D. J. Gaussian 09, Revision D.01; Gaussian, Inc.: Wallingford, CT, **2013**.

(24) (a) Becke, A. D. *J. Chem. Phys.* **1997**, *107*, 8554-8560. (b) Chai, J.-D.; Head-Gordon, M. *Phys. Chem. Chem. Phys.* **2008**, *10*, 6615–6620.

(25) Marenich, A. V., Cramer, C. J. & Truhlar, D. G *J. Phys. Chem. B.* **2009**, *113*, 6378–6396.

(26) Fukui, K. *J. Phys. Chem.* **1970**, *74*, 4161–4163.

(27) GaussView, Version 6.1, R. Dennington, T. A. Keith, J. M. Millam, Semichem Inc., Shawnee Mission, KS, **2016**.

Conclusion

In this doctoral dissertation, the author developed carbon–carbon bond-forming reactions via the cleavage of carbon–fluorine bonds in aryl fluorides and carbon–silicon bonds in acylsilanes.

In Chapter 1, the annulative coupling reaction of aryl fluorides with alkynes involving the cleavage of a carbon–fluorine bond is described. By using a carboxylic acid moiety as a directing group, demonstrating that nickelate complexes can be formed at a key intermediate.

In Chapter 2, the aromatic nucleophilic substitution reaction of non-activated aryl fluorides (without an electron-withdrawing group) with enolates of amides as nucleophiles is described. This study demonstrated that amide enolates can be used as effective carbon nucleophiles in concerted nucleophilic aromatic substitution reactions, expanding the scope of nucleophiles applicable in such transformations.

In Chapter 3, the nickel-catalyzed reactions of acylsilanes with norbornenes is investigated. This study demonstrated that Fischer carbene complexes can be generated from acylsilanes using a nickel catalyst, a salient feature previously unreported. Furthermore, computational studies clarified the differences in reactivity between nickel and palladium catalysts, offering valuable mechanistic insights.

In summary, this dissertation highlights the development of innovative carbon–carbon bond-forming reactions using aryl fluorides and acylsilanes. The findings contribute to the advancement of carbon–carbon bond formation methodologies, which are pivotal to organic synthesis across diverse fields, including natural product synthesis, pharmaceuticals, agrochemicals, and materials science. Additionally, the mechanistic insights into concerted aromatic nucleophilic substitution and Fischer carbene–nickel complex formation lay the groundwork for the future development of novel transformations based on these fundamental processes.

List of Publications

1. **Matsuura, A.**; Chatani, N.
   Nickel-Catalyzed C–F/O–H [4+2] Annulation of Ortho-Fluoro Aromatic Carboxylic Acids with Alkynes.
   Chem. Lett. **2021**, *50*, 1990–1992.
2. **Matsuura, A.**; Ano, Y.; Chatani, N.
   Nucleophilic Aromatic Substitution of Non-Activated Aryl Fluorides with Aliphatic Amides.
   Chem. Commun. **2022**, *58*, 9898–9901.
3. **Matsuura, A.**; Ito, Y.; Inagaki, T.; Kodama, T.; Tobisu, M.
   Generation of Nickel Siloxycarbene Complexes from Acylsilanes for the Catalytic Synthesis of Silyl Enol Ethers.
   ACS Catal. **2024**, *14*, 18216–18222.

Supplementary List of Publication

1. Teranishi, T.; Nishikawa, K.; **Matsuura, A.**; Kumagai, M.; Morimoto, Y.
   Divergent Synthesis of Nerolidol-Type Sesquiterpenoids Produced by Soil Bacterium from an Identical Starting Material via Diepoxide Precursors: Stereochemical Revision and Absolute Configuration of a THF Natural Product.
   Chem. Lett. **2022**, *51*, 1062–1066.
2. Morishige, A.; **Matsuura, A.**; Chatani, N.
   Nickel-Catalyzed Hydrodefluorination of Ortho-Fluoro Aromatic Amides with 2-Propanol.
   Chem. Lett. **2023**, *52*, 63–66.